DEVELOPMENT OF ELECTROCHEMICAL AND FLUORESCENT SENSORS

Thesis submitted to

Cochin University of Science and Technology

in partial fulfilment of the requirements

for the award of the degree of

Doctor of Philosophy

in

Chemistry

by

Divya Thomas

Department of Applied Chemistry

Cochin University of Science and Technology

Kochi – 22

May 2015

Development of Electrochemical and Fluorescent Sensors

Ph.D. Thesis under the Faculty of Sciences

By

Divya Thomas
Research Fellow
Department of Applied Chemistry
Cochin University of Science and Technology
Kochi, India 682022
Email: divyakariankal@gmail.com

Supervising Guide

Dr. K. Girish Kumar
Professor of Analytical Chemistry
Department of Applied Chemistry
Cochin University of Science and Technology
Kochi, India 682022
Email: giri@cusat.ac.in

Department of Applied Chemistry
Cochin University of Science and Technology
Kochi, India 682022

May 2015

DEPARTMENT OF APPLIED CHEMISTRY
COCHIN UNIVERSITY OF SCIENCE AND TECHNOLOGY
KOCHI - 682022, INDIA

Dr. K. Girish Kumar
Professor of Analytical Chemistry

Tel: 0484 - 2575804
E-mail: chem.@cusat.ac.in

Date: 27th May 2015

Certificate

Certified that the work entitled **"Development of Electrochemical and Fluorescent Sensors",** submitted by Ms. Divya Thomas, in partial fulfilment of the requirements for the degree of Doctor of Philosophy in Chemistry to Cochin University of Science and Technology, is an authentic and bonafide record of the original research work carried out by her under my supervision at the Department of Applied Chemistry. Further, the results embodied in this thesis, in full or in part, have not been submitted previously for the award of any other degree. All the relevant corrections and modifications suggested by the audience during the pre-synopsis seminar and recommended by the Doctoral committee have been incorporated in the thesis.

K Girish Kumar
(Supervising Guide)

Declaration

I hereby declare that the work presented in this thesis entitled **"Development of Electrochemical and Fluorescent Sensors"** is based on the original work carried out by me under the guidance of Dr. K.Girish Kumar, Professor of Analytical Chemistry, Department of Applied Chemistry, Cochin University of Science and Technology and has not been included in any other thesis submitted previously for the award of any degree.

Kochi-22
27/05/2015

Divya Thomas

Dedicated to,

my Parents…

Acknowledgement

The work presented in this thesis would not have been possible without the help and support of so many people who have always been there for me throughout the course of this research. They stood by my side when I needed them most. I take this opportunity to acknowledge their kindness and extend my sincere gratitude for helping me in making this Ph.D. thesis a reality.

I would like to express my deepest gratitude to my supervising guide, Dr. K. Girish Kumar, Professor of Analytical Chemistry, Department of Applied chemistry, Cochin University of Science and Technology for his excellent guidance, caring and patience. When I felt down with my work, he gave me the moral support and motivation to overcome and move on.

I express my thankfulness to Dr. K. Sreekumar, Doctoral Committee Member, for his inspiration and help. I extend my thanks to Dr. N. Manoj, Head of the Department of Applied Chemistry, CUSAT and all other faculty members for their encouragement and support. I sincerely thank all the non-teaching staff for their timely help and support.

I am grateful to Dr. Anita I, Associate Professor, Department of Chemistry, Maharajas College for her support and help.

I take this opportunity to sincerely acknowledge the Council of Scientific and Industrial Research (CSIR), Government of India, New Delhi, for providing financial assistance in the form of Fellowship which buttressed me to perform my work comfortably. I would also like to acknowledge Directorate of Extramural Research and Property Rights, DRDO, New Delhi and Kerala State Council for Science Technology, Environment, Kerala for the funding assistance. I thank STIC, CUSAT for analysis.

I am forever indebted to all the teachers who have taught me since my childhood because they are the ones who has built the foundation of this humble achievement. A special note of thanks to Sr. Lilly and Sr. Rosily.

I would also like to place on record my gratefulness to all those people who have been with me since the early days of my research tenure. Dr. Sindhu, Dr. Renjini,

Dr. Leena, Dr. Laina, Dr. Sobhana and Theresa were the chief persons who kept me going at the beginning. Let me also express my love and thanks to my dear lab mates Jesnychechi, Soumya, Zafna, Ajith, Anuja, Sreejith, Meera, Rajitha, Shruthi, Ammu, Shanty, Unni, Sheela miss, Ambily, Shalini, Lakshmi and Sreelakshmi for their support. I will always cherish the sweet moments I have had with them. Special thanks to Anuja, Jesnychechi, Soumya, Zafna, Meera, Sheela Miss, Unni, Ammu and Shalini

I would like to extend my gratefulness to all my friends in polymer, biochemistry, physical, organic and inorganic labs. A special thanks to Maheshattan for his help and support.

Literally I lack words to express my love and indebtedness to my Chachan and Amma. With their immense love, ardent prayers and constant support they have lighted my paths ever since the beginning of my life. Let me also make a special mention of Deepu, my wonderful brother, who has been there for me through the thick and thin of my life. He has been with me as a source of strength and inspiration at the toughest points of my research.

I am greatly indebted to my devoted husband Mr. Jerald and my loving daughter Minnu mol. They form the backbone and origin of my happiness. Their unconditional love and support has enabled me to complete my Ph.D. My special thanks to Minnumol, the best daughter one could ever have, for her radiant smiles which helped me to overcome the difficulties I came across in the pursuit of Ph.D. programme. Dear Minnus, when you grows up, I hope you will not complain for the time I gave to my research instead of caring you. I owe to you my dear ones, every feather of success and achievement in my life.

A big thanks to my dear in-laws Appachan, Amma, Ammu, Justin, Ittu, Riya and Hannah mol for their love and support. Your prayer has been the force which sustained me this far.

I would like to acknowledge the people who mean the world to me, my uncles, aunties and cousins. I extend my respect to my paternal and maternal grandparents.

Above all, I thank God for showering me the strength and blessings to complete my thesis, despite all of the obstacles I have faced.

Divya Thomas

Preface

Chemical sensors have growing interest in the determination of food additives, which are creating toxicity and may cause serious health concern, drugs and metal ions. A chemical sensor can be defined as a device that transforms chemical information, ranging from the concentration of a specific sample component to total composition analysis, into an analytically useful signal. The chemical information may be generated from a chemical reaction of the analyte or from a physical property of the system investigated. Two main steps involved in the functioning of a chemical sensor are recognition and transduction. Chemical sensors employ specific transduction techniques to yield analyte information. The most widely used techniques employed in chemical sensors are optical absorption, luminescence, redox potential etc. According to the operating principle of the transducer, chemical sensors may be classified as electrochemical sensors, optical sensors, mass sensitive sensors, heat sensitive sensors etc.

Electrochemical sensors are devices that transform the effect of the electrochemical interaction between analyte and electrode into a useful signal. They are very widespread as they use simple instrumentation, very good sensitivity with wide linear concentration ranges, rapid analysis time and simultaneous determination of several analytes. These include voltammetric, potentiometric and amperometric sensors.

Fluorescence sensing of chemical and biochemical analytes is an active area of research. Any phenomenon that results in a change of fluorescence intensity, anisotropy or lifetime can be used for sensing. The fluorophores are mixed with the analyte solution and excited at its corresponding wavelength. The change in fluorescence intensity (enhancement or quenching) is directly related to the concentration of the analyte. Fluorescence quenching refers to any process that decreases the fluorescence intensity of a sample. A variety of

molecular interactions that can lead to quenching are excited-state reactions, molecular rearrangements, energy transfer, ground-state complex formation and collisional quenching. Generally, fluorescence quenching can occur by two different mechanisms, dynamic quenching and static quenching.

The thesis presents the development of voltammetric and fluorescent sensors for the analysis of pharmaceuticals, food additives metal ions. The thesis is divided into nine chapters.

The first chapter is a general introduction to electrochemical and fluorescent sensors. The principle and applications of the sensors are also discussed. A detailed review of the scientific literature relevant to the development of electrochemical and fluorescent sensors for food and pharmaceutical analysis is also included.

Chapter 2 provides the details of the methods adopted for the fabrication of electrochemical sensors. Procedures followed for the preparation of buffer solutions and cleaning of various electrodes are also presented in this chapter. The details of the instruments used for carrying out the studies are also given in this chapter.

Chapter 3 describes the development of a voltammetric sensor for the determination of nitrite in food samples. The developed sensor was based on the electrochemical oxidation of nitrite on TMOPPMn(III)Cl modified gold electrode.The experimental conditions for electrochemical determination of nitrite were optimized.An excellent catalytic activity and stability for nitrite oxidation was exhibited by the sensor. The determination of nitrite in food samples were carried out using the proposed sensor and the results were found to be in good agreement with those obtained by standard spectrophotometric method.

In chapter 4, fabrication of an electrochemical sensor based on the catalytic activity of gold nanoparticles deposited on a glassy carbon electrode

(AuNP/GCE) for the determination of Sudan I is discussed. The electrochemical behavior of sudan 1 on AuNP/GCE was found to be quasi reversible. The kinetic parameters such as charge transfer coefficient and heterogeneous electron transfer constant involved in the study were calculated and reported in the chapter. The practical utility of the proposed sensor was evaluated by the determination of Sudan I in food products using AuNP/GCE sensor.

Chapter 5 details the electrochemical behavior of artificial antioxidant, butylated hydroxyanisole (BHA), at a glassy carbon electrode modified with poly L- cysteine. The modified electrode showed good electrocatalytic activity towards the oxidation of BHA under optimal conditions. The modified electrode was characterized by scanning electron microscope (SEM). The kinetic parameters were studied using cyclic voltammetry and the results are interpreted in the chapter. Analytical application of the developed sensor for the determination of BHA in oil samples were carried out.

Chapter 6 – 8 are devoted to the development of fluorescent sensors, study of fluorescence quenching mechanism and its application studies.

Chapter 6 outlines the design of a TOPO capped CdSe quantum dots based fluorescent sensor for the selective determination of NIM, a non-steroidal anti-inflammatory drug. The experimental parameters were optimized and the analytical characteristics were determined. The photo induced electron transfer mechanism was explained for selective quenching of fluorescence intensity by NIM and application of present sensor for the determination of NIM in pharmaceutical formulations were performed and presented in the chapter.

Chapter 7 focuses on the determination of BHA based on the fluorescence quenching of CNDs in the presence of BHA. The effect of other phenolic antioxidants on the fluorescence intensity of CNDs was studied. The

developed sensor was employed for the determination of BHA in oil samples and the details are presented in this chapter.

Chapter 8 demonstrates the development of a fluorescent sensor for the selective determination of Fe^{3+} ion in presence of other transition metals. The experimental parameters were optimized and mechanism of fluorescence quenching was also studied. Practical utility of the developed sensor was evaluated by the determination of Fe^{3+} ion in pharmaceutical formulation using the sensor.

Chapter 9 presents the summary and conclusions of the present study.

Contents

List of Tables

List of Figures

List of Scheme

.....ooo.....

Chapter 1

INTRODUCTION

Contents

"If we knew what it was we were doing, it would not be called research, would it?"

— ***Einstein***

Sensors play a crucial role in clinical research, food safety, environmental protection etc. The development of chemical sensors is an active area of analytical research. Chemical sensor can be defined as a device that transforms chemical information, ranging from the concentration of a specific sample component to total composition analysis, into an analytically useful signal[1]. It consists of a receptor and a transducer. The receptor, where the active chemistry occurs, transforms the chemical information of the analyte into a form of energy which can be measured with the transducer. At the transducer, the energy carrying the chemical information about the sample is

converted into a useful analytical signal. Based on the operating principle of the transducer, chemical sensors may be divided into:

i) Electrochemical sensors: They are based on the measurement of current or potential as a function of concentration of the analyte. Volta metric, amperometric and potentiometric sensors fall under this category.

ii) Optical sensors: Optical devices transform the changes of optical phenomena into useful analytical signal. Different optical properties measured are absorbance, reflectance and luminescence. They are also known as optodes.

iii) Mass sensitive sensors: They rely on the change in the mass of a substance at a specially modified surface. The two types of mass sensitive sensors are surface acoustic wave sensors and piezoelectric devices. The surface acoustic wave devices are based on the measurement of change in propagation velocity of an acoustical wave upon deposition of a definite mass of analyte. The piezoelectric devices measure the change in frequency of the quartz oscillator caused by change in the mass of adsorbed analyte.

iv) Heat sensitive sensors: They are commonly called as calorimeter. The heat change associated with a chemical reaction is monitored with a transducer such as a thermistor or platinum thermometer.

1.1 Voltammetry

Voltammetry, one of the important techniques in electro analytical chemistry, was developed from polarography in 1922 by the Czech chemist Jaroslav Heyrovsky, for which he was bestowed the Nobel Prize in chemistry in 1959. In voltammetric techniques, a potential (E) is applied to an electrode and the resulting current is monitored. Under the applied potential, the electroactive species undergo an electrochemical reaction (oxidation or reduction). Since the occurrence of electrochemical reaction can cause a change in the concentration of electroactive species at the electrode surface occurs, voltammetry is considered as an active technique.
The analytical advantages of the various voltammetric techniques include excellent sensitivity with a very large useful linear concentration range for both inorganic and organic species (10^{-12} to 10^{-1} M), a large number of useful solvents and electrolytes, a wide range of temperatures, rapid analysis times (seconds), simultaneous determination of several analytes, the ability to determine kinetic and mechanistic parameters, a well-developed theory and thus the ability to reasonably estimate the values of unknown parameters and the ease with which different potential waveforms can be generated and small currents measured.

1.2 Voltammetric cell set up

The voltammetric cell integrates three electrodes immersed in asolution containing an excess of a non- reactive electrolyte called a supporting electrolyte. The three electrode system consists of a working electrode where the electrochemical process of interest occurs, a reference electrode and an auxiliary electrode. In a voltammetric experiment the

potential is applied to the working electrode with respect to the reference electrode. Usually, reference electrode maintains a constant potential. Any current generated as a result of the applied potential will be measured between the working and counter electrodes.

1.2.1 Reference electrode

The potential of a reference electrode remains constant and no current is allowed to flow through it. They are completely insensitive to the composition of the solution under study. The most commonly used reference electrodes are saturated calomel electrode (SCE) and silver/silver chloride (Ag/AgCl) electrodes. In SCE, the half - cell is mercurous chloride (Hg_2Cl_2, calomel) which is in contact with mercury metal, either as a pool or as a paste with calomel. A platinum wire serves as an electrical contact. The Ag/AgCl reference electrode comprises of a silver wire (Ag) coated with a layer of solid silver chloride (AgCl) immersed in a saturated solution of KCl and AgCl. The potential of SCE is 0.241 V and that of Ag/AgCl electrode is0.197 V with respect to the SHE at 25^{o}C. Pseudo-reference electrodes such as silver or platinum wire in conjunction with an internal reference compound (usually ferrocene with well-defined potentials) are also employed in case of non-aqueous electrochemistry[2].

1.2.2 Counter electrodes

The counter electrode, also known as auxiliary electrode, allows the control of the potential of a working electrode. In an electrochemical system current flows between the counter and working electrodes. The area of a counter electrode is usually larger than that of a working electrode. Generally,

a coil of platinum wire is used as counter electrode due to its inertness. Graphite or glassy carbon electrodes are also used as counter electrodes.

1.2.3 Supporting electrolytes

The primary role of a supporting electrolyte is to reduce the ohmic or ir voltage drop, thereby eliminating the migration current. Chlorides, sulfates and nitrates of lithium, sodium and potassium and tetraalkylammonium salts of the general formula $NR_4^+X^-$ (R = methyl, ethyl, n-butyl and X - =Cl-, Br-, I-, ClO4-) are generally used as supporting electrolytes. Acids (HCl, H_2SO_4), bases (LiOH, NaOH, $NR_4^+OH^-$) and buffer solutions are also used as supporting electrolytes. The concentration of the supporting electrolyte is nearly hundred times greater than the concentration of analyte.

1.2.4 Working electrode

A polarizable microelectrode is usually used as working electrode in voltammetry. In a voltammetric method, the electrochemical process occurs at the working electrode and performance of the method relies upon the material of working electrode. For an ideal working electrode, the range of potentials at which an electrode behaves as polarizable one should be large, the material used should be inert and it should provide reproducible response. The materials usually used as working electrodes include mercury, noble metals and various types of carbon such as glassy carbon and graphite[3-5]. Noble metal electrodes are considered as excellent anodes but as poor cathodes. Glassy carbon electrodes possess a wide potential window.

1.2.4.1 Mercury electrodes

Mercury serves as a working electrode because of its versatile physical and chemical properties. It possesses high overvoltage for reduction of hydrogen ions and has a highly reproducible, continually renewable and smooth surface[6-9]. The most frequently used mercury electrodes are dropping mercury electrode (DME), hanging mercury electrode (HME) and mercury film electrodes.

Traditional mercury electrode, called dropping mercury electrode (DME), consists of a drop of mercury created periodically and dispatched at the tip of a glass capillary immersed in an electrolyte solution. The mercury film electrode is used in stripping and flow amperometric analysis. It is made by coating a thin layer of mercury on conducting substrate. Iridium and glassy carbon are the most commonly used substrates for the preparation of mercury film electrode due to its ability to adhere the oxide film on its surface. A hanging mercury drop electrode (HMDE) is used in cyclic voltammetry and for stripping analysis. The main shortcomings of mercury electrodes are its limited anodic range and toxicity.

1.2.4.2 Solid Metal Electrodes

Metal electrodes possess wide anodic potential windows and are mechanically stable. Also, the handling of solid electrodes is easy. Metals such as platinum, gold and carbon are the most widely used solid electrode substrates. Metals such as copper, nickel, an alloy of Pt-Ru and alloy of Ni- Ti etc are also employed as electrode substrates[10-11]. Solid electrodes are available in different shapes and dimensions such as tubular, ring, rotating

disk etc. The surface of solid electrodes can be reproduced by mechanical polishing and potential cycling depending on the material of electrode.

Noble metal electrodes are conducting and can be obtained in high purity. Platinum electrodes are limited to a range of positive potentials. Gold electrodes being more inert, has a lesser tendency to form stable oxide films[12-13]. The characteristic property of gold to form Au-sulfur covalent linkage is utilized for the formation of self - assembled monolayer of organo sulfur compounds on the surface of gold electrodes[14-15]. The low hydrogen overvoltage at noble metals restricts their cathodic potential window.

1.2.4.3 Carbon electrodes

Carbon-based electrodes usually have a wider potential range, low background current, rich surface chemistry, chemical inertness and low cost. Carbon electrodes can be homogenous (glassy carbon, graphite, vitreous carbon, screen printed, fullerenes, carbon nanotubes and diamond) or heterogeneous (carbon paste and modified carbon paste). Even though all carbon-based electrode materials have a six-membered aromatic ring with sp^2 bonding they differ from each other in their relative density of the edge and basal plane toward electron transfer and adsorption. The excellent electrical conductivity of carbon electrodes can be attributed to the high degree of electron delocalization and weak Vander Waals forces.

Among carbon electrodes, the most popular is glassy carbon or vitreous carbon electrode. It is glass-like carbon and has both the properties of glass and industrial carbon. It has excellent electrical and mechanical properties, wide potential range, extreme chemical inertness and relatively

reproducible performance[16-18]. Carbon paste electrodes, in which various modifiers can be introduced by physical mixing, are also an important class of carbon based electrodes[19-22].

1.3 The electrical double layer

In an electrochemical cell an electrode can transfer electrons from a layer of solution adjacent to the electrode. Electrical double layer can be defined as the accumulation of charge at the electrode surface and the solution adjacent to the surface. Electrical double layer have composition different from the bulk of the solution. The electrical layer has an inner layer, where potential decreases linearly with distance from the surface of the electrode and a diffuse layer in which an exponential decrease in potential is observed.

The transfer of electrons can be due to two processes such as faradaic and non-faradaic processes. The faradaic processes are referred to processes that involve the transfer of electrons or charges across the electrode-solution interface. Electrodes at which faradaic processes occur are sometimes called charge-transfer electrodes and the processes cause oxidation or reduction reactions to occur at the electrode surface. The magnitude of the faradaic current is determined by the rate of the resulting oxidation or reduction reaction at the electrode surface. They are governed by faradaic laws which state that an amount of chemical reaction at an electrode is proportional to the current i.e. faradaic current.

In addition to faradaic process, non-faradaic process or capacitive process also contribute to the current in an electrochemical cell and the generated current is known as non-faradaic current. The non-faradaic

process may be due to the electrical double layer, adsorption and desorption. It does not involve a chemical reaction. In a voltammetric cell, both faradaic and non-faradic process occurs and the total current is the sum of two. Under potentiostatic conditions, charging process tends to be very fast and resulting non-faradaic current will perish in a short interval.

The factors contributing to the faradaic current in an electrochemical reaction are mass transport and kinetics of electron transfer at the electrode surface

1.3.1 Mass transport

The pathways of reactions occurring in an electrochemical cell are considered to be complex. The overall steps in an electrochemical reaction involves the mass transport of electroactive species to the electrode surface, transfer of electrons across the interface and passage of products back to the bulk. The measured current is therefore proportional to the mass transport and electron transfer rate. The current measured is considered to be mass transport-limited, if only the rate of the transfer of electroactive species contribute to the current. Three different modes of mass transport are diffusion, convection and migration.

Diffusion: It is the movement of chemical species from a region of higher concentration to a region of lower concentration. The flux in diffusion was described by Fick's law[23]as;

$$Jo = -Do \left(\frac{\delta Co}{\delta x}\right), \quad \text{.....(1.1)}$$

where J_o is the diffusional flux and D_o is the diffusion coefficient.

Migration: It is the movement of charged particles under the influence of an electric field. The factors affecting migration are the concentration and charge of the ion, diffusion coefficient and magnitude of the electric field.

Convection: The two types of convections are natural convection and forced convection. Natural convection is due to density gradients whereas forced convection occurs as a result of stirring of solution or by the rotation or vibration of electrode.

The mass transport in a voltammetric cell is complex due to three modes of mass transport. Usually in an electrochemical reaction, migration is eliminated by adding a high concentration of an inert supporting electrolyte to the analyte solution and convection is eliminated by performing the experiment in an unstirred condition. If migration and convection are successfully eliminated, the mass transport is solely due to diffusion and the current in a voltammetric cell is given by

$$i = \frac{nFAD\,(C_{bulk} - c_{x=0})}{\delta} \quad \text{.....(1.2)}$$

where n isthe number of electrons in the redox reaction, F is Faraday's constant, A is the area of electrode, D is the diffusion coefficient, C_{bulk} and $C_{x=0}$ are concentration of reactive species in bulk solution and at the electrode surface and δ is the thickness of the diffusion layer.

1.3.2 Kinetics of electrode reactions

(i) **Reversible Systems**

A system is considered to electrochemically reversible, when electron transfer kinetics at the electrode surface is fast and the concentrations

of oxidized and reduced species at the electrode are those specified by the Nernst equation. The peak current for a reversible reaction is given by the equation;

$$ip = \left(2.69 \times 10^5\right) n^{3/2} A D_o^{1/2} C_0 n^{1/2} \quad \text{.....(1.3)}$$

where, n is the number of electrons, A is the area in cm^2, D_o is the diffusion coefficient in cm^2s^{-1}, C_0 is the concentration in M, v is the scan rate in Vs^{-1} and i_p is the peak current in amperes.

The separation between the peak potentials (for a reversible couple) is given by:

$$\Delta E_p = E_{pa} - E_{pc} = 59mV/n \quad \text{.....(1.4)}$$

In a reversible system**,** the peak potential (Ep) is independent of the scan rate (v) and the peak current (ip) is proportional to $\nu^{1/2}$.

(ii) Irreversible Systems

When electron transfer kinetics at the electrode surface are slow (those with sluggish electron exchange), the concentration of oxidized and reduced species are not in equilibrium. Such systems are considered electrochemically irreversible. The peak current for irreversible systems is given by;

$$i_p = (2.99 \times 10^5)(\alpha)^{1/2} A C_o D_o^{1/2} \nu^{1/2} \quad \text{.....(1.5)}$$

The peak potential for an irreversible reaction is given by the equation 1.6;

$$E_p = E^0 - \frac{RT}{\alpha F}\left[0.780 + ln\left(\frac{D_0^{1/2}}{k_0}\right) + ln\left(\frac{\alpha F \nu}{RT}\right)^{1/2}\right] \quad \text{.....(1.6)}$$

Totally irreversible systems are characterized by a shift of the peak potential with the scan rate.

(iii) Quasi-reversible system

Current in a quasi - reversible system is controlled by both charge transfer as well as mass transfer[24]. The term Quasi reversible was proposed by Matsuda and Ayabe[25]. For a quasi- reversible system; ΔEp = 60-200 mV. The current in a quasi - reversible system is given by,

$$i= FAD_o^{1/2}C_of^{1/2}\nu^{1/2}\psi(E) \quad \text{.....(1.7)}$$

where, $f = \frac{F}{RT}$, and $\psi(E)$ is a function of quasi reversible system, A is the area in cm^2, D_0 is the diffusion coefficient in $cm^2\ s^{-1}$, C_0 is the concentration in M and ν is the scan rate in Vs^{-1}.

$$\Delta= k^o/[D_o^{1/2}(F/RT)^{1/2}\nu^{1/2}] \quad \text{.....(1.8)}$$

where k^o is rate transfer constant of a heterogeneous reaction. As the value of Δ increases, the process tends to be reversible. The rate constant for heterogeneous electron transfer, k^o, for a quasi - reversible reaction lies between 10^{-1} to 10^{-3} cm s^{-1}.

1.4 Heterogeneous rate transfer constant

Nernst and Butler– Volmer equations were employed to define the relation of applied potential to the concentrations of the redox species and the rate of the reaction (k^0) respectively.

For the oxidation reaction involving n electrons;

$$Red \rightleftarrows Ox + ne^- \quad \text{.....(1.9)}$$

the relationship between the potential and the concentrations of the oxidized and reduced form of the redox species at equilibrium(at 298 K) is given by Nernst Equation as in equation 1.10:

$$E = E^{0'} + \frac{0.059}{n}\log_{10}\frac{[\mathrm{Ox}]}{[\mathrm{Red}]} \quad \text{.....(1.10)}$$

where E is the applied potential and $E^{0'}$ the formal potential; [OX] and [Red] represent the concentrations of oxidized and reduced species at the electrode/solution interface.

Butler-Volmer equation (1.11) explains relation between the current on an electrode to the electrode potential, on the assumption that both cathodic and anodic process occur on the same electrode.

$$I = A \cdot i_0 \cdot \left\{ \exp\left[\frac{(1-\alpha)\cdot n \cdot F}{R \cdot T} \cdot (E - E_{eq})\right] - \exp\left[-\frac{\alpha \cdot n \cdot F}{R \cdot T} \cdot (E - E_{eq})\right] \right\} \quad \text{.....(1.11)}$$

where, I is current at electrode (Amps), i_o is exchange current density (Amp/m^2), E is electrode potential (V), E_{eq} is equilibrium potential (V), A is active surface area of electrode (m^2), T is absolute temperature (K), n is number of electrons involved in the electrode reaction, F is Faraday constant, R is universal gas constant and α is the symmetry factor or charge transfer coefficient. The first part of Butler – Volmer equation represents the current densities for the anodic process and second part represents the current densities for the cathodic process.

The heterogeneous rate transfer constant in an electrochemical reaction can be obtained from cyclic voltammetric study. Various equations have been developed for the calculation of heterogeneous rate constant k^o on the

basis of peak separation potential i.e. $\Delta Ep = E_{pc} - E_{pa}$, where E_{pc} and E_{pa} are cathodic and anodic peak potential respectively.

Nicholson method[26] was used to estimate the observed standard heterogeneous electron transfer rate constant (k^o, cm s^{-1}) using the following equation;

$$\Psi = k^o[\pi D n\nu F/(RT)]^{-1/2} \quad \text{.....(1.12)}$$

where Ψ is the kinetic parameter, D is the diffusion coefficient. A plot of Ψ against $[\pi D n\nu F/(RT)]^{-1/2}$ allows the deduction of standard heterogeneous rate transfer constant, (k^o). This method is applied for peak separation ranging between 57 mV and 250 mV (in this range the electrode process progress from reversible to irreversible).

Klingler and Kochi[27] developed a method based on peak separation for the calculation of the heterogeneous rate transfer constant.

$$K^o = 2.18\,[D n\nu F/(RT)]^{-1/2} \exp[-(\alpha^2 n F \Delta Ep/RT)] \quad \text{.....(1.13)}$$

Whereα is electron the transfer coefficient, *n* is the number of electrons transferred and D_o is the diffusion coefficient of the oxidized species in cm^2s^{-1}, $\Delta Ep = Ep^c - E_p^a$. For a reversible reaction the value of α is considered to be 0.5.

A simple method for the determination of the heterogeneous electron transfer rate constant was proposed by Gileadi[28]. The value of peak separation is not considered in this method. A reversible process gradually changes to irreversible process, as the scan rate increases.

On plotting peak current against scan rate, at lower scan rate a linear plot and at higher scan rates an ascending curve was observed. According to equation 1.14, the critical scan rate, ν_c obtained as the intersect of these plots is linearly related to k^o;

$$\log k^o = -0.48\,\alpha + 0.52 + \log\left[nF\,\alpha\,\nu_c D_o / 2.303RT\right]^{1/2} \quad \text{.....(1.14)}$$

This method is applicable for irreversible systems also.

1.5 Chemically modified electrodes

The need for chemically modified electrodes arises from the unpredictable surface reactivity, surface passivation, surface fouling, sluggish kinetics and poor sensitivity of bare electrodes. The surface modification provides a greater control of electrode characteristics and reactivity. It improves the rate of electro catalysis, selectivity and sensitivity of the system. The modification of platinum electrode with olefin compounds by Lane and Hubbard marked the emergence of chemically modified electrodes in the field of electrochemistry[29]. According to IUPAC, a chemically modified electrode is a conducting or semiconducting material that has been coated with a monomolecular, multi-molecular, ionic, or polymeric film which alters the electrochemical, optical and other properties of the interface[30-31]. Chemically modified electrodes find applications in electro catalysis, corrosion protection, electro chromic devices and in bio/chemical sensing. CMEs can be generated by chemisorption, covalent attachment, multimolecular layer deposition, composite formation and electropolymerization of various functionalities on the electrode surface.

The various materials reported for electrode modification includes metal nanoparticles, macro cyclic compounds such as metalloporphyrins, calixarenes etc, electropolymerized films of conducting materials, nanocomposites etc. In the present study, metalloporphyrins, gold nanoparticles (AuNPs) and electropolymerised film of L-cysteine modified electrodes were used for sensor fabrication.

1.5.1 Metalloporphyrins

Porphyrins are a ubiquitous class of macrocyclic compounds, which plays an important role in essential biological activities ranging from photosynthesis to oxygen transport [32-34]. They have an extensive system of delocalized π electrons. They contain four pyrrole rings linked through four methine bridges. They exhibit excellent photophysical, photochemical and electrochemical properties. These properties and the appearance of strong Soret and Q bands of porphyrins are responsible for choosing them as materials for the fabrication of optochemical sensors[35-36]. Porphyrins have found wide application in the field of photodynamic therapy[37-38], light-energy conversion[39-40], molecular wires[41-43], fluorescence switches[44] and sensor fabrication[45].

These compounds are found to be good candidates for modifying electrode surfaces due to their ability to change oxidation states without affecting stability and molecular structure during electrocatalysis. The redox properties of porphyrins depend on the ring substituents and central metal atom. The catalytic activity of metalloprorphyrins can be attributed to the presence of unpaired d electrons and unfilled d orbitals which are available to form bonds with the adsorbate in axial position. The various strategies employed for the

modification of electrodes with metalloporphyrins include dip-dry method, drop dry method, spin coating, electrode position, self- assembled monolayer formation and Langmuir-Blodgett film formation. The use of metalloprphyrin modified electrodes for food and drug analysis is reported[46].

1.5.2 Gold nanoparticles (AuNPs)

Nan materials have attractive electronic, optical, thermal and catalytic properties and possess potential applications in the fields of catalysis, microelectronics and sensor fabrication[47-48]. The important advantages of metal nanoparticles modified electrodes over macroelectrodes in the field of electro analysis are enhancement of mass transport, catalysis and high effective surface area[49-51]. They possess excellent conductivity and catalytic properties which make them suitable for enhancing the electron transfer between the analyte and the electrode surface.

Among the different metal nanoparticles, gold nanoparticles (AuNps) being most stable are used extensively due to their excellent properties such as high electrical conductivity, chemical stability and biocompatibility. They also possess electrocatalytic ability, high surface-to-volume ratio, biocompatibility and functions as an electron antennae between the electrode and electroactive substrate[52-55]. The size confinement effect of AuNps is responsible for its unique optical properties[56]. Various methods reported for the synthesis of gold nanoparticles include chemical synthesis[57-58], UV light or electron-beam irradiation[59], magnetron sputtering, radiolytic and photolytic method[60-61] and electrochemical methods[62-63]. Among the various methods, electrodeposition provides a complementary easy, rapid and cheap alternative for the preparation of gold nanoparticles. AuNPs modified

electrochemical interface behaving as nanoelectrode ensembles have been widely used for the development of electrochemical sensors[64-68].

1.5.3 Electropolymerised film modified electrodes

Conducting polymers (CPs) are good candidates for use in chemical and biochemical sensors due to its selectivity, sensitivity, homogeneity in electrochemical deposition, strong adherence to electrode surface and chemical stability of the film[69-71]. Their unusual electrochemical properties are caused by the conjugated π-electron backbones. Electropolymerisation of various monomers onto high-work function electronic conductors such as platinum, gold and carbon offers a unique route toward electrochemical sensors. Electropolymerization is performed under galvanostatic, potentiostatic, or most commonly potentiodynamic conditions. The thickness, permeation and charge transport characteristics of the polymeric films can be controlled by the potential and current applied.

In addition to conducting polymers, non-conducting films prepared by electro polymerization method has also been employed for electrode fabrication. Their small thickness, which can be controlled by the increase in electrical resistance during its growth on the electrode, allows the rapid diffusion of substrates and products. The advantages of electropolymerised non-conducting films include fast response time and high selectivity. Electrodes modified with electropolymerized films of conducting polymers, such as polypyrrole, polyaniline, polyacetylene, polyindole, polythionine, polythiophene and poly (L-cysteine) has been reported for the development of voltammetric sensors[72-73]. Non-conductive polymers obtained from

amino acid or their derivates and phenol and its derivates are reported in the literature for electrode modification[74].

1.6 Luminescence

Luminescence is the emission of light from any substance and occurs from electronically excited states. Based on the nature of the excited sate luminescence can be of two types: fluorescence and phosphorescence. Other nonradiative deactivation processes occurring are intersystem crossing (ISC), internal conversion (IC), and vibrational relaxation.

Processes which occur between the absorption and emission of light are usually illustrated by a Jablonski or electronic transitions diagram (Fig1.1). The ground, first and second excited states are depicted as S_0, S_1 and S_2 respectively. According to the Franck –Condon principle, transitions between the states occur in a short time (~10^{-15}s) without any significant change of nuclei. Upon absorption of light a fluorophore is excited to a higher vibrational level S_1 or S_2. If the photon emission occurs from S_1 to So, the process is fluorescence. Molecules in S_1 state can undergo a spin conversion to first triplet state and the process is called intersystem crossing (ISC). ISC occur within the lifetime of 10^{-8} s. The mechanism for intersystem crossing involve vibrational coupling between the excited singlet state and a triplet state. If the emission is from triplet excited state (T_1) to ground state (S_0) the process is phosphorescence. Transitions to the ground state are forbidden and the emission rates are slow (10^3-100 s^{-1}), so phosphorescence lifetimes are typically milliseconds to seconds. If vibrational energy levels strongly overlap electronic energy levels, a possibility exists that the excited electron can undergo transition from a vibration level in one electronic state

to another vibration level in a lower electronic state. This process is called internal conversion and mechanistically is identical to vibrational relaxation. Vibrational relaxation occurs very quickly (<1 x 10^{-12} seconds) and is enhanced by physical contact of an excited molecule with other particles with which energy, in the form of vibrations and rotations, can be transferred through collisions[75].

1.6.1 Delayed Fluorescence

In certain cases, a weak emission with spectral characteristics similar to fluorescence but with a shorter life time is observed. This process is known as delayed fluorescence. Two important types of delayed fluorescence are; E-type delayed fluorescence and P-type delayed fluorescence. ; E-type delayed fluorescence was first observed in eosin whereas P-type delayed fluorescence was observed in pyrenes. E-type delayed fluorescence can be defined as the process in which the first excited singlet state becomes populated by a thermally activated radiationless transition from the first excited triplet state. Since in this case the populations of the singlet and triplet states are in thermal equilibrium, the lifetimes of delayed fluorescence and the concomitant phosphorescence are equal. P-type delayed fluorescence is the process in which the first excited singlet state is populated by interaction of two molecules in the triplet state(triplet-triplet annihilation) thus producing one molecule in the excited singlet state. In this biphotonic process the lifetime of delayed fluorescence is half the value of the concomitant phosphorescence[76].

The term fluorescence was introduced by Sir Gabriel Stokes. Fluorescence is emission of light from singlet-excited states to the ground state. According to IUPAC, fluorescence is defined as, '*spontaneous emission of*

radiation from an excited molecular entity with the formation of a molecular entity of the same spin multiplicity'. Return to the ground state is spin-allowed and occurs rapidly by emission of a photon. Fluorescence occurs with an emission rate of 10^8 s^{-1}. Since fluorescence does not require any spin reorientation, the process takes place at a shorter lifetime of nearly 10 ns.

1.6.2 Characteristics of Fluorescence Emission

Fluorescence emission occurs at lower energy compared to absorption. This difference in energy or wavelength between the band maxima of the absorption and emission spectra of the same electronic transition was observed by Sir G. G Stokes and explained as stokes shift[77]. Rapid decay to lower and higher vibrational levels, solvent effect, excited state reactions, complex formation and energy transfer are the common causes of Stokes shift. Kasha's rule[78] states that fluorescence emission spectra are usually independent of the excitation wavelength. The emission is the mirror image of the $S_0 \rightarrow S_1$ absorption.

Emission occurs from a population of *n* excited fluorophores with intensity *I:*

$$I = nE \quad \text{.....(1.15)}$$

The emission lifetime is within the picosecond-to-nanosecond range. Thus, emission is a very fast process, and so in order to observe fluorescence emission, the fluorophore should be excited continuously.

Excitation and emission spectra are the characteristics of fluorescent compounds. Excitation spectrum gives a clear picture of the distribution of electron in the ground state. The excitation spectra can be obtained by

measuring the emission intensity at a fixed wavelength whereas the emission spectra are obtained by measuring the variation in emission intensity wavelength for a fixed excitation wavelength. The intensity, position of the emission wavelength and lifetime are characteristics of a particular fluorophore.

1.6.3 Fluorescence lifetimes and quantum yields

The fluorescence lifetimes and quantum yields are the most important characteristics of a fluorophore. Fluorescence quantum yield is the ratio of number of photons emitted to the number of photons absorbed. Quantum yields typically range between a value of zero and one

$$Q = \frac{\Gamma}{\Gamma + k_{nr}} \quad \text{.....(1.16)}$$

where Γ is the number of photons emitted and k_{nr} is all forms of non-radiative decay from the excited to the ground state. The quantum yield can be close to unity if the radiationless decay rate is much smaller than the rate of radiative decay, that is knr<Γ.

Fluorescence lifetime (τ) can be defined as the mean time a fluorophore remain in the excited state followed by excitation. Generally, fluorescence lifetimes ranges from the 10^{-9} s to 10^{-12} s. If n_0 is the initial population of fluorophores in the excited state, the rate of decay of excited state population is given by the equation 1.17as:

$$\frac{dn(t)}{dt} = (\Gamma + k_{nr})n(t) \quad \text{.....(1.17)}$$

Where n(t) is the number of molecules after excitation at time t, Γ is the emission rate and k_{nr} is the non radiative decay rate. Since radiation is a random event, the exponential decay of excited state population is given as:

$$n(t) = n_0 \exp(-t/\tau) \quad \text{.....(1.18)}$$

In fluorescence experiments, intensity (I) is measured rather than number of excited molecules. Therefore;

$$I(t) = I_0 \exp(-t/\tau) \quad \text{.....(1.19)}$$

where I(t) and I_0 are fluorescence intensities at time t and at time 0.The inverse of total decay rate, $\tau = (\Gamma + k_{nr})^{-1}$is termed as lifetime($\tau$). The fluorescence life time is measured from the slope of a plot of log I *(t)* versus t. The lifetime measured assuming that all processes that compete for excited state deactivation are absent is called intrinsic or natural lifetime (τ_n) and the measured lifetime after considering all non - radiative processes are termed as excited state or measured fluorescence lifetime. The natural lifetime is given as

$$\tau_n = \frac{1}{\Gamma} \quad \text{.....(1.20)}$$

and it can be calculated from measured lifetime (τ) and quantum yield using the equation:

$$\tau_n = \tau / Q \quad \text{.....(1.21)}$$

In actual practice measured fluorescence lifetime is always less than intrinsic or natural lifetime. The two popular methods for the determination of fluorescence lifetimes are the pulse or photon-counting and the phase modulation method[75].

1.7 Fluorescence Quenching

Fluorescence quenching can be defined as any process that reduces the fluorescence intensity of a fluorophore. Quenching is an important phenomenon in fluorescence as it provides information about the nature of the fluorophore, type of interaction between fluorophore and quencher and also about the concentration of quencher. Quenching requires molecular interaction between the fluorophore and quencher. Variety of molecular interactions such excited state reactions, molecular rearrangements, ground state complex formation; collisional quenching and energy transfer can result in quenching. The two basic types of molecular interactions leading to quenching are dynamic quenching and static quenching. Dynamic quenching or collisional quenching takes place as a result of diffusive interaction of quencher to the fluorophore whereas static quenching occurs due to the formation of non-fluorescent complex formation between fluorophore and the quencher.

1.7.1 Collisional or Dynamic quenching

In collisional quenching, at the excited state quencher diffuses into the fluorophore and fluorophore returns to the ground state without emission of a photon. Collisional quenching occurs without a photochemical reaction. The decrease in fluorescence intensity due to collisional quenching is described by the Stern-Volmer equation:

$$\frac{F_0}{F} = 1 + k_q\tau_0[Q] = 1 + K_D[Q] \quad \text{.....(1.22)}$$

where F_0 and F are the fluorescence intensities in the absence and presence of quencher, k_q is the bimolecular quenching constant;τ_0 is the lifetime of

the fluorophore in the absence of quencher, Q is the concentration of quencher and K_D is the Stern – Volmer constant. An important characteristic of collisional quenching is represented as equation 1.23:

$$\frac{F_0}{F} = \frac{\tau 0}{\tau} \quad \text{.....(1.23)}$$

The observed equivalent decrease in fluorescence intensity and lifetime is due to the depopulation of excited state by quenching.

1.7.2 Static or Contact quenching

Fluorescence quenching resulting from the formation of a complex between fluorophore and quencher is known as static quenching. When this complex absorbs energy from light, the excited state immediately returns to the ground state without emission of a photon and the molecules do not emit fluorescent light. The relation between fluorescence intensity and quencher concentration is derived by considering the association constant for complex formation and is given by;

$$K_s = \frac{[F-Q]}{[F][Q]} \quad \text{.....(1.24)}$$

where K_S is the fluorophore-quencher association constant, $[F-Q]$ is the concentration of the complex, [F] is the concentration of the uncomplexed fluorophore and [Q] is the concentration of quencher. On substituting fluorophore concentration by fluorescence intensities and rearranging equation1.24;

$$\frac{F_0}{F} = 1 + K_s[Q] \quad \text{.....(1.25)}$$

A plot of $\frac{F_0}{F}$ against [Q] is linear for both dynamic and static quenching and from the slope of the plot Stern – Volmer constant can be obtained. The dynamic and static quenching can be distinguished by the measurement of fluorescence lifetime and also their dependence on temperature and viscosity. For static quenching $\frac{\tau 0}{\tau} = 1$; whereas for collisional quenching $\frac{F_0}{F} = \frac{\tau 0}{\tau}$.

A characteristic feature of static quenching is a change in the absorption spectra of the fluorophore. In case of collisional quenching as it affects only the excited state of fluorophore no change in the absorption spectra is observed. At higher temperature, the collision is very fast and results in large amount of collisional quenching. Since the dissociation of weakly bound complexes occurs at higher temperature, the extent of static quenching is lesser when the temperature is high. Comparison of dynamic and static quenching[75] is given in figure 1.2

In certain cases fluorescence quenching can be by both dynamic and static quenching. Such situations can be visualized by an upward curvature in the Stern – Volmer plots and can be expressed as:

$$\frac{F_0}{F} = (1+ K_D [Q])(1+ K_s[Q]) \quad \text{.....(1.26)}$$

The modified Stern -Volmer equation combines dynamic and static quenching effect on the fluorescence intensity and displays as a second-order in [Q].

1.8 Mechanism of fluorescence quenching

Predicting the mechanism of quenching is a challenging task. The fluorescence quenching can be explained by considering either one or by the combination of different mechanisms. The three important mechanisms for explaining quenching are; intersystem crossing or the heavy atom effect, electron exchange or Dexter interactions and photoinduced electron transfer (PET).

1.8.1 Intersystem crossing or the heavy atom effect

The quenching of fluorescence intensity observed in the presence of heavy atom halogens and oxygen can occur by intersystem crossing. In the excited state, upon interaction with a triplet oxygen or heavy atom the fluorophore undergoes intersystem crossing from an excited singlet state to triplet state. The fluorophore in the excited triplet state can return to the ground state by non- radiative decay, leading to a decrease in the fluorescence intensity. Figure 1.3 represents the quenching by intersystem crossing[75].

1.8.2 Electron exchange or Dexter interactions

The electron exchange or Dexter interaction[79-82] is as shown in Figure 1.4. Dexter interaction can be explained on the basis of an interaction between a donor, D, and an acceptor, A. An electron in lowest unoccupied orbital of the excited donor is transferred to the acceptor.

The acceptor remains in an excited state after transferring an electron from its highest occupied orbital to the donor.

1.8.3 Photoinduced electron transfer (PET)

Photo induced electron transfer (PET) is the third type of mechanism for quenching.PET involves the formation of a complex ($D_p^+A_p^-$) between the electron donor (D_P) and the electron acceptor (A_P). The formed complex can return to the ground state without emission of a photon or by an exciplex emission (Fig 1.5).

Among the various mechanisms for quenching the energy transfer occurring in PET can be predicted by basic principles of electrochemistry i.e, Rhem-Weller equation:

$$\Delta G = E(D^+/D^-) - E(A/A^-) - \Delta G_{00} - \frac{e^2}{\varepsilon d} \quad \text{.....(1.27)}$$

where the reduction potentials E (D^+/D^-) and E(A/A^-) are obtained from the process $D_p^+ + e \rightarrow D$ and $Ap + e \rightarrow A_p^-$ respectively. ΔG_{00} is the energy of the S_0S_1 transition of the fluorophore. ε is the dielectric constant of the solvent, and *d* is the distance between the charges. Since energy is lost when the light energy is dissipated and the ions experience columbic attraction, ΔG_{00} and $\frac{e^2}{\varepsilon d}$ will have a negative sign. As E (D^+/D) and E (A/A^-) represents the reduction potentials, they will have an opposite sign.

1.8.4 Fluorescent Resonance Energy Transfer

Fluorescence resonance energy transfer (FRET) or Forster type energy transfer is another important mechanism used to explain the energy transfer between a donor (D) molecule in the excited state and an acceptor (A) molecule in the ground state. The requirements for FRET are dipole–dipole interactions between the donor and acceptor, and extent of spectral overlap

of the emission spectrum of the donor with the absorption spectrum of the acceptor. The effective distances between the donor and acceptor molecules are in the 10 to 100 Å range

1.9 Fluorophores

Fluorescence is a powerful tool in biological research, the relevance of which relies greatly on the availability of sensitive and selective fluorescent probes. Fluorophores have a key role in fluorescence sensors. Afluorophore can be defined as a component that causes a molecule to absorb energy of a specific wavelength and then re-remit energy at a different but equally specific wavelength. The amount and wavelength of the emitted energy depend on both the fluorophore and the chemical environment of the fluorophore[83].

1.9.1 Quantum Dots (QDs)

Colloidal quantum dots were discovered by Alexie Ekimov in 1980s in glass matrix[84] and by Louis E Brus in colloidal solutionsin1982[85].The term "quantum dot" was coined by Mark Reed[86]. Quantum Dots (QDs) are semiconductor nanoparticles usually made from the periodic groups II-VI (CdSe, CdS etc.) or III-V (InP, InAs etc.). Their size ranges from 1 nm to 10 nm and possesses unique optical, electrical and chemical properties due to quantum confinement effects. Semiconductor QDs exhibit novel optical and electronic properties and emerged as a versatile class of fluorescent probes for bioimaging and biodiagnostics. Being zero dimensional, QDs have a sharper density of states than higher dimensional structures. QDs typically have very broad continuous absorption spectra that depend on the

particle size, broad excitation and narrow size-tunable emission spectra, negligible photobleaching and high photochemical stability. QDs have large extinction coefficients (Ɛ), particularly significant for optical properties. In electronic properties QDs have band gap energies that vary as a function of size. The physical and chemical properties of QDs can be governed by two factors such as the high surface/ volume ratio of the nanoparticles and the size of the particle, which determines the electronic and physical properties of the material. Chemical and photochemical stability of QDs can be improved by modifying the surface of QDs with materials of higher band gap, thiols, silica and polymers[87-89]. Quantum dots have been used as fluorophores in pH sensors[90], for detection of heavy metal ions[91], organic compounds[92], biomolecules[93], drugs[94], proteins and enzymes[95]. Even at relatively low concentrations, QDs have reported to be serious toxic[96-97].

1.9.2 Carbon nitride dots (CNDs)

Carbon dots (CDs), metal-free polymeric photocatalyst, is a promising alternative to traditional toxic metal-based semiconductor QDs[98]. In order to tune the fluorescence efficiency of CDs substitution of carbon atoms with heteroatoms such as nitrogen, sulfur, and silicon was achieved[99-100].Among these, nitrogen (N) atom has been widely used for substitution because of the comparable atomic size of nitrogen atoms with carbon atoms. As the nitrogen substitution disorder the carbon hexagonal rings and create emission energy traps through the radiative recombination induced by electron–hole pairs, the obtained carbon nitride dots (CNDs) emitted blue luminescence upon UV excitation[101].They exhibited stable photoluminescence (PL), strong fluorescence, broad excitation spectra, tunable emission spectra,

low cytotoxicity and excellent biocompatibility. These unique properties and non toxicity in the physiological condition proved them to be effective fluorescent probes. They are of several nanometers in size and exhibit excellent stability in aqueous media[102-106]. The unique properties and wide applications in catalysis, sensors and corrosion protection, etc made CNDs the focus of materials research[107-109]. Several synthetic strategies such as laser ablation[110], electrochemical oxidation[111], chemical oxidation[112-113], thermolysis[114-115] and microwave-assisted methods[116-117], have been adopted for the preparation of CDs. Among these approaches, the microwave-assisted method is the most economical, facile and green synthetic route.

1.10 Literature Review

Voltammetric sensors based on chemically modified electrodes (CMEs) have been reported for the analysis of different food additives such as colorants, preservatives, antioxidants etc. CMEs have excellent sensitivity, selectivity and they can also enhance the electrocatalysis process. A brief review on various chemically modified electrodes for quantification of food additives is reported here.

Wang et al.[118] developed an electrochemical sensor using polyvinylpyrrolidone (PVP)-modified carbon paste electrode for the sensitive determination of quinoline yellow. In 0.1 M phosphate buffer (pH 6.5), the developed sensor showed an irreversible oxidation peak at 0.97 V. The experimental parameters such as the effect of pH, amount of PVP, accumulation potential and time were studied and optimized. The linear range was from 5.0×10^{-8} to 1.0×10^{-6} M, and the limit of detection was evaluated to be 2.7×10^{-8} M. The developed sensor was applied for the

determination of quinoline yellow in different soft drink samples and the results were compared with high-performance liquid chromatography.

A voltammetric sensor for determination of sunset yellow in soft drinks based on hexadecyltrimethylammonium bromide (CTAB) functionalized graphene supported platinum nanoparticles composite (CTAB-Gr-Pt) modified glassy carbon electrode was reported[119]. The method utilizes the synergistic effect of the large surface area and electrocatalytic activity of both Gr and Pt NPs for the development of sensor. Under the optimized experimental conditions, the oxidation peak currents of sunset yellow were proportional to its concentrations in the range of $8.0 \times 10^{-8} – 1.0 \times 10^{-5}$ M and the limit of detection was 4.2×10^{-9} M. The developed method was successfully applied to determine sunset yellow in soft drinks.

A carbon nanotubes modified carbon paste electrode sensor was developed by Santos et al.[120] for the voltammetric determination of sulphite in beverages. The method is based on the electrochemical reduction of suphite on a carbon-paste electrode chemically modified with multiwalled carbon nanotubes. The developed sensor showed a linear relationship from 2.5×10^{-5} to 5.0×10^{-4} M with a limit of detection of 1.6×10^{-6} M was obtained. The selectivity of proposed method was proved by the absence of interference from other common coexisting species in beverage such as ascorbic acid, fructose, and sucrose. The proposed method was utilized for determination of sulphite in various beverage samples.

Chandran et al.[121] studied the electrochemical behavior of amaranth at multiwalled carbon nanotube (MWCNT) modified gold electrode. In 0.1 M acetate buffer solution (pH 5.0), a well-defined peak at 0.792 V was

observed for the oxidation of amaranth. The electrochemical behavior of amaranth was found to be diffusion controlled. The experimental parameters such as supporting electrolyte, pH of the solution and amount of MWCNT–Nafion suspension were optimized. The oxidation current of amaranth varies linearly with concentration in the range of 1.0×10^{-5} - 1.0×10^{-6} M with a limit of detection at 6.8×10^{-8} M. The sensor was successfully employed for the determination of amaranth in soft drink samples.

Carbon nanotube and poly (pyrrole) composites modified electrode was developed by Zhao et al.[122] for the simultaneous determination of amaranth and Ponceau 4R. The decoration of poly (pyrole) on CNTs has increased the dispersibility and effective surface area of the proposed electrode. The proposed sensor exhibited linear response ranges for amaranth and ponceau 4R from 5.0×10^{-9} M– 5.0×10^{-7} M and 8×10^{-9} –1.0×10^{-6} M and corresponding detection limits were 5.0×10^{-10} M and 1.0×10^{-9} M, respectively. The potential application of proposed sensor was evaluated by the determination of ponceau 4R and amaranth in fruit drink samples.

A highly sensitive alumina microfibers modified carbon paste electrode based electrochemical sensor for the determination of ponceau 4R and tartrazine was developed by Wu et al.[123]. The oxidation of ponceau 4R and tartrazine was observed at 0.67 and 1.01 V. The oxidation process of ponceau 4R and tartrazine at the modified electrode involves one electron and one proton. The detection limits for ponceau 4R and tartrazine were 8.0×10^{-8} M and 2.0×10^{-9} M respectively. The sensor was also applied for the quantification of ponceau 4R and tartrazine in soft drinks.

Mo et al.[124] reported the electrodeposition of nitrogen-doped graphene/ carbon nanotubes (NGR–NCNTs) nanocomposite on a glassy carbon electrode (GCE) for the electrochemical determination of caffeine and vanillin in food products. Microscopic techniques such as scanning electron microscopy (SEM) and transmission electron microscopy (TEM) were used for the characterization of modified electrode. The electrochemical performance of NGR–NCNTs modified GCE towards caffeine (CAF) and vanillin (VAN) was demonstrated by cyclic voltammetry (CV) and square wave voltammetry (SWV). Under optimized conditions, the developed sensor was linear in the range of 6.0×10^{-8} –5.0×10^{-7} M for CAF and 1.0×10^{-8} –1.0×10^{-7} M for VAN respectively.

A Pt: Co nanoalloy modified carbon ionic liquid paste electrode (Pt:Co/IL/CPE) utilizing n-hexyl-3-methylimidazolium hexafluorophosphate as a binder was developed for the study of electrochemical behavior of vitamin B9[125]. Compared with unmodified carbon paste electrode, a decrease in overpotential for the oxidation of vitamin B9 was about 110mV with 2.6-fold increment in the oxidation peak current when using Pt:Co/IL/CPE. The mechanism involved in the electro-oxidation of vitamin B9 on the surface of the modified electrode was studied. Pt: Co/IL/CPE was successfully applied for the determination of vitamin B9 in fortified food and mint vegetable samples.

Thomas et al.[126] reported the development of a sensitive voltammetric method for the determination of tert-butyl hydroquinone (TBHQ) using multiwalled carbon nanotube modified gold electrode (MWCNT/GE). The electro oxidation of TBHQ on the modified electrode was found to be

perfectly reversible with the involvement of two electrons and two protons. A linear relation between anodic peak currents and concentrations of TBHQ was observed in the range 4.0×10^{-6} - 1.0×10^{-4} M. The practical utility of developed sensor was tested by applying the developed sensor for the determination of TBHQ in commercially available coconut oil.

An electrochemical sensor combining the advantages of two nanostructured materials, AuNPs and MWNTs, was developed for the determination of synthetic food color, sunset yellow (SY)[127]. A pair of well - defined quasi-reversible peak with the formal potential ($E^0 = -108$ mV) was observed in phosphate buffer solution (PBS). The kinetic and thermodynamic parameters of the redox reaction such as standard heterogeneous rate constant ($ks = 7.944 \times 10^{-1}\ s^{-1}$), electron transfer coefficient ($\alpha = 0.487$) and free energy of activation (G) were calculated. Under optimum conditions, the nanocomposite film modified electrode showed a linear response in the range from 1.0×10^{-6} - 1.0×10^{-5} M, with a limit of detection 4.0×10^{-8} M. Analytical application of the developed sensor for quantitative determination of SY in commercially available soft drink samples were discussed.

A differential pulse voltammetric method for the determination of the propyl gallate (PG) was reported by Vikraman et al.[128]. The sensor was based on the oxidation of PG at multiwalled carbon nanotube (MWNT)-modified gold electrode (GE). The observed anodic peak of PG may be due to the two electron oxidation of hydroxyl group. The experiment conditions such as the amount of MWNT, effect of various supporting electrolyte, and the influence of the pH of the supporting electrolyte were optimized. Under optimized conditions, the developed sensor showed a linear response range

from 1.0×10^{-4} - 1.0×10^{-5} M. The amount of PG in vegetable oils was determined using the developed sensor.

The electrochemical oxidation and determination of amaranth using a carbon nanotube modified glassy carbon electrode (MWNT/GCE) was reported by Wu et al[129]. Compared to unmodified GCE, at MWNT/GCE, an irreversible well-defined oxidation peak was observed. The observed enhancement can be attributed to the electrocatalytic property of MWNT. Under optimized conditions, the oxidation peak current of amaranth at MWNT/GCE was linear to its concentration over the range from 4.0×10^{-8} to 8.0×10^{-7} M. The performance of this method was tested by applying it for the determination of amaranth in various soft drinks.

A new and sensitive electrochemical sensor based on hexadecyltrimethylammonium bromide (CTAB) functionalized graphene supported platinum nanoparticles (CTAB-Gr-Pt) composite was fabricated for the determination of sunset yellow[130]. The improved oxidation activity of sunset yellow at (CTAB-Gr-Pt) modified electrode may be due to the synergistic effect of the large surface area and electrocatalytic activity of both Gr and Pt NPs. The electrochemical behavior of sunset yellow was investigated using cyclic voltammetry (CV) and differential pulse voltammetry (DPV). Under the optimized experimental conditions, the oxidation peak current of sunset yellow was linear in the range of 8.0×10^{-8} – 1.0×10^{-5} M and the limit of detection was 4.2×10^{-9} M. The developed was successfully applied to determine sunset yellow in soft drinks with satisfactory recoveries.

An electrochemical sensor based on the multi-wall carbon nanotube (MWNT) thin film-modified GC electrode was developed for sensitive determination of Sudan I^{131}. Even though the oxidation potential at modified electrode is same as that at bare GCE, an enhancement in the oxidation peak current of Sudan I at the MWNT film-modified GCE was observed. The enhancement in peak current can be attributed to the subtle electronic properties and catalytic ability of MWNT. The developed sensor exhibited a linear response over the range of 4.0×10^{-8}– 4.0×10^{-6} M. Limit of detection obtained was 2.0×10^{-8} M. The practical utility of the developed sensor was established by employing the present sensor for the determination of Sudan I in hot chili samples.

Lin et al.[132] reported the development of gold nanoparticles (AuNPs) modified glassy carbon electrode for simultaneous determination of butylated hydroxyanisole (BHA), butylated hydroxytoluene (BHT) and butylated hydroquinone (TBHQ). The redox reactions of BHA, BHT and TBHQ were electrocatalytically enhanced at AuNP/GCE. Also, the redox reactions at the surface of AuNPs/GCE were found to be diffusion controlled. Peak current versus concentration of BHA, BHT and TBHQ were linear in the range of 1.0×10^{-7} – 1.5×10^{-6} M, 2.0×10^{-7} - 2.2×10^{-6} M and 2.0×10^{-7} – 2.8×10^{-6} M respectively. The developed sensor was successfully applied for the determination of the three analytes in edible oil samples.

Porphyrins and metalloporphyrin are used to modify electrode surfaces due to its ability to electrocatalyse the electron-transfer reactions. Modification of electrodes with these macrocyclic compounds has found to increase the sensitivity and selectivity of the electrode[133-135].

A glassy carbon electrode was modified with an alternated layers of iron (III) tetra-(*N*-methyl-4-pyridyl)-porphyrin (FeT4MPyP) and cobalt(II) tetrasulfonatedphthalocyanine (CoTSPc)[136]. Since the modified electrode showed an excellent catalytic activity and stability towards the oxidation of nitrite, it was used for the voltammetric determination of nitrite. The linear response was in the range of $2.0 \times 10^{-7} – 8.6 \times 10\text{-}^{6}$ M and limit of detection obtained was 4.0×10^{-8} M. The developed sensor was applied for the determination of nitrite in water samples.

Wu[137] reported the development of an electrochemical sensor by modifying a glassy carbon electrode with iron-porphyrin (5,10,15,20-tetraphenyl-21H, 23H-porphine iron(III) chloride) and carbon nanotubes for the determination of Sudan 1. The electrocatalytic ability of iron (III)-porphyrin and the unique physiochemical properties of carbon nanotubes was responsible for the excellent electrochemical reduction of Sudan 1. Under optimum conditions, the linear relationship of Sudan I was from $5.03 \times 10^{-8} – 2.0 \times 10^{-6}$ M and limit of detection was 1×10^{-8} M. The modified electrode was used for the determination of Sudan 1 in real samples such as hot chili powder, hot chili juice and ketchup samples.

The electrodes modified with poly(p-aminobenzenesulphonic acid) (poly(p-ABSA)) has reported to have excellent stability, more active sites, reproducibility,homogeneity in electrochemical deposition and can adhere strongly to the electrode[138]. Li et al.[139] reported the development of a poly(p-aminobenzenesulphonic acid)-based electrochemical sensor for sensitive determination of Sudan I. The large number of π–π bonds, electron-rich N atoms, and high electron density among sulphonic group in

poly(p-ABSA) film enables the strong adsorption of Sudan I on the surface of poly(p-ABSA) film, leading to an increased electrochemical signal. Under optimum conditions the concentration of Sudan I was linear in the range of $4.0 \times 10^{-9} – 2.0 \times 10^{-6}$ M and limit of detection was 1.2×10^{-9} M. The sensor was also employed for the determination of Sudan I in hot chili and ketchup samples.

Ye et al.[140] reported a poly (L-cysteine) modified glassy carbon electrode sensor for the determination of sunset yellow (SY) in Fanta. Cyclic voltammetry and electrochemical impedance spectroscopy was used for the characterization of electrode. The kinetic parameters of the redox reaction of SY were also studied. The developed sensor exhibited stability, good selectivity, low cost and simple fabrication. The peak current was linear with the concentration of SY from $8.0 \times 10^{-9} – 7.0 \times 10^{-7}$ M.

A highly sensitive and selective determination of nitrite at electropolymerized film of 5-amino-1, 3, 4-thiadiazole-2-thiol (p-ATT) on glassy carbon electrode (GCE) was reported by John et al[141]. The electrochemical oxidation of nitrite at 0.84 V at p-ATT modified electrode with an enhanced peak current may because of the attraction between the positively charged backbone of the p-ATT film and negatively charged nitrite ions. Compared to bare GCE a two times increase in the heterogeneous rate constant for the oxidation of nitrite at (p-ATT)/GCE indicates that the oxidation of nitrite was faster at (p-ATT)/GCE. The developed was successfully applied for by the determination of nitrite in water samples.

Single-walled carbon nanotubes (SWNTs) possess excellent catalytic properties. The aggregation of SWCNTs can be prevented by its interaction

between conducting polymers. A polypyrrole/single-walled carbon nanotubes composite modified glassy carbon electrode was developed for the determination of quinoline yellow[142]. Under the optimal conditions, the fabricated electrode exhibits excellent electrochemical activity toward the oxidation of quinoline yellow in the range of $8.0 \times 10^{-7} – 1.0 \times 10^{-5}$ M, and the detection limit was 8.0×10^{-8} M. The excellent stability and reproducibility of the developed sensor was attributed to particular properties of polypyrrole, single walled carbon nanotubes and synergic interaction between them. The practical application of the developed sensor was evaluated by applying the sensor for determination of quinoline yellow in soft drinks.

Pacheco et al.[143] reported the development of an electrochemical sensor for the determination of OchratoxinA (OTA) in food samples. The sensor was based on modifying glassy carbon electrode with multiwalled carbon nanotubes (MWCNTs) and an electropolymerized moleclarly imprinted polymer of pyrrole. The ability of pyrrole to form hydrogen bonds between the oxygen groups of OTA and the N–H group of polypyrrole was the basis of sensing mechanism. The increased conductivity and the surface area of the sensor were achieved by MWNTs. Under optimized conditions, the oxidation peak current of OTA was linearly proportional to the concentration in the range of 5.0×10^{-8} - 1.0×10^{-6} M. The developed sensor was applied for the determination of OTA in spiked beer and wine samples.

An electropolymerized molecularly imprinted polymer (MIP) of para-aminobenzoic acid (pABA) modified gassy carbon electrode sensor was developed for the determination of melamine in milk[144]. The mechanism of sensing is based on the fact that the benzene ring of pABA can provide

recognition sites through a "$\pi - \pi$ stacking" interaction with the aromatic structure of melamine. The MIP sensor was successfully applied to the determination of melamine in milk products and showed high selectivity, sensitivity, and reproducibility the experimental parameters were optimized and under optimized conditions, the concentration was linear in the range of 4.0×10^{-6} - 4.5×10^{-5} M.

A poly (diallyldimethylammonium chloride) functionalized reduced graphene oxide (PDDA-RGO) nanocomposite modified carbon paste electrode sensor was developed for the electrochemical determination of quinoline yellow (QY)[145]. SEM, FTIR and Raman spectroscopic techniques were used as evidence for the formation of PDDA-RGO nanocomposite. Under the optimal conditions, the peak current of proposed sensor was linear to the concentration of QY in the range of 1.0×10^{-8} – 1.0×10^{-5} M. The sensor also exhibited excellent repeatability and stability. The developed electrochemical sensor was also successfully applied for the determination of QY in soft drink.

The modification of electrodes with ionic liquids (ILs) has received great attention due to its ability to increase electron transfer rate. ILs was reported to have good chemical and thermal stability, negligible vapor pressure, high ionic conductivity and wide electrochemical windows[146-148].

Elyasiet al.[149] reported the development of a Pt/CNTs nanocomposite ionic liquid modified carbon paste electrode (Pt/CNTs/ILCPE) for the determination of Sudan 1. The increased oxidation peak current and the decreased oxidation peak potential at modified electrode was a clear

evidence for the catalytic activity of Pt/CNTs/IL towards the oxidation of Sudan I. The kinetic parameters were calculated. The developed sensor exhibited excellent electrochemical response, high sensitivity, long term stability and a lower detection limit.

Fluorescence sensing has fascinated extensive interest in field of research as it is simple, sensitive and rapid. It has found profound application in environment monitoring, clinical diagnostics and food quality control. A detailed literature review focus on the utilization of fluorescent probes for the quantitative determination of drugs and metal ions.

A simple, rapid and specific method for spironolactone determination based on the quenching of the fluorescence of CdSe quantum dots (QDs) by spironolactone was developed by Yang et al[150]. The developed sensor exhibited a linear response in the range of 6.0×10^{-6} -1.7×10^{-3} M with 4.8×10^{-7} M limit of detection. The developed sensor was satisfactorily applied for the determination of spironolactone in pharmaceutical tablets and the results agreed with the claimed values. The possible mechanism for the reaction was also discussed.

The development of an efficient fluorescent sensor based on the quenching of the fluorescence intensity of functionalized CdS quantum dots by sulfadiazine was reported[151]. Water soluble thioglycollic acid (TGA) modified CdS QDs synthesized by microwave assisted method was used as the fluorescent probe. Upon addition of sulfadiazine to CdS QDs quenching of fluorescence emission at 489 nm due to the electrostatic interaction of surface of CdS QDs in aqueous medium occurred. Under optimum condition, the fluorescence intensity versus sulfadiazine concentration gave

a linear response in the range of 1.2×10^{-5} - 2.1×10^{-3} M. The concentration of sulphadiazine as low as 1.3×10^{-6} M can be detected using the developed sensor. The developed method was employed for the determination of sulfadiazine in injections.

An enhancement in the fluorescence intensity of thioacetamide functionalized CdS QDs on treatment with ciprofloxacin was observed and it was used as an assay method for the determination of ciprofloxacin[152]. At pH 7.4, the developed showed a linear response in the range of 2.6×10^{-6} – 3.6×10^{-4} M with the detection limit of 2.31×10^{-8} M. This method made the quantitative determination of ciprofloxacin in human serum samples without separation of foreign substances possible.

Liang et al.[153] developed a fluorescent sensor for the determination of drug, methimazole. The method was based on the quenching of fluorescence emission from CdSe quantum dots by methimazole. All the experimental parameters were optimized and it was found that under optimum conditions, the concentration of methimazole was linear in the range of 5.0×10^{-8} M - 5×10^{-6} M with a detection limit of 3.0×10^{-8} M. CdSe QDs based fluorescent probe was applied to determine methimazole in pharmaceutical tablets. Quenching of fluorescence intensity of CdSe quantum dots by methimazole can be attributed to exchange of surface capping organic molecules of quantum dots induced by methimazole.

A metalloporphyrin-based fluorescence sensor for levamisol (LEV) was reported by Gong et al[154]. Metal complex of glycosylated 5, 10, 15, 20-tetrakis[2-(2, 3, 4, 6-tetraacetyl--D-glucopyranosyl)-1-O-phenyl] porphyrin in chitosan matrices was used as the fluorophore. The increase in the

fluorescence intensity of metalloporphyrin modified optode membrane in presence of LEV was due to the complexation with the central metal moiety of metalloporphyrin. The calibration graph obtained with the proposed sensor was linear over the range of 1.3×10^{-5}- 3.5×10^{-7} M. The developed sensor was also applied for the determination of LEV in pharmaceutical preparations.

Based on the quenching of the fluorescence of CdTe QDs by pazufloxacin, a rapid and specific method for determination of pazufloxacin was reported[155]. Fluorescence intensity of thioglycolic acid (TGA) capped QDs were quenched linearly by pazufloxacin in a range of 2.7×10^{-9} to 8.5×10^{-5} M. The proposed method was used for the determination of pazufloxacin in freeze-dried powder injection and sodium chloride injection and the results obtained were in good agreement with the reported values.

Semiconductor quantum dots and carbon nitride dots have many unique properties that offer significant advantages as fluorescent probes in ion sensing. The interaction of metal ions with these nanoparticles can either lead to quenching or enhancement of fluorescence intensity. The use of luminescent QDs as ion selective probes was first demonstrated by Chen and Rosenzweig[156]. Water-soluble luminescent CdS quantum dots (QDs) capped by l-cysteine, and thioglycerol have a profound effect on the luminesence response of CdS QDs in presence of metal ions. Fluorescence intensity of thioglycerol-capped CdS QDs was quenched in presence of copper ions whereas zinc ions showed an enhancement in the florescence intensity of l-cysteine-capped CdS QDs. The sensor was successfully applied for the determination of copper with a limit of detection of 1.0×10^{-10} M and zinc ions as low as 8.0×10^{-10} M.

CdSe/ZnS nanocrystals modified with bovine serum albumin was used for the detection of copper[157]. Even though the fluorescent probe was sensitive to Cu^{2+} and Fe^{3+} ions, the interference of Fe^{3+} was eliminated by removing itas a complex (FeF_6^{3-}) by the addition of F^- ions. The fluorescence intensity of fluorophore was quenched linearly with the concentration of Cu^{2+} ions. The quenching is due to the displacement of Cd^{2+} ions and the formation of CuSe on the surface of QDs. The developed sensor was able to determine concentration of Cu^{2+} ions as low as 1.0×10^{-8} M.

Li et al.[158] developed a cysteamine (CA)-capped CdTe quantum dots (QDs) (CA–CdTe QDs) for the determination of Hg^{2+} ions. Under optimum conditions, the fluorescence quenching of CA–CdTe QDs was linear in the concentration range of 6.0×10^{-9}–4.5×10^{-7} M. The detection limit using the developed sensor was 4.0×10^{-9} M. Upto 10- fold excess of Pb^{2+}, Cu^{2+} and Ag^+ does not interfere on the determination of Hg^2. The strong affinity of mercury for nitrogen atoms can result in the effective transfer of electrons from the amide groups of cysteamine to the Hg^{2+} ion and this may be the reason for the observed fluorescence quenching. The applicability of the proposed method for the determination of Hg^{2+} was investigated by the analysis of lake water samples using proposed sensor.

The decrease in the fluorescence intensity of N-acetyl-L-cysteine-capped CdTe quantum dots (QDs) by Hg^{2+}ions was the basis of fluorescent sensor developed by Zhao et al.[159]. The selectivity of the system was established by studying the effect of Li^+, Na^+, K^+, Ca^{2+}, Mg^{2+}, Zn^{2+}, Cd^{2+}, Pd^{2+}, Fe^{3+}, Pb^{2+}, and Cu^{2+}ions on the fluorescence intensity of NAC-capped CdTe QDs and the study revealed that only Hg^{2+} ions quench the fluorescence

intensity. The quenching of fluorescence intensity of NAC-capped CdTe QDs by Hg^{2+} ions was linear in the range from 2.0×10^{-8} - 4.3×10^{-6} M.

An effective and simple quantification method for the determination of iron in biodiesel using water-soluble mercaptopropionic acid (MPA)-capped CdTe quantum dots (QDs) was reported by Santos et al[160]. The mechanism of quenching was based on the iron binding on the surface of QDs inducing recombination centers for electrons and holes, resulting in the decrease of fluorescence intensity of QDs. Under the optimized experimental conditions, the reported method showed a linear working from 7.5×10^{-8} -1.8×10^{-6} M. The determined limit of detection (LOD) was about 2.2×10^{-8} M.

Narayanaswamy et al.[161] developed a mercaptoacetic acid (MAA) capped CdS QDs as a fluorescent sensor for the determination of Hg^{2+} ions. The sensor is based on the fluorescence quenching of MAA/CdS QDs by Hg^{2+} ions. The strong interaction of functional group present in capping agent and Hg^{2+} ions led to the fluorescence quenching process. Under the optimum conditions, the fluorescence intensity of CdS QDs was linear to the concentration of mercury ion in the range 5.0×10^{-9} - 4.0×10^{-7} M with a detection limit of 4.2×10^{-9} M. The selectivity of proposed method was evaluated by examining the effect of different cations on the fluorescence intensity of MAA capped CdS QDs and the results indicate that these ions did not interfere in the analysis.

Zhu et al.[162] reported the development of an L-cysteine modified CdS quantum dots (QDs) for the determination of Ag^{+} ions. The working of sensor was based on the fluorescence enhancement of CdS QDs at 545 nm by silver

ions. Under optimum conditions, the fluorescence intensity of CdS QDs is linearly proportional to silver concentration from 2.0×10^{-8} - 1.0×10^{-6} M with a detection limit of 5.0×10^{-9} M. Possible fluorescence enhancement mechanism was also studied.

Wanget al.[163] described the synthesis of water soluble L-cysteine-coated CdSe/CdS core-shell QDs. The synthesized QDs have an excellent quantum yield and stability. The sensitivity of L-cysteine-coated QDs towards Cu^{2+} ions in presence of other physiologically important cations, such as Ca^{2+}, Mg^{2+}, Zn^{2+}, Al^{3+}, Fe^{3+}, Mn^{2+} and Ni^{2+} etc. led to the development of a L-cysteine-coated QDs based fluorescent sensor for Cu^{2+} ions. The application of proposed method for the determination of Cu^{2+} ions in vegetable samples with good recoveries proved the practical utility of proposed method.

Water-soluble cadmium telluride quantum dots capped with mercaptosuccinic acid (MSA-CdTe QDs) were prepared for the selective and sensitive fluorescence probing of silver (I) ion[164]. The fluorescence intensity of the MSA-CdTe QDs was quenched linearly only in the presence of Ag^{+} ions. The common interfering metal ions did not affect the fluorescence intensity of MSA-CdTe QDs. The concentration of Ag^{+} was linear over the range of 4.0×10^{-7} - 8.0×10^{-6} M. The proposed method was applied for the determination of Ag^{+} in two fixer samples. The results obtained with the proposed method were compared with the standard AAS method.

Chen et al.[165] developed a highly blue fluorescent carbon nanodots (CNDs) based ratiometric fluorescence sensor for Al^{3+} ions. Quercetin (QCT) and its fluorescent metal-ion complex (QCT-Al^{3+}) efficiently coordinated on the surface of CNDs. The mechanism of sensing was

explained on the basis of fluorescence resonance energy transfer (FRET) with CNDs as donor and QCT-Al^{3+} as acceptor. The detection limit for determination of Al^{3+} was 5.6×10^{-7} M.

The fluorescence efficiency of QDs depends on the presence and nature of capping agents at the surface of QDs[166]. The molecular recognition properties of host molecules such as calixarenes, crown ethers and porphyrins decorated on the surface of QDs and the unique optical properties of QDs have paved way for the development of fluorescent sensors for metal ion sensing. Frasco and Chaniotakis[167]were the first to report that QD surface passivated with calixcrown moiety can be employed for ion sensing. Luminescent and stable CdSe/ZnS core/shell quantum dots (QDs) capped with sulfur calixarene was synthesized and they were applied for the selective determination of mercury ions in acetonitrile with high sensitivity[168]. The fluorescence intensity of S-calix capped QDs was quenched by mercury ions and was described by Stern – Volmer relation. The limit of detection was 15×10^{-9}M.

A 15-crown-5 functionalized CdSe/ZnS quantum dots (QDs) was synthesized and were exploited for the sensing of K^+ ions in aqueous medium[169]. The recognition was supposed to be achieved by sandwich type of complexation between the 15-crown-5/K^+ /15- crown-5.

Thiacalix[4]arene carboxylic acid (TCC) modified CdSe/ZnS QDs were reported as fluorescent probes for Cu^{2+} ion[170]. The surface modification of trioctylphosphine oxide (TOPO) capped CdSe/ZnS QDs with TCC has improved its solubility in water. Fluorescence of the TCC-coated QDs was selectively quenched by Cu^{2+} ions in the presence of other transition metal

ions such as Cd^{2+}, Zn^{2+}, Co^{2+}, Fe^{2+} and Fe^{3+} ions. The Stern-Volmer plot for the fluorescence quenching by Cu^{2+} ions showed a linear relationship upto 3.0×10^{-5} M of Cu^{2+} ions. The fluorescence quenching was selective to Cu^{2+} ions in presence of other biologically important ions such as Na^{+}, K^{+}, Mg^{2+} and Ca^{2+} indicating the practical utility of TCC-coated QDs as a fluorescent probe for the determination Cu^{2+} ion in biological samples.

The use of 1,10-diaza-18-crown-6 modified CdS:Mn/ZnS QDs for the detection of Cd^{2+} was reported[171]. 1,10-diaza-18-crown-6 was attached on QDs by zero-length covalent coupling. The detection is based on an electron transfer process between the QDs and the ligand, and subsequent complex formation between $Cd^{2+}$and 1,10-diaza-18-crown-6. The sensor relies on the enhancement of fluorescence intensity in presence of Cd^{2+}. The sensor was found to be selective to Cd^{2+} ions in presence of other environmentally relevant metal ions.

Chaniotakiset al.[172] reported the development of a highly fluorescent and selective nanosensor for the detection of zinc ion in organic medium. The sensor was based on the fluorescence enhancement of 5,10,15,20-tetra(4-pyridyl)porphyrin [$H_2P(pPyr)_4$] decorated CdSe QDs by Zn^{2+} ions. The response of sensor to Zn^{2+} ions was linear in the range of 5.0×10^{-7} - 5.0×10^{-5} M with a limit of detection 5.0×10^{-7}M. The sensing of Zn^{2+} ions may be due to the coordination of $Zn^{2+}$with the nitrogen atom in the pyridyl-substituted porphyrins.

The use fluorescence sensing system for the determination of food colorant was reported by Zhou et al.[173]. The sensor was based on the quenching of fluorescence intensity of oleic acid-functionalized Mn-ZnS

quantum dots (QDs) by Sudan dyes. The quenching was due to the inner filter effect. The sensor could detect Sudan I, II, III, and IV as low as 2.4×10^{-8} M, 3.2×10^{-8} M, 2.1×10^{-9} M and 3.2×10^{-9} M respectively. The method was applied for the determination of Sudan dyes in hot chili sauce, sausage and tomato sauce.

1.11 Scope of the present investigation

Chemical sensors have found applications in food quality control, clinical analysis, pharmaceutical analysis and metal ion sensing. The present study aims at the development of electrochemical and optical sensors for the quantitative determination of food additives, drugs and metal ions. The thesis aims at the development of electrochemical sensor for food additives such as nitrite, Sudan 1 and butylated hydroxyanisole. The effect of various parameters such as supporting electrolyte, pH and scan rate was studied. The analytical figures of merit and interference study for each sensor were established. The developed sensors were applied for the determination of food additives in different food samples.

Also, fluorescence based optical sensors was developed for the determination of drug (nimesulide), food additive (butylated hydroxyanisole) and metal ion (Fe^{3+}). Fluorophores used for sensor fabrication were synthesized and characterized. The experimental parameters for the development of sensors were studied. The developed fluorescence sensors were applied for real sample analysis.

It is hoped that the developed electrochemical and fluorescent sensors may be used for real applications after a thorough study for application aspects.

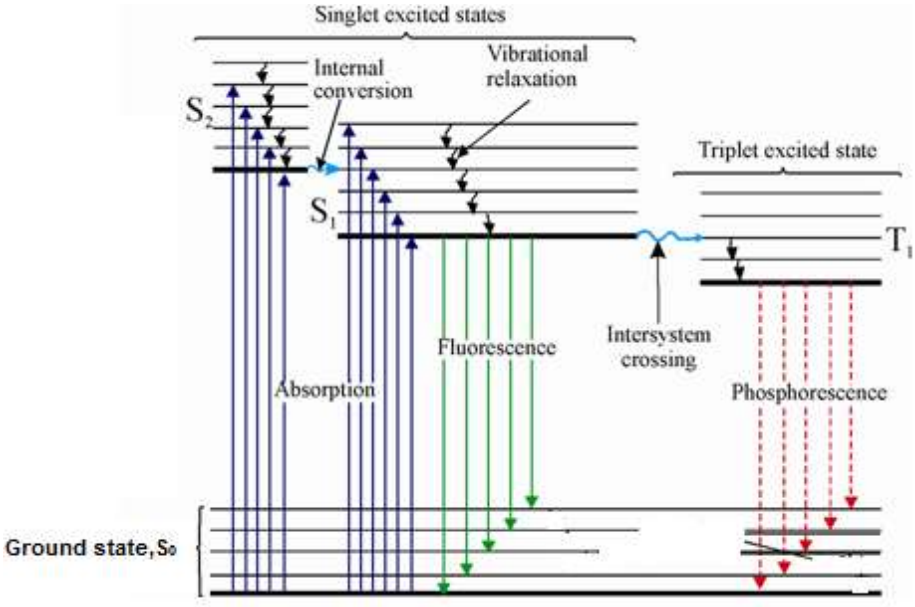

Figure 1.1 Jablonski diagram

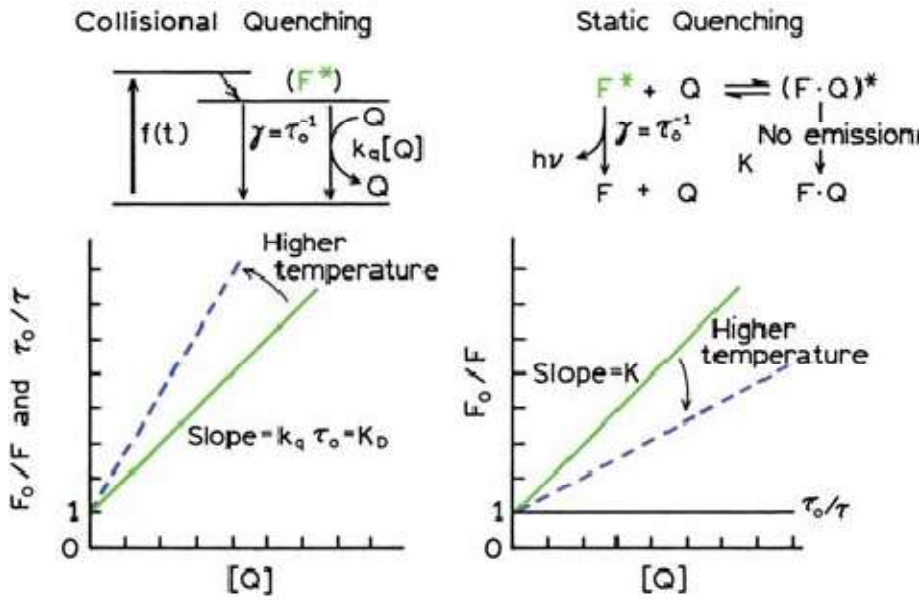

Figure 1.2 Comparison of dynamic and static quenching

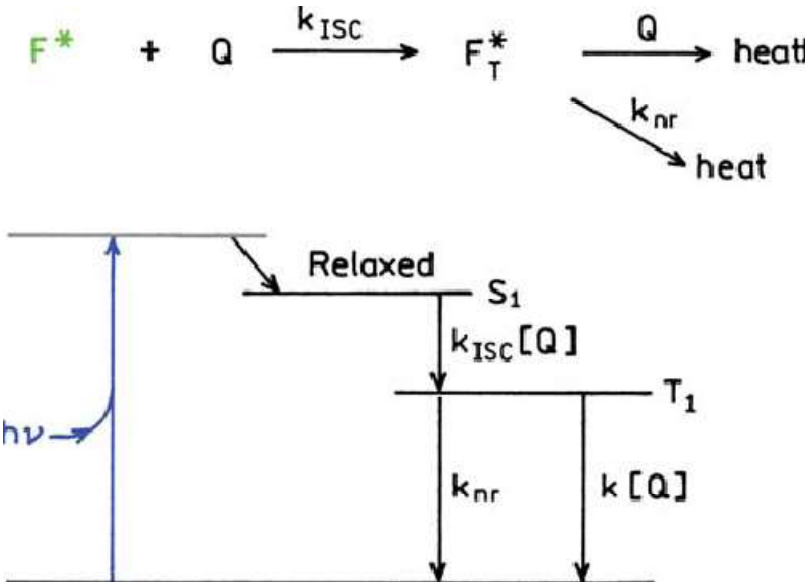

Figure 1.3 Quenching by intersystem crossing

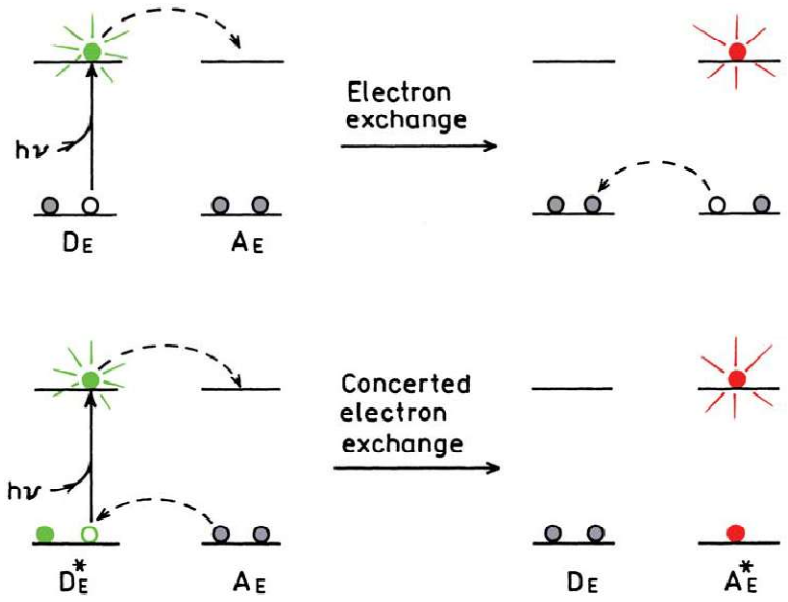

Figure 1.4 Scheme for electron exchange

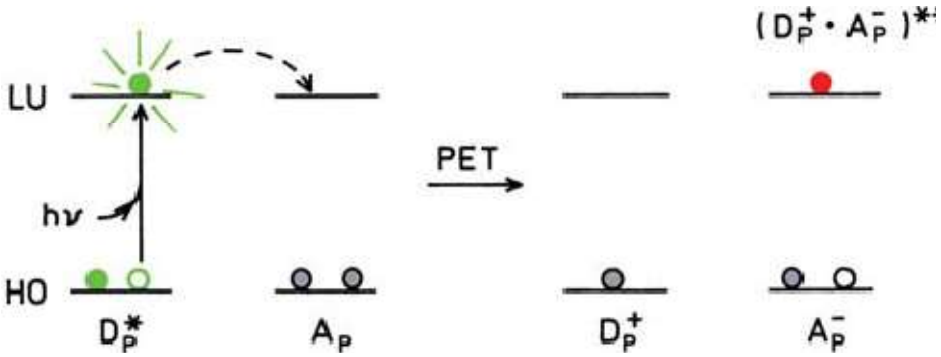

Figure 1.5 Schematic diagram for photoinduced electron transfer

Chapter 2

MATERIALS AND METHODS

Contents

This chapter gives a brief description about the reagents and instruments involved in the development of both voltammetric and fluorescent sensors. The cleaning of various electrodes and procedure for the preparation of buffer solution is also included in this chapter.

2.1 Reagents

All reagents and solvents used for the investigations were of analytical grade and Millipore water was used throughout the studies. All chemicals were used as received. Nafion, alumina and L-cysteine were purchased from Sigma Aldrich Corporation, USA. Chloroauric acid was purchased from SRL Chemicals, India. Ethanol, sodium dihydrogen orthophosphate, disodium hydrogen orthophosphate and sodium acetate trihydrate were purchased from Merck, Germany. Sodium nitrite, butylatedhydroxyanisole (BHA), Sudan 1, trioctylphosphine, trioctylphosphine oxide, hexadecylamine, dimethylformamide, selenium powder and zinc acetate (Zn $(CH_3CO_2)_2$) were purchased from SD Fine chemicals (Mumbai, India).

Pure drugs such as nimesulide (NIM), mefenamic acid (MEF), ibuprofen (IBU), rofecoxib (ROF), diclofenac sodium (DIC), sulfamethoxazole (SMZ) and tinidazole (TNZ) were obtained as gift samples.

2.2 Instruments Used

Electrochemical measurements were performed on a BASi Epsilon Electrochemical analyzer (Bioanalytical system, USA) and a CH Instruments (Austin, TX) with a conventional three-electrode system. Chemically modified glassy carbon electrodes/gold electrodes served as the working electrode and a platinum wire was used as auxiliary electrode. All potentials in the electrochemical studies were referenced to Ag/AgCl reference electrode and all experiments were performed at room temperature. Scanning Electron Microscopic (SEM) images were obtained on a JEOL 6390LV. The pH measurements were carried out in a Metrohm pH meter. Ultrasonic cleaning

of the electrode was carried out in an Ultrasonicator (Oscar Ultrasonics, Pvt. Ltd. Mumbai). UV-Visible spectrum was recorded using Spectro UV-Visible Double Beam UVD-3500 instrument, using quartz cuvettes of 1.0 cm optical path length.

Fluorescence measurements were recorded using a JAZ- EL-200-X. Diode lasers of appropriate wavelength were used as excitation source. Transmission electron microscopy (TEM) was performed with a Hitachi H600, operating at an accelerating voltage of 80kV. For TEM analysis, purified QDs in dry form was redispersed in chloroform and deposited on the surface of the copper grid with a sprayer.

2.3 Cleaning of Gold Electrode (GE)

The working GE was mechanically polished with aqueous slurries of alumina (50 nm) on a flat pad prior to surface modification. After polishing, it was rinsed ultrasonically with absolute ethanol to remove residual alumina particles from the surface and then cleaned with a piranha solution (H_2O_2:H_2SO_4 = 1:3, v/v) for 10 minutes. Further the electrode was sonicated successively in ethanol and water for 3 minutes each. Following the mechanical cleaning, an electrochemical cleaning process was carried out using cyclic voltammetry, performed from 0 to 1.5 V in 0.5 M H_2SO_4 solution at a scan rate of 0.1 Vs^{-1} until a stable cyclic voltammogram was obtained.

2.4 Cleaning of Glassy Carbon Electrode (GCE)

Prior to modification, the GCE was mechanically polished with alumina slurry down to 0.05µm on a polishing cloth. The electrode was then rinsed with millipore water thoroughly. The electrode was sonicated in

methanol, water, aqueous HNO_3 (1:1 v/v) and acetone respectively in order to remove any adsorbed substances on the electrode surface.

2.5 Preparation of supporting electrolyte

The supporting electrolytes used for the present voltammetric studies are phosphate buffer solution and citrate buffer solution. Phosphate buffer solutions of different pH are prepared by mixing NaH_2PO_4 and Na_2HPO_4 in double distilled water. The amount of NaH_2PO_4 and Na_2HPO_4 required for different pH are given in Table 2.1. Citrate buffer solutions are prepared by mixing different ratios of sodium citrate and citric acid in double distilled water. The exact amount of sodium citrate and citric acid needed for the preparation of citrate buffer with different pH are given in Table 2.2.

Table 2.1 Preparation of 0.1M phosphate buffer solution

pH	NaH_2PO_4 (g/L)	Na_2HPO_4 (g/L)
2	13.799	0.002
3	13.790	0.003
4	13.780	0.036
5	13.615	0.360
6	12.143	3.218
7	5.836	15.466
8	0.940	24.97
9	0.100	26.605
10	0.010	26.781

Table 2.2 Preparation of 0.1M citrate buffer solution

pH	Sodium citrate (g/L)	Citric acid (g/L)
2	0.65	20.54
3	4.26	17.93
4	4.27	13.11
5	18.64	7.69
6	25.70	2.65
7	28.8	0.37
8	29.35	0.039
9	29.40	0.004

.....ൠ.....

Chapter 3

VOLTAMMETRIC SENSOR FOR NITRITE

Contents

This chapter presents the development of a simple and sensitive voltammetric method to determine nitrite by using gold electrode modified with [5,10, 15,20-tetrakis (4-methoxyphenyl) porphyrinato] manganese (III)chloride (TMOPPMn(III)Cl). An excellent catalytic activity and stability for nitrite oxidation was exhibited by the sensor. The effect of various experimental parameters on voltammetric response of nitrite was studied. Under optimized conditions nitrite concentration as low as 2.9×10^{-9} M can be determined. Effect of common foreign ions has been examined in simulated mixtures and the sensor was found to be tolerant against these ions. The proposed sensor was used for the determination of nitrite in various food samples such as chicken ham, sausage and pickled vegetables and the results were found to be consistent with the values obtained by standard Griess protocol.

3.1 Introduction

Nitrite ion (NO_2^-) is one of the active intermediate species in the nitrogen cycle and a useful indicator of equilibrium state of the oxidative and reductive pathways of the nitrogen cycle. It is a simple oxy-anion of nitrogen with a pKa of 3.2 at 20°C[174]. Nitrites are both of environmental and biological importance. Nitrite is ubiquitous within environment, physiological systems, and commonly used in some food as preservatives[175-176]. Nitrite is used in meat curing due to three functions; (a) antimicrobial action (as preservative), (b) gives characteristic flavour of cured meat and (c)gives characteristic pink colour to cured meat due to the formation of nitrosomyoglobin. Moreover, nitrite can be formed in the production of pickled vegetables because of the biodegradation of nitrate or other nitrogenous substances[177]. Nitrite is found to be effective in preventing growth of Clostridium botulinum which produces the botulinum toxin.

The health hazards caused by the build-up of high nitrite concentrations in food samples, considering their use as preservatives, are subjects under investigations[178]. Once NO_2^- is taken by the human body, it combines with blood pigments to produce methaemoglobinaemia (Blue baby syndrome), in which oxygen is no longer available to the tissues. In addition, nitrite can also react with amines and amides in stomach to produce carcinogenic N-nitrosamines[179-180]. Therefore, the quantitative determination of nitrite concentrations is of great importance, especially for food quality control.

Various analytical methods have been used to determine nitrite ions, such as[181-183], gas chromatography[184-185], ion chromatography[186] and chemiluminescence[187]. However, these methods proved to have limitations

with respect to specificity, sensitivity, simplicity and analysis time. Even with the Griess assay[181], the widely used classical method for the determination of nitrite is highly sensitive and specific; it is often associated with drawbacks such as longer coupling time, use of carcinogenic reagents and large sample volumes.

Electrochemical techniques provide useful alternatives as they follow simple, cheap and safe analyses. In general, the main electrochemical methods involve the reduction and oxidation of nitrite on the electrode[188-191]. However, the electrochemical methods based on the reduction of nitrite suffer from poor sensitivity and interference of some co-existent species[192], while its oxidation, is a straight forward reaction. The oxidation of nitrite occurs at higher over potential on bare electrodes and also it can result in poor sensitivity and reproducibility through cumulative electrode passivation effects. A good way to overcome these drawbacks is modification of the electrodes with redox mediators that facilitate electron transfer processes. It is well documented that functionalization of an electrode surface can offer significant analytical advantage in voltammetric experiments.

The modification of electrodes with deposition of various functional compounds has attracted much interest due to its potential application[193-194]. The porphyrins, a class of naturally occurring macrocyclic compounds, play a very important role in the metabolism of living organisms. The porphyrin molecule contains four pyrrole rings linked via methine bridges. The excellent thermal, chemical, electrochemical and photochemical stability of metalloporphyrins make them suitable candidates for the modification of electrodes [195-196]. The strong complexing properties and

catalytic behaviour of metalloporphyrins, are responsible for their numerous applications in chemical analysis[197-198]. The various factors contributing to the sensing properties of these compounds are the coordinated metal, peripheral substituents and the conformations of the macrocyclic skeleton. The catalytic property of transition metal ion porphyrins is due to the presence of unpaired d electrons and unfilled d orbitals which are available to form bonds with the adsorbate in axial position[199].

The present chapter describes the development of a gold sensor based on manganese (III) complex of a porphyrin for the determination of nitrite in food samples. A [5,10,15,20-tetrakis (4-methoxyphenyl) porphyrinato] manganese (III) chloride (Fig 3.1), (TMOPPMn(III)Cl) modified gold electrode sensor was fabricated dropping adequate amount of metalloporphyrin solution on a cleaned gold electrode.

The analytical parameters involved in the development of sensor were optimized and the proposed sensor was applied for the determination of nitrite in various food samples. The reliability of proposed method was established by comparing the results with the standard spectrophotometric work.

3.2 Experimental

3.2.1 Fabrication of TMOPPMn(III)Cl modified gold electrode

As a first step to modification of electrode, the mechanical and electrochemical cleaning of gold electrode was carried out as in section 2.3. The cleaned gold electrode was modified by dropping 3 µl of 2.5 mg mL^{-1} (0.5% w/v) of TMOPPMn(III)Cl solution onto the clean electrode surface

and evaporating the solvent at room temperature. TMOPPMn(III)Cl solution was prepared by dissolving 2.5 mg of TMOPPMn(III)Cl in a mixture of 0.3 μl nafion and 0.2 μl of ethanol.

3.2.2 Standard stock solutions

Working standard solutions of nitrite were obtained by dilution of the standard stock solution of nitrite. The stock solution of nitrite (1×10^{-1} M) was prepared by dissolving 0.068 g of sodium nitrite in 10.0 mL of double distilled water.

3.2.3 Analytical Procedure

Adequate amount of sodium nitrite solution was transferred into an electrochemical cell containing 10.0 mL of 0.1M phosphate buffer solution and the three electrode system consisting of TMOPPMn(III)Cl/GE as working electrode, Pt wire as auxiliary electrode and Ag/AgCl as reference electrode was installed on the cell. The solution was de-aerated with nitrogen for 5 minutes. Differential pulse voltammograms were recorded between 0.1 and - 0.1V at a scan rate of $0.1Vs^{-1}$. Pulse amplitude of 50 mV, pulse period of 200 ms and pulse width of 50 ms were used. The potential step was 4 mV. The peak current for oxidation of nitrite at a potential of 0.690 V was measured.

3.2.4 Standard method for the determination of nitrite

0.5 g of sulfanilamide (SAA) was dissolved in 150 mL of 1M HCl and 6.0 mL of 0.20 % N-(1-naphthyl) ethylenediamine hydrochloride (NEDA) was added to it[181]. The solution was diluted to 200.0 mL. 5.0 mL of this solution was transferred into ten 25.0 mL standard flasks. Nitrite solutions

of different concentration were added into the flask and solution was made up to the volume. The absorbance of resulting solution was measured at 540 nm.

3.2.5 Sample preparation for electrochemical assay

Samples of chicken ham, sausage and pickled vegetables were purchased at local stores. Food samples were treated with saturated borax solution, followed by the addition of zinc acetate (5%) solution to precipitate proteins. The mixture was diluted with water and filtered. Spiked samples were prepared by adding a known amount of nitrite to the samples before extraction. Solutions of different concentrations were prepared by serial dilution of the stock solution with supporting electrolyte. The resulting filtrate solution was refrigerated under 4°C for further studies[177]. The nitrite concentration in real samples was determined using differential pulse voltammetric (DPV) technique and compared with those obtained with the standard spectrophotometric method.

3.3 Results and Discussions

3.3.1 Surface area study

The microscopic areas of the bare gold electrode (GE) and TMOPPMn(III)Cl/GE were obtained by cyclic voltammetry (Fig.3.2 a and 3.3b) using 2.0 mmolL^{-1} $K_3Fe(CN)_6$ as a redox probe containing 0.1M KCl at different scan rates. According to Randels –Sevcik equation[200], for a reversible process, the anodic peak current (i_p) is linear to square root of scan rate ($\nu^{1/2}$);

$$ip = (2.69 \times 10^5)n^{3/2}AC_0 D_R^{1/2} \nu^{1/2} \quad \text{.....(3.1)}$$

where A refers to the surface area of the electrode and C_o concentration of $K_3Fe(CN)_6$. For 2.0 mM $K_3Fe(CN)_6$, the electron transfer n = 1 and the diffusion coefficient $D_R = 7.60 \times 10^{-6}$ cm^2s^{-1}. Thus, from the slope of i_p vs $v^{1/2}$ relation, the microscopic areas of TMOPPMn(III)Cl modified GE was calculated to be 0.0197 cm^2, which was about three times greater than the bare GE (0.0082 cm^2). The increase in surface area of modified electrode is an evidence for the effective modification of gold electrode.

An additional evidence for the modification of GE was obtained from surface morphological studies of bare GE and TMOPPMn(III)Cl/GE carried out by scanning electron microscopy (SEM) (Fig. 3.3a and 3.3b). A smooth surface was observed for the bare gold electrode. Comparison of SEM images of bare GE and TMOPPMn(III)Cl/GE demonstrates the modification of GE.

3.3.2 Electrocatalytic oxidation of nitrite on modified gold electrode

Differential pulse (DP) and square wave (SW) voltammetric techniques were used for the study of electrochemical behaviour of nitrite at TMOPPMn(III)Cl/GE. Figure 3.4 displays the differential pulse voltammetric response of 1×10^{-3} M nitrite in 0.1M phosphate buffer solution (pH 6) at a) bare GE and b) TMOPPMn(III)Cl/GE. At bare GE, nitrite does not generate a voltammetric response. On the other hand, at TMOPPMn(III)Cl/GE a well - defined irreversible anodic peak at a potential of 0.690 V was observed. The observed peak at 0.690 V may be due to the oxidation of nitrite. This result illustrates that the TMOPPMn(III)Cl could present a favourable activity towards the oxidation of nitrite, suggesting that TMOPPMn(III)Cl/GE will be an excellent sensor for nitrite determination. Since oxidation of

nitrite occur at a lower potential of 0.69 V (43 μA) using DPV compared to square SWV (0.74 V, 39 μA) further studies were carried out using DPV technique.

3.3.3 Optimizing the experimental conditions

The conditions for sensor fabrication and effect of amount of TMoPPMn(III)Cl, effect of buffer solution, influence of pH of buffer and effect of scan rate on the anodic peak potential and peak current of nitrite were studied and optimized.

3.3.3.1 Effect of the amount of TMOPPMn(III)Cl

The amount of TMOPPMn(III)Cl solution on the GE directly determines the thickness of TMOPPMn(III)Cl film. The influence of amount of modifier on the peak current is as shown in Fig. 3.5. As the amount of TMOPPMn(III)Cl was increased from 1 to 3 μL, oxidation peak current greatly enhanced.

The enhancement of current indicates that number of catalytic sites increase with increase in the amount of TMOPPMn(III)Cl. Further increasing the volume of TMOPPMn(III)Cl solution, results in decrease of the peak current. The insulating property of nafion might have reduced the electron transfer rate thereby reducing the peak current[201]. Hence, the volume of TMOPPMn(III)Cl solution was fixed to be 3μL (0.5%w/v).

3.3.3.2 Effect of buffer solution and pH

The influence of supporting electrolyte on the electrochemical oxidation of nitrite was tested with different electrolytes of 0.1 M concentration

(H_2SO_4, HCl, NaCl, KCl, NaOH, citrate, acetate and phosphate buffer solution) and the results are given in Table 3.1. Since best response was obtained with phosphate buffer solution it was selected for further studies.

The effect of pH of solution on the electrochemical response of nitrite was studied in the pH range from 2.0 to 8.0 in 0.1 M phosphate buffer solution. Figure 3.7 depicts the effect of pH on the oxidation peak current of 1×10^{-3} M nitrite. It was observed that the anodic peak current increased with pH in the range of 2.0–6.0. In strongly acidic conditions nitrite ions are unstable[202] due to the decomposition of NO_2^- to NO and NO_3^- according to the Eq. (3.2):

$$2H^+ + 3NO_2^- \rightarrow 2NO + NO_3^- + H_20 \quad \text{.....(3.2)}$$

This is evidenced from the small peak currents at lower pH (<4.0). When pH was above 6.0, a decrease in current was observed. This can be attributed to the shortage of protons at higher pH[203-204] which makes the electrocatalytic oxidation of nitrite difficult. The maximal peak current appeared at pH 6.0. Therefore, pH 6.0 was chosen for further studies.

3.3.3.3 Effect of Scan rate

The effect of scan rate on the oxidation peak current was studied by DPV and the overlay of differential pulse voltammograms for the oxidation of nitrite at different scan rates is represented in figure 3.7. It was found that oxidation peak current of 1×10^{-3} M nitrite shows a linear relationship with square root of scan rate (ν) and can be expressed as: $ip = 0.028\ v^{1/2} - 0.026$, R = 0.999 (Fig. 3.8), where i_p is the peak current in μA. The linear dependency between square root of scan rate and peak current

demonstrates that the oxidation of nitrite at TMOPPMn(III)Cl modified gold electrode is controlled by the mass transport of nitrite ion from the bulk solution to the electrode surface. In addition, it was observed that the oxidation peak potential (*E*p) shifted slightly to more positive potentials with increasing the scan rate, indicating the chemical irreversibility of electrocatalytic oxidation process of nitrite[205]. From Fig. 3.9, it was found that E_p varied linearly with lnν, Ep = 0.023 lnν + 0.58, R = 0.995, where E_p is the peak potential. According to Laviron's equation[206], slope of this plot, b, is equal to RT/αnF, where b is the slope, R is the Universal gas constant, T is the temperature, α is the transfer coefficient (for a totally irreversible electrode process the value of α is assumed to be 0.5) and F is 96500 C. From the slope a value of n = 2.23, was obtained, indicating that oxidation of nitrite at the electrode surface was a two electron process[207] as represented in eqn 3.3:

$$NO_2^- + H_2O \rightleftharpoons NO_3^- + 2H^+ + 2e^- \quad \text{.....(3.3)}$$

3.3.3.4 Interferences study

The selectivity of TMOPPMn(III)Cl/GE was tested by studying the effects of common ions in the determination of nitrite and results are incorporated in Table 3.2. No obvious interference was seen in nitrite determination, on addition of upto 100-fold excess of Ca^{2+}, Cu^{2+}, K^+, PO_4^{2-}, CO_3^{2-} and NO_3^-. However, a 50-fold excess of ascorbic acid showed a noticeable interference in nitrite determination using TMOPPMn(III)Cl/GE sensor.

3.4 Analytical characteristics of the sensor

Under optimized conditions (0.1 M phosphate buffer solution of pH 6), differential pulse voltammetric studies for oxidation of nitrite was carried out at different concentrations (Fig 3.10). The proposed sensor showed a linear response range from 1.0×10^{-6} to 8.0×10^{-8} M (Fig. 3.11) with a limit of detection of 2.9×10^{-9} M. This indicates that the presence of nitrite in food samples with concentration as low as 2.9×10^{-9} M can be determined using the proposed sensor. The regression equation is expressed as i_p (μA) = 0.20 C (M) -1.8, R = 0.997, where C is the concentration of nitrite.

The analytical characteristics of TMOPPMn (III)Cl/GE are summarized in Table 3.3, in comparison with those reported in the literature. The oxidation of nitrite occurs at a lower potential using the developed sensor compared to other reported voltammetric sensors. Also the reported sensor has a lower limit of detection.

The relative standard deviation of the peak current, corresponding to the oxidation of 1×10^{-3} M nitrite, for five determinations was found to be 1.46 %. The TMOPPMn(III)Cl modified gold electrodes were found to have reserved 97% of their initial activity for more than 2 weeks. These results demonstrated the good reproducibility and stability of the proposed sensor.

3.5 Application of TMOPPMn(III)Cl/GE sensor for determination of nitrite

To confirm the validity and accuracy of the developed sensor, nitrite content in chicken sausage, chicken ham and pickled vegetables were determined. The concentration of nitrite in food samples was determined by

standard addition method. Each test was repeated five times. The obtained results are in good agreement with the standard spectrophotometric method (Table 3.4). The satisfactory results indicate that the proposed electrochemical sensor is reliable for the determination of nitrite in real samples.

3.6 Conclusion

The electrocatalytic oxidation of nitrite at TMOPPMn(III)Cl modified gold electrode sensor can be used as a new method for the determination of nitrite. Under optimized conditions the developed sensor has high sensitivity, good stability, reproducibility and a marked selectivity for the determination of nitrite. The sensor is also promising for determination of nitrite in food samples and the results are consistent with those obtained with standard spectrophotometric method. The use of less toxic reagents in the proposed method makes it more advantageous over the standard method, based on carcinogenic reagents.

Table 3.1 Effect of supporting electrolyte

Supporting electrolyte	Potential (mV)	Current (μA)
H_2SO_4	940	6.1
HCl	928	7.8
KCl	840	9.58
KNO_3	825	1.1
NaOH	924	6.9
Acetate buffer solution	724	20.4
Citrate buffer solution	696	10.4
Phosphate buffer solution	690	43.4

Table 3.2 Effect of foreign species on the oxidation peak current of 1×10^{-4} M nitrite

Foreign species	Concentration (M)	Signal change
K^+	1×10^{-2}	1.3
Ca^2	1×10^{-2}	1.3
Cu^{2+}	1×10^{-2}	2.1
PO_4^{2-}	1×10^{-2}	1.9
CO_3^{2-}	1×10^{-2}	2.3
NO_3^-	1×10^{-2}	3.6
ascorbic acid	5×10^{-3}	22.1

Table 3.3 Comparison of different voltammetric sensors for determination of nitrite in phosphate buffer solution

Electrode	Ep (V)	Analytical range	LOD (M)	References
MC/GCE[a]	0.810	5.0×10^{-7} - 1.0×10^{-4}	1.0×10^{-7}	208
Thionine/ACNTs/GCE[b]	0.800	3.0×10^{-6} -1.0×10^{-2}	9.0×10^{-7}	209
FeT_4MPyP/CuTSPc/GCE[c]	0.710	5.0×10^{-7} - 7.5×10^{-6}	1.4×10^{-7}	177
TMOPPMn (III)Cl/GE	0.690	5.0×10^{-2} -9.0×10^{-8}	2.9×10^{-9}	Proposed method

[a] MC/GCE : chitosan-carboxylated multiwall carbon nanotube modified glassy carbon electrode

[b] Thionine/ACNTs/GCE : Thionine modified aligned carbon nanotube electrode

[c] FeT_4MPyP/CuTSPc/GCE : alternated layers of iron (III) tetra- (N-methyl-4-pyridyl)-porphyrin (FeT_4MPyP) and copper tetrasulfonated phthalocyanine (CuTSPc) modified glassy carbon electrode

Table 3.4 Determination of nitrite in food samples (n=5)

Samples	Added (M)	Griess assay			Proposed method		
		Found (M)	R.S.D* (%)	Recovery ** (%)	Found (M)	R.S.D* (%)	Recovery** (%)
Chicken sausage	5×10^{-4}	4.98×10^{-4}	2.1	99.6	5.04×10^{-4}	2.2	100.8
	5×10^{-5}	5.01×10^{-5}	1.1	100.2	5.10×10^{-5}	1.4	102.0
Chicken ham	5×10^{-4}	4.95×10^{-4}	0.9	99.0	4.95×10^{-4}	1.1	99.0
	5×10^{-5}	4.97×10^{-5}	1.9	99.4	5.09×10^{-5}	2.7	101.8
Pickled vegetable	5×10^{-4}	5.08×10^{-4}	1.1	101.6	4.96×10^{-4}	2.7	99.2
	5×10^{-5}	5.03×10^{-5}	1.33	100.6	4.97×10^{-5}	2.5	99.4

* Relative standard deviation

** Average of 6 determinations

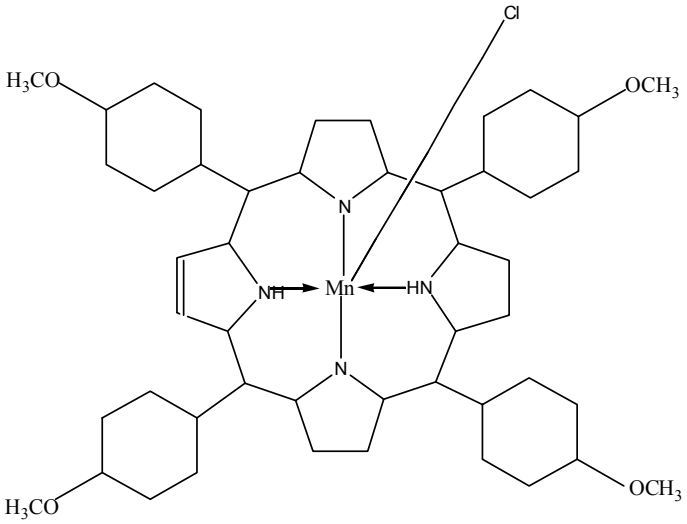

Figure 3.1 Structure of TMOPPMn(III)Cl

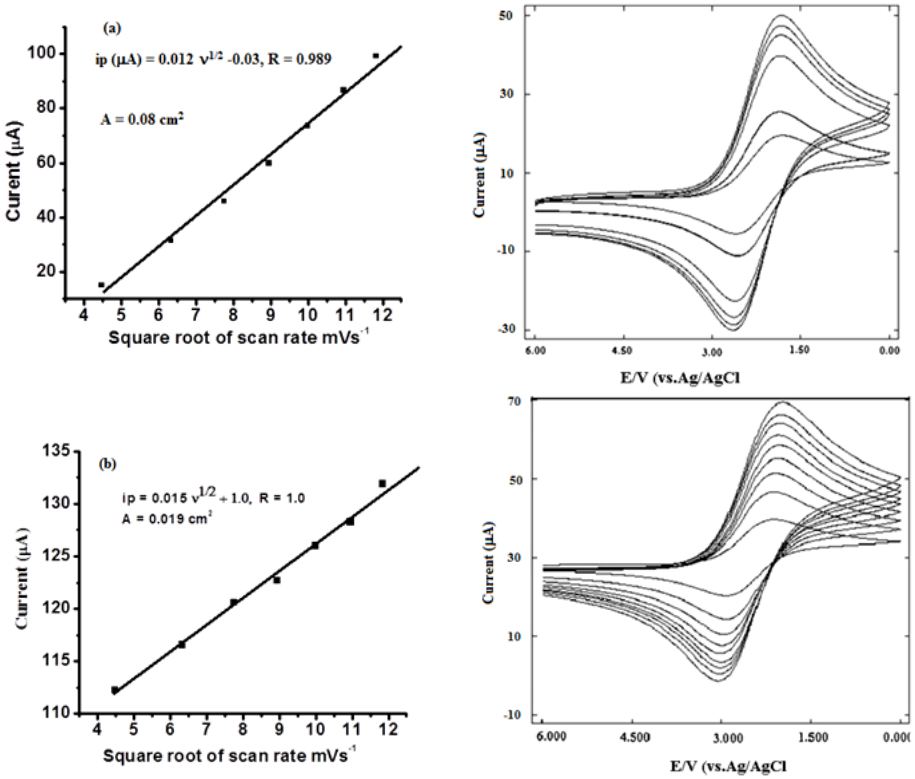

Figure 3.2 Surface area study of a) bare GE and b) TMOPPMn(III)Cl/ GE in 2.0×10^{-3} M $K_3Fe(CN)_6$ at different scan rates

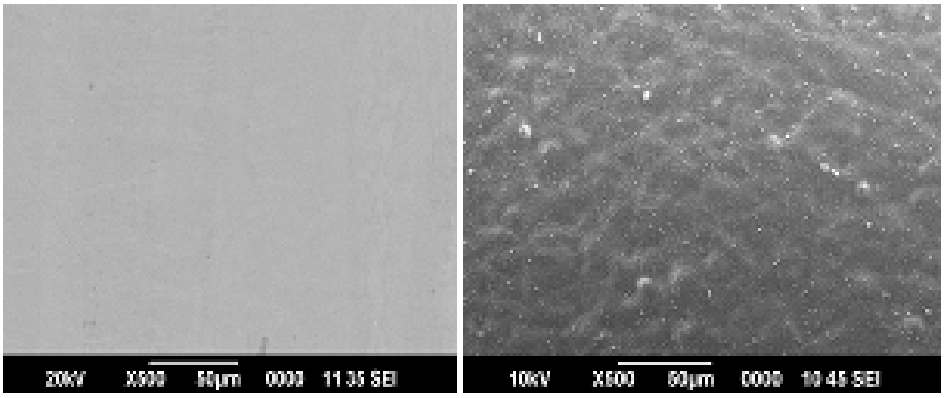

Figure 3.3 SEM image of a) bare GE and b) TMOPPMn(III)Cl/ GE

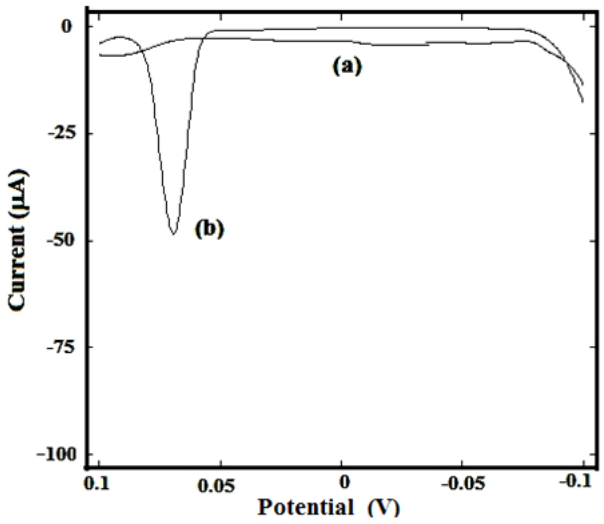

Figure 3.4 Differential pulse voltammogram of nitrite at a) bare GE b) TMOPPMn(III)Cl/GE

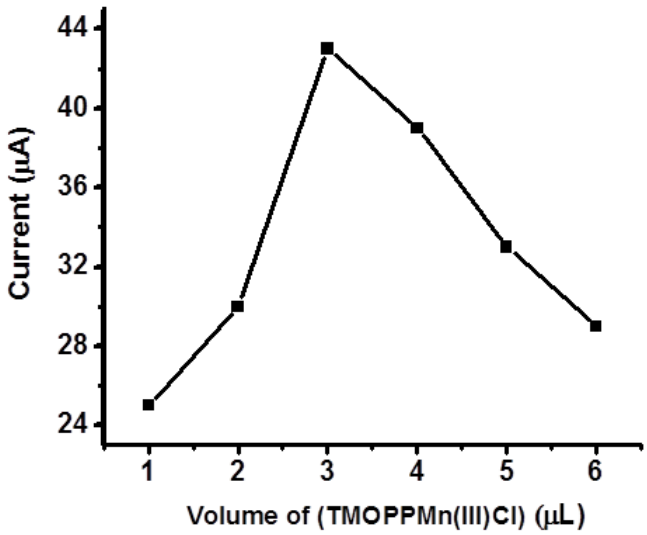

Figure 3.5 Effect of the amount of TMOPPMn (III)Cl

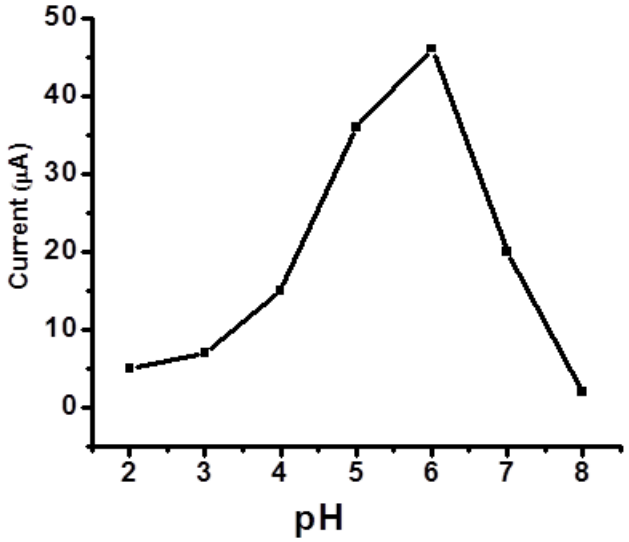

Figure 3.6 Effect of pH

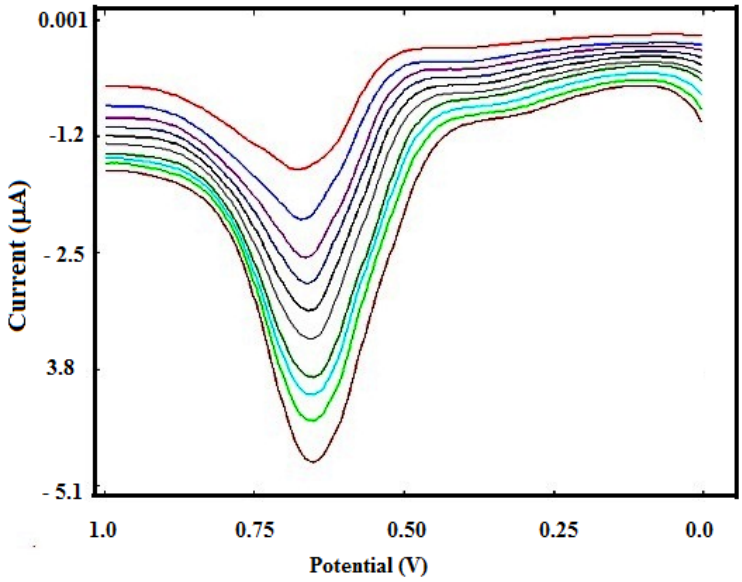

Figure 3.7 Overlay of Differential Pulse Voltammograms for oxidation of nitrite at various scan rates

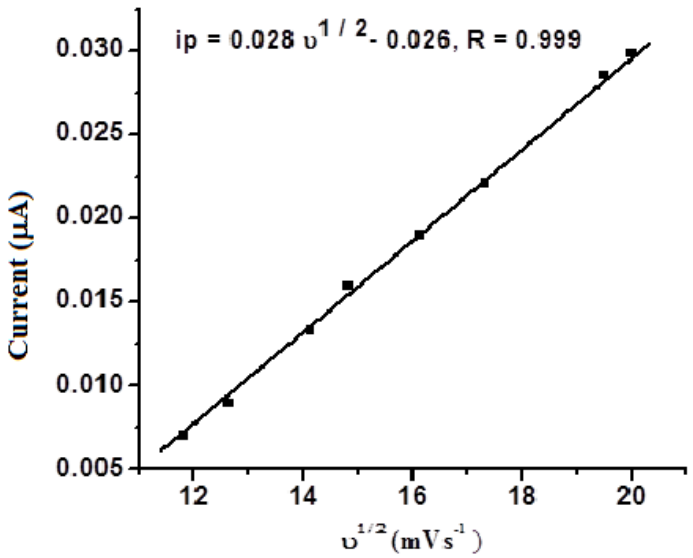

Figure 3.8 Plot of anodic peak current versus square root of scan rate

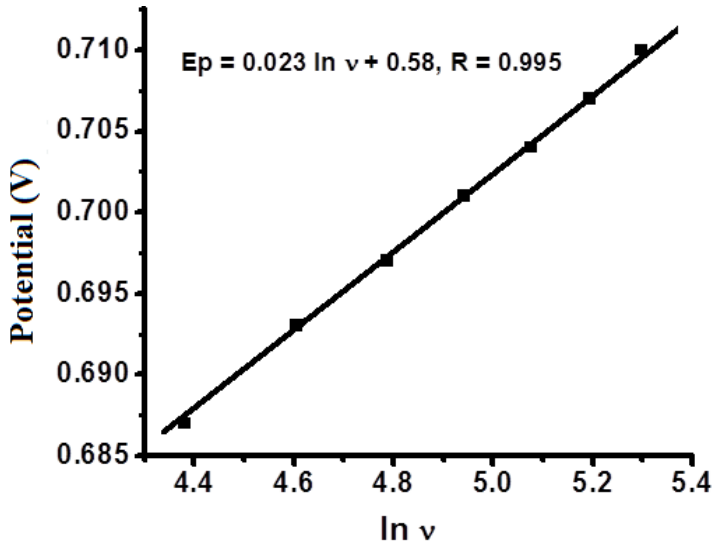

Figure 3.9 Plot of peak potential versus ln scan rate

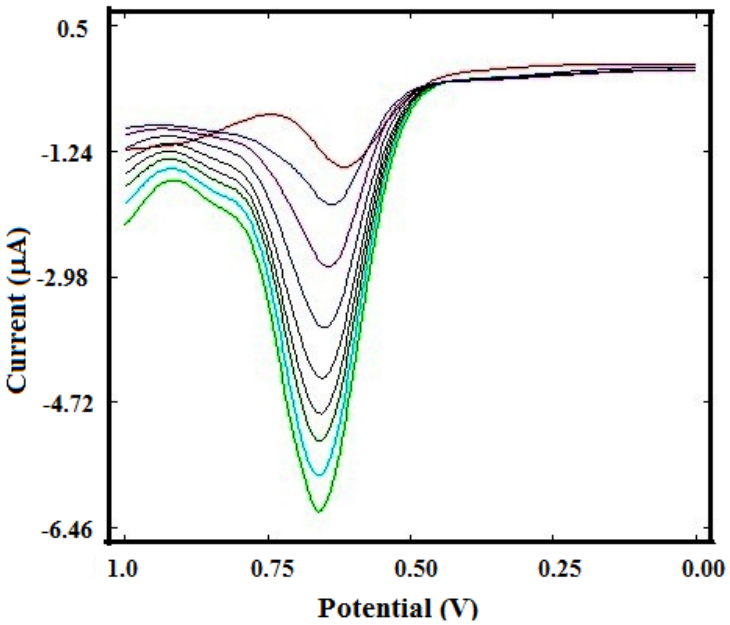

Figure 3.10 Overlay of Differential Pulse voltammograms for oxidation of nitrite at various concentrations

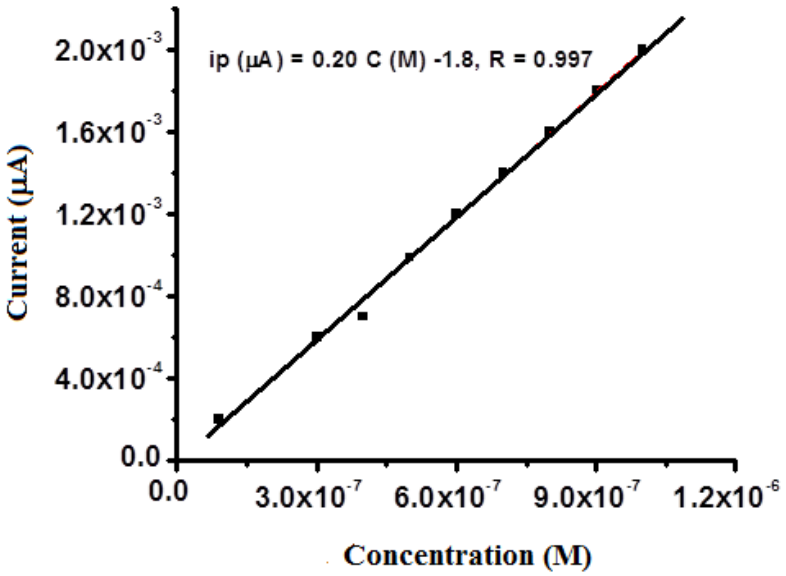

Figure 3.11 Plot of peak current against various concentrations of nitrite

Chapter 4

VOLTAMMETRIC SENSOR FOR SUDAN 1

Contents

This chapter describes the development of an electrochemical sensor, based on the catalytic activity of gold nanoparticles deposited on a glassy carbon electrode (AuNP/GCE), for the determination of Sudan 1 in food samples. The electrocatalytic activity of AuNPs towards the oxidation of Sudan 1 was studied by cyclic voltammetry and square wave voltammetry (SWV). The cyclic voltammogram of the modified electrode has a pair of well-defined quasi-reversible redox peaks with a formal potential of 0.295 V (*vs.* Ag/AgCl) at a scan rate of 0.1 Vs^{-1}. The sensor exhibited two distinct linear response ranges of 4.0×10^{-5} - 1×10^{-3} M and $2 \times 10^{-5} - 7 \times 10^{-7}$ M. The heterogeneous electron transfer constant (k_s) for the oxidation of Sudan 1 was evaluated to be 1.5×10^{-1} s^{-1}. The average surface concentration of Sudan 1 on the surface of AuNP/GCE was 1.2×10^{-9} mol cm^{-2}. The proposed sensor has been successfully used for the determination of Sudan 1 in food products such as ketchup and chilly powder.

4.1 Introduction

Color is often the first sensory quality by which food is judged. Food colorants have been used to make food more attractive and delicious for centuries[210]. Copper sulfate was used to impart green color to pickles and candies were colored using lead[211]. Even though, natural food colors are available, artificial colors remain the most popular type of food colorings because of their brightness, stability, low cost and effectiveness. They are also added to compensate for the loss of natural colors of food, which are destroyed during processing and storage, and to provide the desired colored appearance. However, the use of synthetic food colorants is controversial as some of them are found to be potentially toxic if they are excessively consumed and also studies have proved that they have no nutritional values. The use of synthetic colorants in foods is strictly controlled by legislation and harmonized across the European Union by formulating the directive 94/36/EC[212].

The food colorants are categorized into five major classes: the azo compounds (E 102, E 110, E 122, E 123, E124, E 128 and E 129), the triarylmethane group (E 131, E 133 and E142), the chinophthalon derivative of Quinoline Yellow (E104), xanthenes as Erythrosine (E 127) and the indigo colorants (Indigo Carmine E 132).

Sudan I (1-phenylazo-2-naphthol, Figure 1), an azo compound, is a non-ionic fat-soluble dye. It is extensively used to enhance the appearance of products such as chilly powder, tomato sauces, salami, olive oil etc[213]. It has also been used in coloring waxes, oils, petroleum solvents and polishes[214-215]. Colorization or amending of the original color with Sudan dyes can make

food unsafe because of the toxicity and carcinogenic properties of such compounds[216-218]. Sudan dyes have evident toxic effect to human's organs as the aniline which is produced during the metabolic decomposition of Sudan dyes could attack the hepatocytes and lead to toxic hepatic disease. Since they posed an increased risk of cancer for humans, the International Agency for Research on Cancer, (IARC) has assessed Sudan I as a group 3 carcinogen[219]. Due to the carcinogenicity, use of Sudan I as coloring agent in food products is forbidden in most countries. Unfortunately, a variety of food stuffs contaminated with Sudan dyes (particularly Sudan I) has been detected[220-221]. For the sake of effective control of the illegal use of Sudan I in foodstuffs, accurate and reliable methods for the determination of Sudan dyes in food products are of great importance and interest.

The analytical techniques adopted for the determination of Sudan 1 usually involves high performance liquid chromatography (HPLC)[222-223], high performance liquid chromatography– mass spectrometry (HPLC–MS)[224-225], gas chromatography–mass spectrometry (GC–MS)[226], capillary electrophoresis[227] and electrochemical methods[228-230]. Electrochemical methods are obviously better due to its convenience, fastness, higher sensitivity and reproducibility.

For electrochemical determination of Sudan 1 using modified electrodes, the modifier is a key factor that can heavily influence the sensitivity and selectivity of determination. The determination of Sudan I based on electrochemical method using various chemically modified electrodes has been reported in the literature[231-234]. Among the different materials used as an electrode modifier in voltammetry, metal nanoparticles,

especially gold nanoparticles (AuNPs), have attracted much attention due to their unique properties and wide varieties of potential applications[235-236]. The application of gold nanoparticles as transducers for electrochemical sensors has led to high sensitivity, wide linear range, and higher selectivity. The reasons for these enhancements are the high surface area and polycrystalline structure of the gold nanoparticles (AuNPs). Gold nanoparticles (AuNPs) can be prepared by chemical synthesis[237-238] or by physical ways such as magnetron sputtering, radiolytic and photolytic methods[239-240]. Electrochemical deposition of gold nanoparticles provides a rapid and convenient method of preparation[241].

This chapter presents the development of a gold nanoparticle modified glassy carbon electrode sensor for the determination of Sudan 1 in food samples. The advantages of the proposed sensor are its high selectivity, sensitivity and wide linear range for the determination of Sudan 1 as well as the long stability of the AuNP/GCE sensor.

Considering the electrode reaction of a single compound, the main physical parameters, that describe the electron transfer reaction between the electrode and the investigated compound, such as the number of exchanged electrons involved in the elementary act of electrochemical transformation n, the electron transfer coefficient α (i.e. the symmetry factor of the energetic barrier) and the standard rate constant of electron transfer k_s. Cyclic voltammetric technique can be employed to characterize the kinetics of electron transfer reactions.

The electron transfer kinetics can depend very much on the electrode material. Laviron's[242] method was used to calculate the heterogeneous

electron transfer constant, ks, for the oxidation of Sudan I on bare and AuNP/GCE electrode. Much less information regarding k_s for the oxidation of Sudan 1 is available in literature[243]. The designed sensor was further used to evaluate Sudan 1 in various food samples.

4.2 Experimental

4.2.1 Fabrication of gold nanoparticle modified glassy carbon electrode (AuNP/GCE)

First step involved in the fabrication of AuNP/GCE is the cleaning of GCE and is performed as mentioned in section 2.4. The cleaned GCE was then immersed in 0.05M H_2SO_4 solution containing 1×10^{-3} M $HAuCl_4$. Electrochemical deposition of AuNPs on GCE was performed by carrying out 30 cyclic scans between 1.3 and 0 V at a scan rate of $0.1Vs^{-1}$ [149] (Fig. 4.2). The anodic peak at 1.1 V can be attributed to the oxidation of deposited gold to Au (III). The cathodic peaks may be due to the reduction of gold surface oxide, reduction of protons and hydrogen evolution[244-246]. A shift in reduction peak in the second cycle to more positive potential was observed and it represents an easier electrodeposition of gold over a previously deposited gold nuclei[247]. The resulting gold nanoparticle modified glassy carbon electrode was washed in double distilled water and dried in air.

4.2.2 Preparation of Sudan 1 solution

1×10^{-1} M stock solution of Sudan 1 was prepared by dissolving 0.248 g of it in 10.0 mL of ethanol. Standard solutions (1×10^{-3} - 1×10^{-8} M) of analyte were prepared by serial dilution of stock solution using 1:1 ethanol and 0.1 M HCl.

4.2.3 Analytical procedure

1:1 mixture of ethanol and 0.1 M HCl was used as the supporting electrolyte. A desired volume of Sudan 1 was pipetted into an electrochemical cell, followed by deareation with pumping O_2 -free nitrogen. An accumulation step was conducted by stirring the solution for 90 sec at open - circuit. After a quiescent interval of 2 s, square wave voltammograms was recorded from –0.50 to 0.70 V at a scan rate of 0.1 Vs^{-1}. The experimental conditions were amplitude of 0.025 V, increment of 0.004 V and frequency of 15 Hz. The peak current for oxidation of Sudan 1 was measured at 0.264 V. Prior to and after each measurement, the AuNPs modified GCE was activated by successive cyclic voltammetric sweeps from –0.50 to 0.70 V at 0.1 Vs^{-1} in the electrolyte solution until the voltammograms kept unchangeable to achieve a reproducible electrode surface.

4.2.4 Procedure for treatment of food samples

Various samples of hot chilly powder and ketch up were purchased from local market. 2.0 g of the sample was exactly weighed and then ultrasonicated with 20.0 mL of ethanol for 20 minutes. The extraction is repeated three times, every time recovering the liquid phase after filtration. The extracts were collected in a 100.0 mL volumetric flask and diluted to volume with ethanol. Spiked samples were prepared by adding a known amount of Sudan 1 to the samples before extraction. Solutions of varying concentrations were made by taking adequate aliquots of the clear filtrate and diluting with ethanol. The concentration of Sudan 1 in food samples were determined from calibration graph.

4.3 Results and discussion

4.3.1 Characterization of AuNP/GCE

In order to illustrate that the electrodeposited AuNPs could improve the surface area, electroactive surface area (A) of AuNP/GCE was determined by cyclic voltammetry using Randle's Sevicik[200] equation as detailed in section 3.3.1 of chapter 3. From Fig. 4.3a and Fig. 4.3b it was found that the peak currents (ip) at AuNPs modified electrode and bare GCE were proportional to the square root of scan rate. From the slopes, effective surface area (A) of AuNPs modified GCE and bare GCE were acquired as 0.029 cm^2 and 0.019 cm^2 respectively.

The surface morphology of a modified electrode greatly impacts its reactivity and performance. Scanning Electron Microscopy (SEM) was employed to gain insights into the surface morphology of bare GCE and AuNP/GCE [Fig. 4.4a. and 4.4b]. The SEM image of modified electrode clearly indicated the effective modification of GCE with AuNPs.

4.3.2 Electrochemical behavior

The electrochemical behavior of Sudan 1 (1×10^{-4} M) on bare GCE and AuNP/GCE was investigated in 0.1 M HCl using cyclic voltammetry [Fig. 4.5]. At the surface of unmodified electrode a pair of redox peaks were observed at E_{pa} = 0.388 V and E_{pc} = 0.255 V. Under identical conditions, at AuNPs modified GCE, the anodic and cathodic peak potentials shifted to 0.355 V (16.06 μA) and 0.235 V (4.99 μA) respectively. The anodic peak potential decreased by 0.033V and an enhancement in peak current (two times) was observed. These results indicate that gold nanoparticles have

significantly improved the performance of the glassy carbon electrode for the oxidation of Sudan 1. The peak –to- peak separation (ΔE_p) of 0.12 V demonstrated that the electrochemical reaction of Sudan 1 on AuNP/GCE is a quasi-reversible process. The formal potential $E^{0\prime} = \frac{E_{pa} + E_{pc}}{2}$ of the electrode was 0.295 V.

Since the electrocatalytic oxidation of Sudan 1 took place at a lower potential (0.264V) with an enhanced peak current (33 μA) using square wave voltammetry (SWV) compared to CV (0.355 V, 16.06 μA), SWV technique was used for further studies.

4.3.3 Optimization of experimental variables for electrocatalytic oxidation of Sudan 1

The influence of experimental variables such as the effect of supporting electrolyte, scan rate and accumulation time on the voltammetric response of Sudan 1 using the proposed sensor was investigated using 1×10^{-4} M of Sudan 1.

4.3.3.1 Effect of supporting electrolyte

Supporting electrolyte can affect the electrochemical properties of electrode and the electrochemical reaction of analyte. The electrochemical behavior of Sudan 1 in different supporting electrolytes (H_2SO_4, HCl, NaCl, KCl, NaOH, citrate and phosphate buffer) of 0.1 M concentration was investigated at AuNP/GCE. From Table 4.1, it was found that the oxidation of Sudan 1 occurred at a lower anodic potential with an enhanced peak current in 0.1M HCl and hence it was used for the electrochemical determination of Sudan 1.

4.3.3.2 Effect of the amount of ethanol

Sudan 1 is insoluble in water whereas soluble in ethanol. In the present investigation, a certain amount of ethanol was added into the supporting electrolyte solution to increase the solubility of Sudan 1. The amount of ethanol exerts great influence on electrochemical response of Sudan 1 at AuNP/GCE. Measurements were made with different ratios of ethanol and 0.1 M HCl. It was found that the maximum oxidation peak current was obtained when 0.1M HCl and ethanol were in the ratio of 1:1. Therefore a supporting electrolyte with 1:1 ratio of 0.1 M HCl and ethanol was used throughout the studies.

4.3.3.3 Effect of cycle number (N)

The optimized condition for the deposition of Au nanoparticles on GCE was studied. The number of potential cycles for the deposition of gold nanoparticles was varied from 10 to 60 cycles. The peak current for oxidation of Sudan 1 was found to increase with the increase of number of cycles up to 40. On further increasing number of cycles beyond 40, a decrease in peak current was observed. The reduction in peak current may be due to the conversion of AuNPs into the bigger clusters of gold at very high gold loading. Since the maximum current was obtained when number of cycles was 40, the optimum number of cycles for the electrochemical deposition of AuNPs was fixed to be 40.

The average surface concentration (Γ) of gold nanoparticles deposited on GCE was calculated using the equation[248] (4.2),

$$Q = nFA\Gamma \quad \text{.....(4.2)}$$

Where Q is the charge passing through the electrode, n is the number of electrons transferred, F is the Faraday's constant and A is the effective surface area of electrode. From the experimental results the amount of AuNPs deposited on the surface of GCE was estimated to be 2.15×10^{-9} mol cm^{-2}.

4.3.3.4 Effect of accumulation time

Open circuit accumulation is used in electro analytical chemistry to improve sensitivity of determination by accumulating analyte on electrode surface. The influence of accumulation time, in the range of 30 to 210 sec, on the anodic peak current of Sudan 1 was as shown in figure 4.6. It can be seen that the anodic peak current increases linearly with accumulation time upto 90 sec. This phenomenon suggests that accumulation is efficient to improve the sensitivity of the proposed sensor. However, further increase on accumulation time did not show any appreciable change in the oxidation peak current. The amount of Sudan 1 on the surface of AuNP/GCE tends to a limiting value may be the reason for this. Thus, an accumulation time of 90 s was optimized for all further measurements.

4.3.3.5 Effect of scan rate

Figure 4.7 represents the overlay of cyclic voltammograms for oxidation of Sudan 1 at different scan rates. A linear dependency was found when peak current, (i_p), was plotted against scan rate, ν [Fig. 4.8] and can be expressed as, i_p (μA) = 0.028 ν + 0.130, R^2 = 0.998. The result indicates that the oxidation of Sudan 1 at AuNP/GCE is an adsorption controlled process. Also, logarithm of peak current, log (i_p), was plotted against logarithm of scan rate, log ν (Fig. 4.9) and the relationship was found to be linear, log i_p (μA) = 1.06 logν - 1.30, R^2 = 0.996, with a slope of 1.06. The

value of the slope is near to the theoretical value of 1.0, for an adsorption controlled process[249] and therefore confirms that the oxidation of Sudan 1 is an adsorption controlled process.

The number of electrons involved in the oxidation of Sudan 1 was calculated using the equation 4. 3;

$$i_p = \frac{nFQv}{4RT} \quad \text{.....(4. 3)}$$

where i_p represents the anodic peak current, Q is the amount of charge integrated from the area of cyclic voltammetric peak, T is the temperature in Kelvin (298K), R is the universal gas constant (8.314 $Jmol^{-1}K^{-1}$), F is the Faraday constant (96500 $Cmol^{-1}$) and n is the number of electrons transferred. From the slope of ip versus v, n was calculated to be 0.92 (≈ 1). The observed oxidation peak may be ascribed to the oxidation of –OH group present in Sudan 1[250].

The apparent charge transfer rate constant, k_s, and the charge transfer coefficient, α, of a surface confined redox couple can be evaluated from cyclic voltammetric experiments by using the variation of anodic and cathodic peak potentials with logarithm of scan rate, according to the procedure of Laviron[242]. Figure 4.10 shows that the Ep values are proportional to the logarithm of scan rate and following equations are used to determine the electron transfer coefficient:

$$E_{pa} = a + \frac{2.303\ RT}{(1-\alpha)n_\alpha F} \log v \quad \text{.....(4.4)}$$

$$E_{pc} = b - \frac{2.303\ RT}{\alpha n_\alpha F} \log v \quad \text{.....(4.5)}$$

From Fig.4.10, E_{pa} = 0.180 + 0.123 log ν, R = 0.998; E_{pc} = 0.317 -0.13log ν, R = 0.996. The kinetic parameters α_a and α_c (anodic and cathodic transfer coefficients) are 0.52 and 0.45 respectively.

The value of the apparent heterogeneous electron transfer rate constant k_s could be calculated based on Laviron's equation [242]:

$$\log k_s = \alpha \log(1-\alpha) + (1-\alpha)\log\alpha - \log\frac{RT}{nF\vartheta} - \alpha(1-\alpha)\frac{nF\Delta Ep}{RT} \quad \ldots (4.6)$$

The calculated value of k_s on bare GCE and AuNP/GCE was found to be 0.9 × 10^{-1} s^{-1} and 1.5 × 10^{-1} s^{-1} respectively. The greater value of k_s on AuNP/GCE than on bare GCE, suggested that AuNPs are excellent promoters for the direct electron transfer between Sudan 1 and GCE.

The average surface concentration (Γ) of Sudan 1 on the surface of AuNP/GCE can be calculated according to the equation[251]:

$$i_p = \frac{n^2F^2A\tau\vartheta}{4RT} \quad \ldots (4.7)$$

where ip is the anodic peak current, n is the number of electrons transferred, ν is the scan rate, A is the effective surface area of modified electrode, Γ is the average surface concentration of Sudan 1, T,R and F are the temperature in Kelvin (298 K), universal gas constant (8.314 $Jmol^{-1}K^{-1}$) and Faraday constant (96500 $Cmol^{-1}$). Based on the equation 4.7, the average surface coverage of Sudan 1 was estimated to be 1.2 × 10^{-9} mol cm^{-2}.

4.3.4 Linearity range and limit of detection

The relationship between the oxidation peak current and the concentration of Sudan I was examined by SWV and is as shown in Figure

4.11. In the plot of oxidation peak current versus concentration of Sudan 1, two linear ranges were obtained. The first linear range (Fig. 4.12) was from $2 \times 10^{-5} - 7 \times 10^{-7}$ M, and the corresponding calibration equation was i_p (μA) = 129.9 C (M) + 8.9 with a correlation coefficient, R=0.998 and the limit of detection was 1.1×10^{-8} M. The second linear range (Fig. 4.13) was between 4.0×10^{-5} and 1×10^{-3} M (i_p (μA) = 252.1 C (M) + 26.5, R = 0.991).

The relative standard deviation of the peak current corresponding to the oxidation of 1×10^{-4} M Sudan 1, for five determinations was found to be 1.5%. The AuNP/GCE was found to have reserved 97% of its initial activity for more than one month. These results demonstrated the good reproducibility and stability of the proposed sensor. Table.4.2 demonstrates the comparison of results for the determination of Sudan 1 using different voltammetric sensors. From the table, it is understood that compared to other reported voltammetric sensors for the determination of Sudan 1, oxidation of Sudan 1 occurs at a lower potential using the proposed sensor. The limit of detection obtained with the present method is in the range of other sensors.

4.4 Effect of interfering species

SWV was used to study the effect of foreign species (commonly contained in chilly powder and ketchup) on the determination of Sudan I (1×10^{-4}M) under the optimized conditions. The oxidation peak current of Sudan I in the absence and presence of various concentration of foreign species was measured. Experimental results, Table 4.3, showed that no interference was observed for the determination of Sudan I in the presence of upto 100- fold excess of Na^+, Ca^{2+}, K^+, Mg^{2+}, glucose, 4-nitrophenol, 4-chlorophenol, phenol and upto 10- fold excess of allura red. Sunset yellow

interferes severely in the determination. The results indicated a good selectivity of the proposed sensor for the determination of Sudan I.

4.5 Application study

Practical utility of the developed sensor has been demonstrated by the analysis of Sudan I in chilly powder and ketchup samples. Samples were prepared and analysed in accordance with procedures described in section 4.2.3. Peak corresponding to Sudan I was not observed in the voltammograms of these samples, indicating the absence of Sudan 1 in these samples or the content is lower than the detection limit. Table.4.4, shows the content of Sudan 1 in different chilly powders and ketchup sample, which was obtained by the standard addition method using AuNP/GCE sensor. The data indicates that this method has reliable recoveries and a good repeatability with the RSD values below 5 %.

4.6 Conclusion

Gold nanoparticles were electrodeposited on GCE and modified electrode was characterized using SEM. Effective surface area calculated using Randles' equation points toward the effective modification of GCE with AuNPs. AuNP/ GCE exhibited excellent catalytic activity towards the oxidation of Sudan 1 due to its large surface area. As demonstrated, at AuNP/GCE surface, Sudan 1 underwent an adsorption controlled and quasi-reversible electron transfer reaction. The oxidation current measured increased linearly with Sudan 1 concentration in the ranges of 4.0×10^{-5} - 1×10^{-3} M and 2×10^{-5} – 7×10^{-7} M. The proposed sensor was used satisfactorily for the determination of Sudan 1 in chilli powder and ketch up sample.

Table 4.1 Effect of supporting electrolyte

Supporting electrolyte	Potential (mV)	Current (μA)
H_2SO_4	385	10.07
HCl	357	16.06
KCl	760	14.01
KNO_3	831	2.51
NaOH	520	4.72
Acetate buffer solution	732	2.02
Citrate buffer solution	547	12.78
Phosphate buffer solution	684	3.46

Table 4.2 Comparison of different sensors for the determination of Sudan 1

Electrode	Potential (Ep, V)	Linear range (M)	Limit of detection (M)	Reference
[1]Pt/CNts/ILCPE	0.650	8.0×10^{-9} to 6.0×10^{-3}	3.0×10^{-9}	149
[2]MWNT/GCE	0.672	1.0×10^{-6} to 1.2×10^{-4}	3.4×10^{-8}	230
[3]MMT-Ca/CPE	0.620	2.01×10^{-7} to 4.0×10^{-6}	8.1×10^{-8}	251
[4]Fe_3O_4/GCE	0.643	1.0×10^{-8} to 1.0×10^{-6}	1.0×10^{-9}	234
[5]OMC/GCE	0.700	4.03×10^{-7} to 6.6×10^{-5}	2.4×10^{-9}	229
AuNP/GCE	0.264	4.0×10^{-5} to 1×10^{-3} 2×10^{-5} to 7×10^{-7}	1.0×10^{-8}	Proposed sensor

1. platinum carbon nanotubes nanocomposite ionic liquid modified carbon paste electrode
2. multiwalled nanotube modified glassy carbon electrode
3. montmorillonite calcium modified carbon paste electrode
4. Fe_3O_4 nanoparticle modified glassy carbon electrode
5. Ordered mesoporous carbon (OMC) modified glassy carbon electrode (OMC/GCE)

Table 4.3 Effect of foreign species

Foreign species	Concentration(M)	Signal change
Na^+	1×10^{-2}	3.6
K^+	1×10^{-2}	4.1
Ca^{2+}	1×10^{-2}	2.1
Mg^{2+}	1×10^{-2}	1.9
glucose	1×10^{-2}	4.8
4-nitrophenol	1×10^{-2}	0.7
4-chlorophenol	1×10^{-2}	2.1
4-aminophenol	1×10^{-2}	3.8
phenol	1×10^{-2}	1.2
Allura red	1×10^{-3}	9.3
Sunset yellow	1×10^{-4}	9.5

Table 4.4 Application study for the determination of Sudan 1 in various food samples (n=5)

Sample	Added (M)	Found (M)	R.S.D* (%)	Recovery** (%)
Chilly powder A	1.00×10^{-6}	1.05×10^{-6}	1.3	105.0
	5.00×10^{-5}	4.91×10^{-5}	3.5	98.2
	7.00×10^{-5}	6.96×10^{-5}	4.5	99.3
Chilly powder B	1.00×10^{-6}	0.99×10^{-6}	1.3	99.7
	5.00×10^{-5}	5.01×10^{-5}	1.7	100.2
	7.00×10^{-5}	6.92×10^{-5}	2.3	98.8
Ketch up	1.00×10^{-6}	1.02×10^{-6}	4.5	102.0
	5.00×10^{-5}	5.16×10^{-5}	5.7	103.2
	7.00×10^{-5}	7.13×10^{-5}	2.8	101.8

*relative standard deviation
**average of 6 replicates

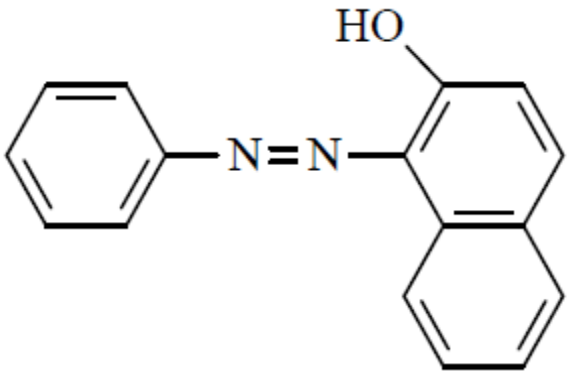

Figure 4.1 Structure of Sudan 1

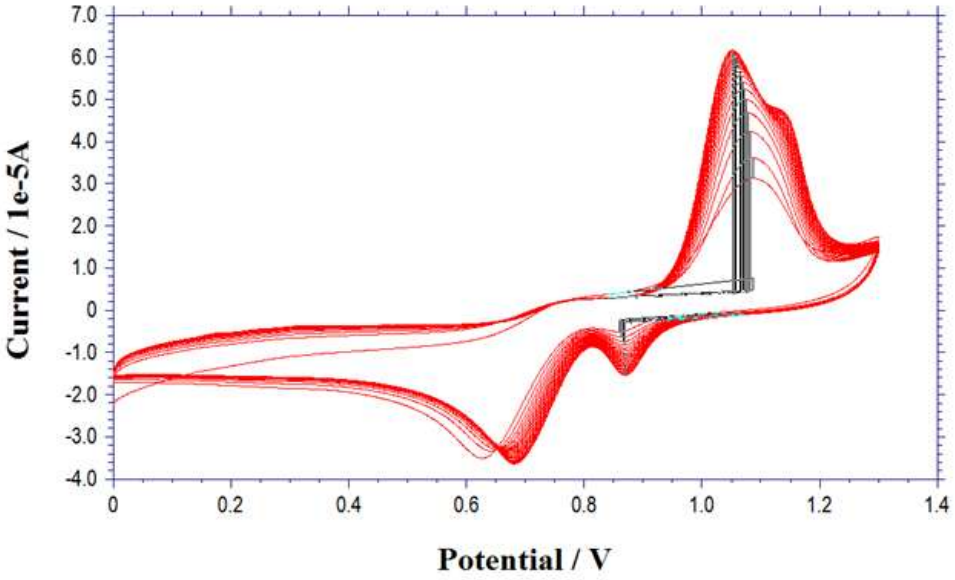

Figure 4.2 Electrodeposition of AuNP at GCE

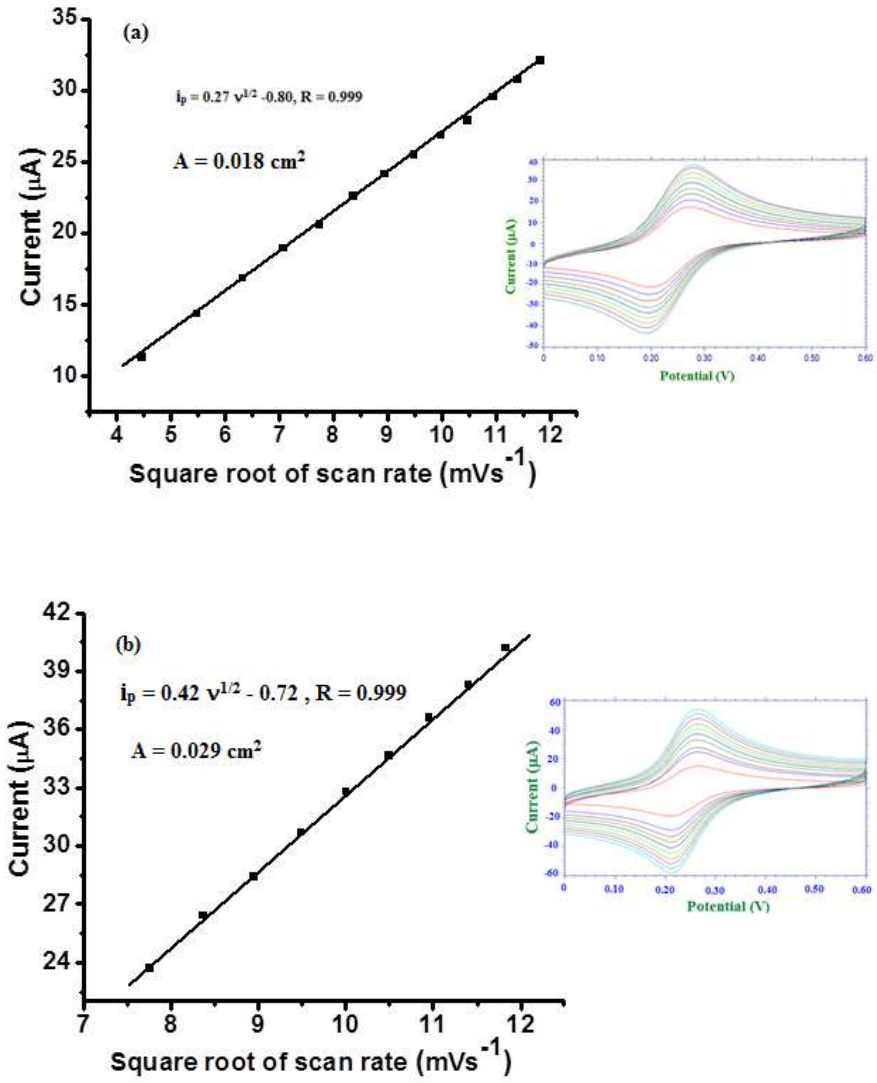

Figure 4.3 Surface area study of a) bare GCE and b) AuNP/GCE in 2.0×10^{-3} M $K_3Fe(CN)_6$ at different scan rates

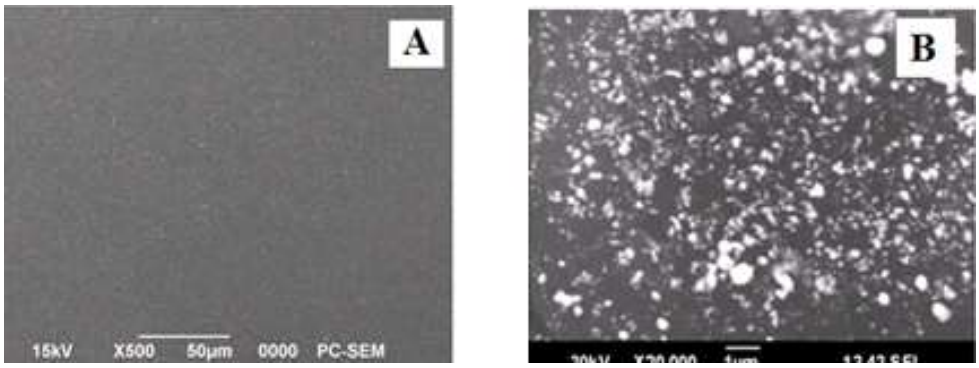

Figure 4.4 SEM images of (a) bare and (b) AuNP/GCE

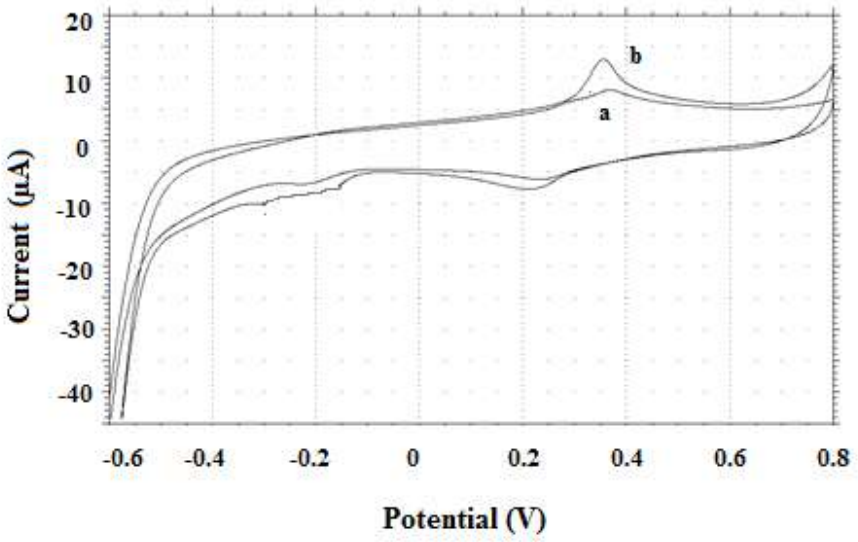

Figure 4.5 Cyclic voltammogram of 1 ×10^{-4}M Sudan 1 at (a) bare GCE and (b) AuNP/GCE in 0.1M HCl, scan rate 0.1Vs^{-1}

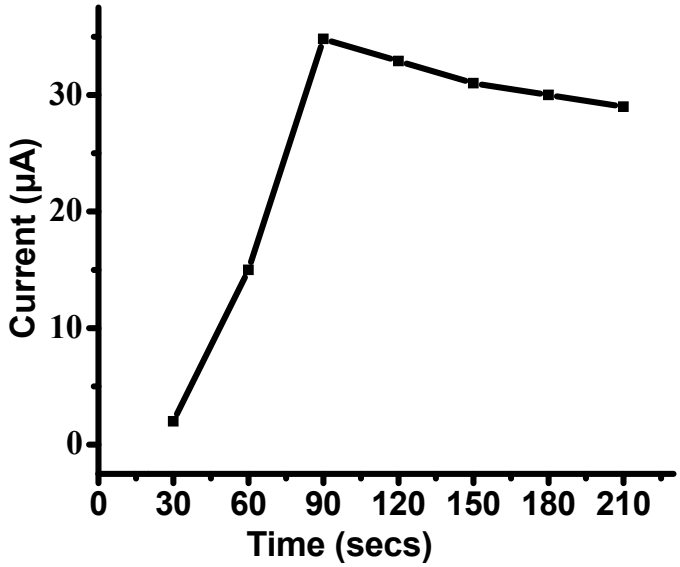

Figure 4.6 Effect of accumulation time

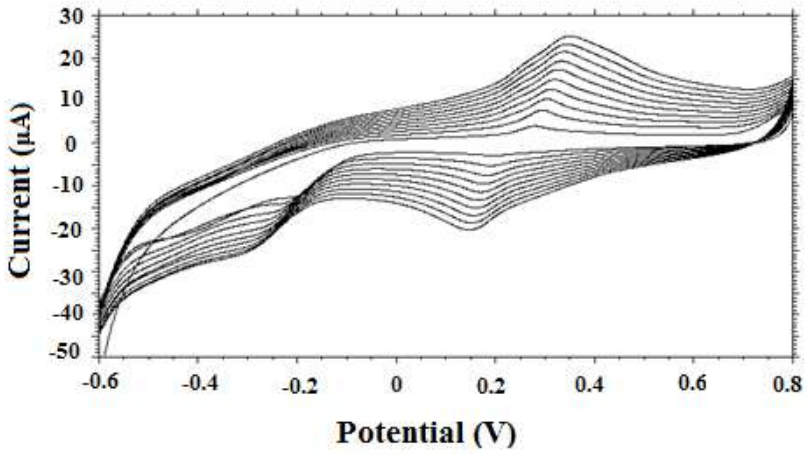

Figure 4.7 Overlay of cyclic voltammograms of the oxidation of 1×10^{-4} M Sudan I at AuNP/GCE in 0.1 M HCl at various scan rates

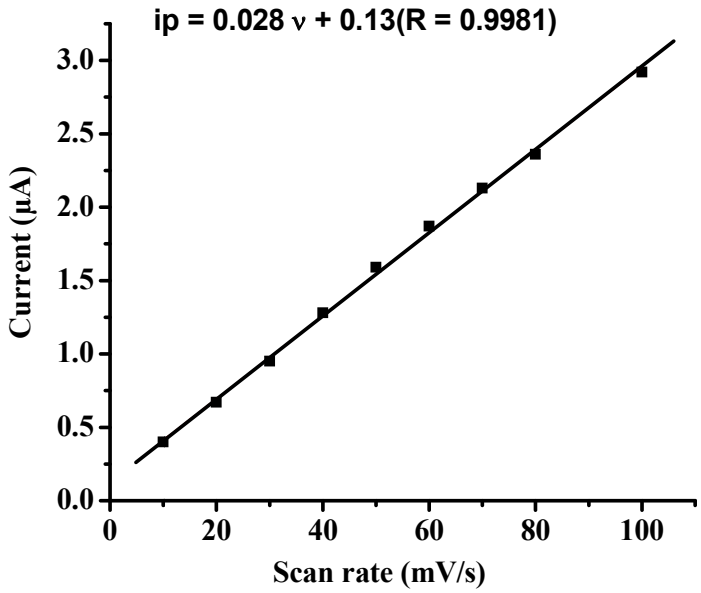

Figure 4.8 Plot of peak current vs scan rate

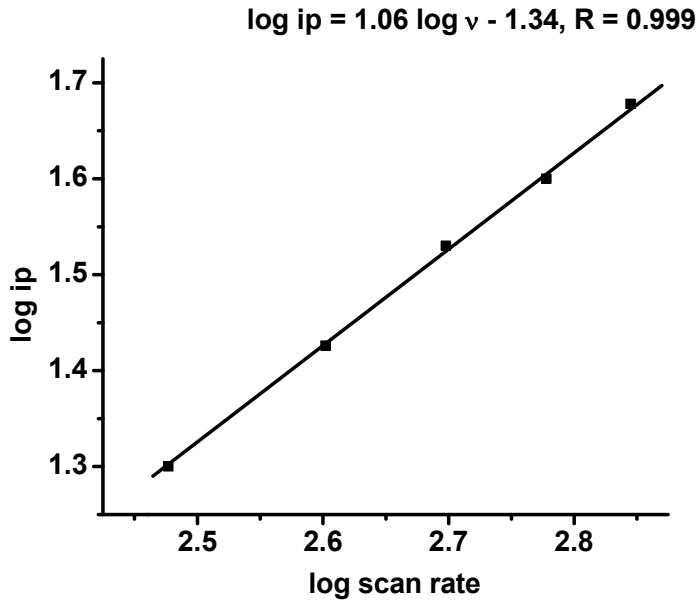

Figure 4.9 Plot of log ip vs log scan rate

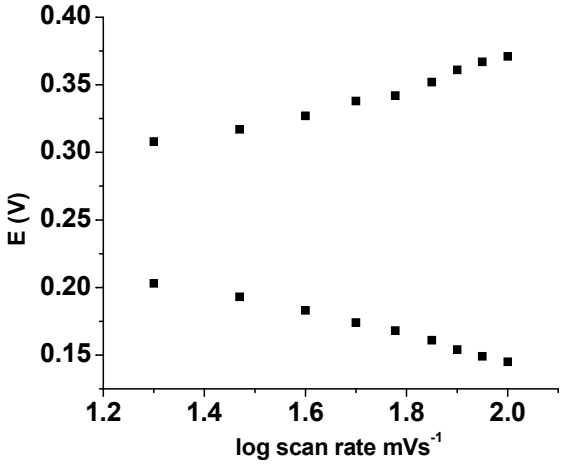

Figure 4.10 Influence of scan rate on the anodic and cathodic peak potential of 1×10^{-4} M Sudan I

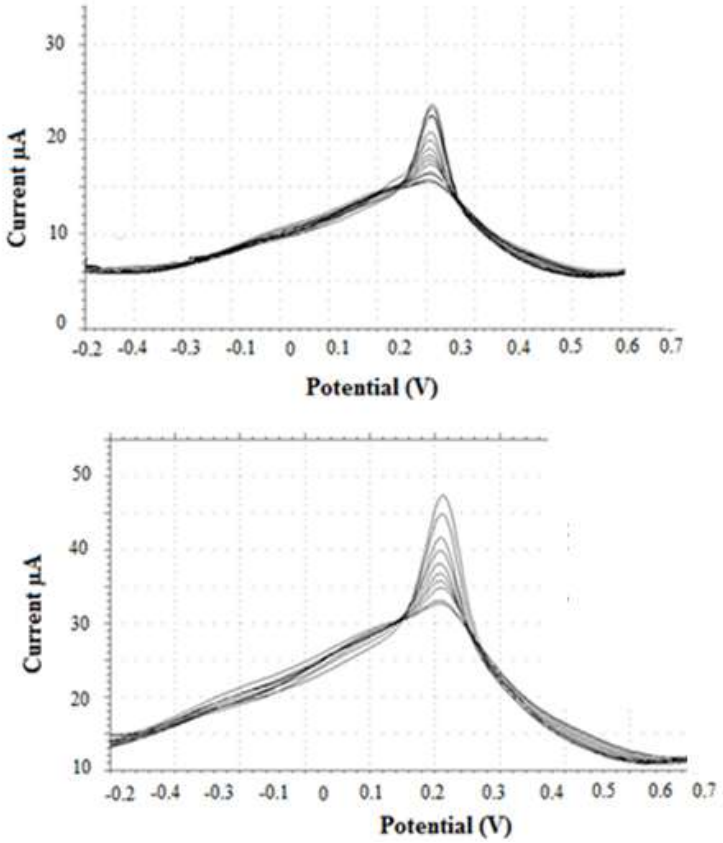

Figure 4.11 SWV response of Sudan 1 at different concentrations in 0.1 M HCl

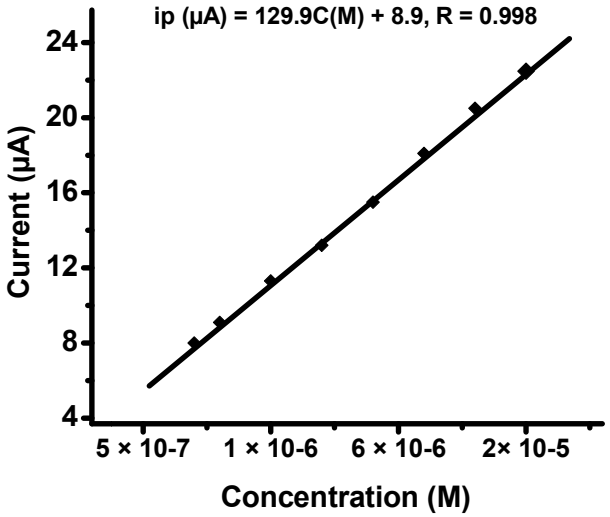

Figure 4.12 Linear plot of oxidation peak current versus various concentration of Sudan 1

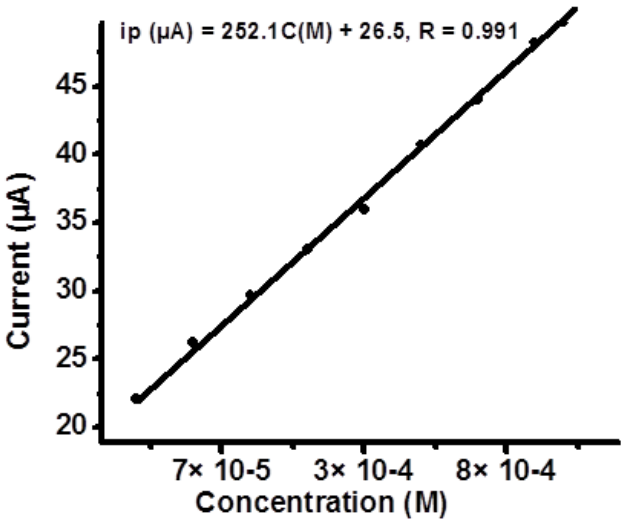

Figure 4.13 Linear plot of oxidation peak current versus various concentration of Sudan 1

.....ꕥ.....

Chapter 5

VOLTAMMETRIC SENSOR FOR BUTYLATED HYDROXYANISOLE (BHA)

Contents

Electrochemical behavior of artificial antioxidant, butylated hydroxyanisole (BHA), is investigated at a glassy carbon electrode modified with poly L- Cysteine [poly (L- Cys/GCE)] and is described in this chapter. BHA exhibits a pair of well - defined redox peak on poly (L- Cys/GCE) with E_{pa} = 0.069 V and E_{pc} = 0.004 V. The modified electrode showed good electrocatalytic activity towards the oxidation of BHA under optimal conditions. The limit of detection was found to be 4.1 $\times 10^{-7}$ M. The heterogeneous electron transfer rate,k_s, and charge transfer coefficient, α, was found to be 1.20 s^{-1} and 0.575 respectively. The average surface concentration of BHA on the surface of poly (L- Cys/GCE) was calculated to be 3.18 $\times$ 10^{-4} mol cm^{-2}. The analytical utility of the proposed sensor was evaluated by the successful determination of BHA in coconut oil and sesame oil samples.

5.1 Introduction

Food is essential for the survival of mankind. It is found to have a short shelf life and undergoes easy spoilage due to its varied composition. Since ancient times, antioxidants have become an essential group of food additives mainly because of their unique properties of enhancing the shelf life of food products without any loss to sensory or nutritional qualities. Antioxidants also help the body to protect itself against damage caused by reactive oxygen species (ROS) as well as those of nitrogen (RNS) and chlorine (RCS)[252]. US Food and Drug Administration (FDA) defined antioxidants as "substances used to preserve food by retarding deterioration, rancidity, or discoloration due to oxidation." Gum guaiac is reported as the first antioxidant approved for the stabilization of animal fats[253-254].

Antioxidants are usually classified into two: natural and synthetic antioxidants. Butylated hydroxyanisole (E-320, Fig. 5.1), a lipophilic organic compound, is a synthetic phenolic antioxidant. It is a mixture of two isomeric organic compounds, 2-tert-butyl-4-hydroxyanisole and 3-tert-butyl-4-hydroxyanisole. BHA has been added to oils and fat-containing foods for its antioxidant properties[255]. In presence of BHA, oxygen has greater affinity towards BHA rather than that on oils or fats thereby protecting them from spoilage. The conjugated aromatic ring of BHA is able to stabilize free radicals, sequestering them. By acting as free radical scavengers, further free radical reactions are prevented[256-257]. It is also used as an additive in cosmetics, pharmaceuticals, jet fuels, rubber, petroleum products and embalming fluid. BHA has a profound antimicrobial effect against aspergillus parasiticus, staphylococcus aureus, escherichia coli and salmonella typhimurium[258].

BHA has been alleged of inducing health menaces such as child hyperactivity, damage to the lungs, liver, kidneys etc. In several countries the use of these additives is subject to regulations, which define specific approved antioxidants, establish permitted use levels, and include labelling requirements. According to JECFA (Joint FAO/WHO Expert Committee on Food Additives), the Allowable Daily Intake (ADI) for BHA is 0–0.5 mg/kg body weight. Hence there is an increasing demand to ensure the fulfillment of legal requirements as well as quality-control procedures in the food industry. Although there have been regulations to limit the usage of BHA in our food products, it is important to thoroughly investigate the quantity of these antioxidants in food products.

Many analytical methods are reported for the quantification of BHA in food samples and these includes colorimetry and spectrophotometry[259-260], chromatographic techniques[261-264], micellar electro kinetics[265-266] etc. Voltammetric methods using modified electrodes[267-269] have also been reported for the determination of BHA in food samples.

Polymer-modified electrodes (PMEs) have received extensive application in voltammetric sensors because of their selectivity, sensitivity and homogeneity in electrochemical deposition, strong adherence to electrode surface and chemical stability of the film[270-272]. Among them, polymeric films obtained from amino acid or their derivates have gained a particular interest. L-cysteine (2-amino-3-mercaptopropanoic acid, L-Cys), one of the sulfur amino acids, is non-essential amino acid present in the human body. The poly (L-cysteine) film has been used to modify electrodes[273-274], due to its excellent electrocatalytic activity.

Electrochemical sensors are based on the electron transfer (ET) occurring at the interfaces during redox reactions: electrons flow from redox species within the bulk solution towards the electrode surface generating an electron flow that can be collected and measured. Cyclic voltammetric technique was employed to characterize the kinetics of electron transfer reactions.

The objective of the present work is to develop a convenient and sensitive electrochemical sensor using a glassy carbon electrode modified with an electropolymerised film of L- cysteine for the determination of BHA. The resulting sensor showed excellent reproducibility and stability when the experimental conditions for the fabrication of the developed method was optimized. Heterogeneous electron transfer constant,k_s, on bare and poly(L-Cys)/GCE electrodes were calculated using Laviron's[242] method. Much less information regarding k_s for the oxidation of BHA is available in literature. The developed sensor was successfully applied for the determination of BHA in oil samples.

5.2 Experimental procedures

5.2.1 Fabrication of poly (L- cysteine) modified glassy carbon electrode

Prior to modification, the bare GCE was polished to a mirror finish using alumina slurries with different powder size down to 0.05 μm. After polishing, the electrode was sonicated in ethanol and doubly distilled water for 5 min, successively, in order to remove any adsorbed substances on the electrode surface. The cleaned GCE was immersed in 5×10^{-3} M L- cysteine solution and 30 cyclic scans were carried out between -0.8 and 2.0 V at a scan rate of $0.1 Vs^{-1}$[275]. The resulting poly (L- cysteine) modified glassy

carbon electrode (poly (L-Cys)/GCE) was thoroughly rinsed with ethanol to remove the physically adsorbed L-cysteine monomers. A schematic representation of fabrication of (poly (L-Cys)/GCE) is represented in scheme 5.1.

5.2.2 Preparation of BHA solution

A stock solution of 1×10^{-1} M BHA was prepared by dissolving 0.180 g of BHA in10.0 mL of methanol. Solutions of different concentrations were prepared by the serial dilution of stock solution.

5.2.3Analytical procedure

10.0 mL of 0.1 M citrate buffer solution of pH 6.0 was used as the supporting electrolyte. A desired volume of BHA was pipetted into an electrochemical cell, followed by deareation with pumping O_2- free nitrogen. After a quiescent interval of 2 s, differential pulse voltammograms (DPV) was recorded from -0.50 to 0.30 V at a scan rate of 0.1 Vs^{-1}, with an amplitude of 0.05 V, pulse width of 0.06 s, sample width of 0.02 s and pulse period of 0.5 s. The peak current for oxidation of BHA was measured at 0.024 V. Prior to and after each measurement, the L- cysteine modified GCE was activated by successive cyclic voltammetric sweeps from -0.50 to 0.30 V at 0.1 Vs^{-1} in the electrolyte solution until the voltammograms kept unchangeable to achieve a reproducible electrode surface.

5.3 Sample preparation

5.3.1Treatment of vegetable oil samples

5.0 g of a vegetable oil sample was placed into a 100.0 mL Erlenmeyer flask (with a screw cap) and 5.0 mL of pure methanol was added. After being

shaken, with the use of a laboratory shaker for 5 min, the mixture was transferred to a 10.0 mL centrifuging tube and centrifuged at 3000 rpm for 5 min. After a settling time of 2 min, the extracts were transferred into a 25.0 mL flask. The above extraction procedure was repeated twice, all the extracts were collected, and transferred into the 25 ml flask; and then the solution was diluted to the mark with methanol[276]. An adequate amount of this sample solution was transferred into an electrochemical cell and BHA was determined by standard addition method.

5.4 Results and discussions

5.4.1 Surface area study

The cyclic voltammetric analysis with redox reactions of 2.0×10^{-3} M $K_3Fe(CN)_6$ was used to evaluate the electrochemical behavior of bare GCE and poly(L- Cys)/GCE at a scan rate of 0.1 V s^{-1}. The effective surface area of the electrodes was determined using the Randles–Sevcik equation: [200]

$$I_p = (2.69 \times 10^5)\, A\, n^{3/2}\, D_R^{1/2} C\, \nu^{1/}2 \quad \text{..... (5.1)}$$

For $K_3Fe(CN)_6$, n = 1 and $D_R = 7.6 \times 10^{-5}$ cm^2 s^{-1}. From equation (5.1), the effective surface area (A) is proportional to the value of $Ip/v^{1/2}$. Based on the slope of the linear relationship between Ip and square root of scan rate, the effective surface areas of the bare and poly (L- Cys)/GCE were calculated to be 0.017 cm^2 and 0.0351 cm^2 respectively. The effective surface area of poly (L- Cys)/GCE was found to be about two times greater than that of bare GCE which is a strong evidence for the successful and effective modification of GCE using L- cysteine.

The morphological features of bare GCE and modified GCE were studied using SEM. The difference in the morphologies of bare and modified electrodes (Fig. 5.2a and 5.2b) is an evidence for the modification of GCE.

5.4.2Electrochemical behavior of BHA

Cyclic voltammetry was used to investigate the electrochemical behavior of 1.0×10^{-5} M BHA in 0.1 M citrate buffer solution (pH 6.0) on a bare glassy carbon electrode (GCE) and a poly (L- Cys)/GCE at a scan rate of 0.1 Vs^{-1}. At bare GCE (Fig. 5.3a), BHA shows an irreversible behavior with an oxidation peak at 0.115V (2.3 μA). However, on poly (L- Cys)/GCE, (Fig. 5.3 b), BHA exhibits a pair of well – defined redox peak with E_{pa} = 0.069 V (i_{pa} = 15 μA) and E_{pc} = 0.004mV (i_{pc} = 10 μA). The overpotential of BHA lowered by 0.045 V on poly (L- Cys)/GCE compared to bare GCE and an enhancement in peak current was also observed. The separation between anodic and cathodic peak potentials, (ΔE_p = 0.065 V), was greater than the value of $\frac{59}{n}$ mV (n=2), indicating that the electrochemical behavior of BHA under optimized conditions is a quasi-reversible two electron process. The formal potential, $E^{0'} = \frac{E_{pa} + E_{pc}}{2}$ of the electrode was 0.036 V.

Comparison of voltammetric studies revealed that the oxidation of BHA (1×10^{-5} M) occurred at a lower potential (E_p = 0.023 V; i_p = 38.8 μA) using DPV than CV. Therefore DPV technique was chosen for further studies.

5.4.3 Optimization studies

5.4.3.1Effect of supporting electrolyte and pH

The electrochemical behavior of 1.0×10^{-5} M BHA in 0.1 M solution of different supporting electrolytes (citrate buffer, phosphate buffer, acetate buffer, HCl, NaOH, KNO_3) were compared by DPV. Since oxidation peak current of BHA in citrate buffer solution was more sensitive and the peak shape was more preferable than in the other supporting electrolytes, it was selected for further studies.

The effect of pH on the oxidation peak potential of BHA at L- cysteine modified GCE was investigated (Fig. 5. 4a). The peak potential corresponding to the BHA oxidation shifted negatively at a slope of −58.3 mV/pH in the range of 1–7, revealing that proton takes part in the oxidation of BHA[277]. A linear relationship between peak potential (Ep) and pH was observed for BHA following the equation, Ep = -58.3 pH + 0.37, R =0.9778. The slope was in agreement with the theoretical value (59 mV/pH), indicating that the oxidation process of BHA occurred with the involvement of equal number of electrons and protons. However, a maximum catalytic peak current was observed at pH 6.0, (Fig. 5.4 b), beyond pH 6.0; the peak current exhibited a gradual decrease. Therefore, citrate buffer of pH 6.0 was used for the determination of BHA to achieve higher sensitivity.

5.4.3.2Effect of scan rate

In order to study the nature of electrode process occurring at the electrode surface, the effect of scan rate on the oxidation peak current of 1×10^{-5} M BHA was studied by cyclic voltammetry (Fig.5.5). The plot of

peak current vs. square root of scan rate ($\nu^{1/2}$) is linear over the whole range of scan rate studied (Fig.5.6), which indicates that it is a typical diffusion controlled system, and the equation can be expressed as $ip\ (\mu A) = 3.71\ \vartheta^{\frac{1}{2}} - 0.14, R^2 = 0.998$. Also, logarithm of peak current, log (ip), was plotted against the logarithm of scan rate, log ν. This relationship was found to be linear, ($\log ip(\mu A) = 0.54\ \log \nu + 0.38, R = 0.999$) (Fig. 5. 7) with a slope of 0.54, which is near to the theoretical value of 0.5 for a diffusion controlled process [249].

The number of electrons involved in the oxidation of BHA was calculated using the equation:

$$i_p = \frac{nFQ\nu}{4RT} \quad \text{.....(5.2)}$$

where i_p represents the anodic peak current, Q is the amount of charge integrated from the area of cyclic voltammetric peak, T is the temperature in Kelvin (298K), R is the universal gas constant (8.314Jmol^{-1}K^{-1}), F is the Faraday constant (96500 Cmol^{-1}) and n is the number of electrons transferred. From the slope of i_p versus υ, n was calculated to be 1.79 (≈ 2). Hence it can be concluded that the oxidation of BHA involves two electrons and two protons[278] (Scheme 2). The anodic peak observed for the oxidation of BHA may be due to the oxidation of the hydroxyl group present in BHA.

The study of rates of electron transfer reactions at the electrode electrolyte solution interface is a fundamental issue in electrochemistry. Based on Laviron's theory[242], the apparent charge transfer rate constant, k_s, and the charge transfer coefficient α, of a surface confined redox couple can

be measured from CV experiments by considering the variation of anodic and cathodic peak potentials as a function of logarithm of scan rate. A plot of peak potentials (E_p)*vs* logarithm of scan rate is depicted in Figure 5.8 and from slopes of the plots the transfer coefficients can be calculated using the equations;

$$E_{pa} = a + \frac{2.303\ RT}{(1-\alpha)n_\alpha F} \log\nu \quad \text{..... (5.3)}$$

$$E_{pc} = b - \frac{2.303\ RT}{\alpha n_\alpha F} \log\nu \quad \text{.....(5.4)}$$

Where E_{pa} is anodic peak potential and $E_{pc}$is cathodic peak potential respectively. The evaluated values for α is 0.58. The heterogeneous electron transfer rate in the redox probe can be determined using the Eq.(5.5):

$$\log k_s = \alpha log(1-\alpha) + (1-\alpha)\log\alpha - \log\frac{RT}{nF\vartheta} - \alpha(1-\alpha)\frac{nF\Delta Ep}{RT} \text{.....(5.5)}$$

The rate constant for the electron transfer process depends on the nature of the electrode material. The value of k_s on bare GCE and poly (cys/GCE) was found to be 2.6×10^{-3} s^{-1} and 1.20 s^{-1} at 0.1 Vs^{-1}. The higher value of k_s on modified GCE revealed that electron transfer through the L-cys/GCE was more facile than that for bare GCE.

The average surface concentration (Γ) of BHA on the surface of modified GCE was estimated based on the slope of ip vs. ν using the equation[230] (5.6) and found to be 3.18×10^{-4} mol cm^{-2}.

$$i_p = \frac{n^2F^2A\tau\vartheta}{4RT} \quad \text{.....(5.6)}$$

5.4.3.3 Interference of coexisting substances

In order to evaluate the selectivity of the poly (L- Cys) modified electrode towards the oxidation of BHA, the effect of various substances, which are commonly present with the antioxidant in commercial food samples, such as butylated hydroxy toluene (BHT), tert- butyl hydroquinone (TBHQ), ascorbic acid, sodium sulfite, citric acid, acetic acid and EDTA, were studied using the proposed sensor and the results are incorporated in Table.5.1.

From Table.5.1, it was concluded that a 100 fold excess of BHT, TBHQ, sodium sulfite, citric acid, NaCl, acetic acid and EDTA had no influence on the voltammetric determination of 1×10^{-5} M BHA using proposed sensor. A 1:1 ratio of ascorbic acid and propyl gallate were found to interfere in the determination of BHA. The above results ascertained that majority of the coexisting substances do not interfere with the determination of BHA and confirmed the acceptable selectivity of the proposed electrode.

5.4.3.4 Linearity range, limit of detection, stability and reproducibility

Figure 5. 9 displays the overlay of differential pulse voltammograms for different concentration of BHA under the optimized conditions using poly (L- Cys)/ GCE. A linear relationship was established between i_{pa} and the concentration of BHA in the range of 1.0×10^{-5} to 1.0×10^{-6} M (Fig. 5.10). The linear regression equation and correlation coefficient are: ip (μA) = 2.8C (M) + 0.41, R = (0.999), where *ip* is the oxidation peak current in μA and C is the concentration of BHA in M. The limit of detection was evaluated to be 4.1×10^{-7} M.

The performance of the modified electrode was evaluated by its repeatability, stability and reproducibility. Five parallel determinations using same poly (L- Cys)/ GCE were carried out in 1×10^{-5} M BHA and the relative standard deviation obtained was 3.9 %. This result infers the good repeatability of the modified electrode. The developed sensor retained 95% of its response for more than a week, pointing to the good stability of proposed sensor. In order to establish the reproducibility of the proposed sensor five determinations using different poly (L- Cys)/ GCE was carried out and the relative standard deviation obtained was 4.2%. These results proved that results can be reproduced at poly (L-Cys)/GCE sensor, without much difference.

A comparison between other voltammetric sensors for the determination of BHA was studied. From Table.5.2, it was concluded that compared to other reported voltammetric sensors, the oxidation of BHA occurred at a lower potential with a wide linear range at the proposed sensor.

5.5 Analytical applications

In order to evaluate the analytical applicability of the proposed sensor, it was applied to the determination of BHA in coconut oil and sesame oil samples by adapting standard addition method. The results presented in Table 5.3 indicate that a good recovery is observed. The good recoveries achieved in oil samples revealed that the developed poly (L-Cys)/GCE sensor has high sensitivity and selectivity for determining BHA in oil samples.

5.6 Conclusion

Poly (L-Cys)/ GCE was fabricated by electropolymerization of L- cysteine on GCE and the modified electrode was characterized by SEM. The electropolymerized film showed promising electrocatalytic activity towards the oxidation of BHA. The sensor exhibited very good linear range of 1.0×10^{-5} to 1.0×10^{-6} M with a detection limit of 4.1×10^{-7} M. The proposed sensor possesses high stability, good repeatability and excellent anti-interference ability. The good recoveries achieved in the real sample studies revealed the promising practical utility of the proposed sensor.

Table 5.1 Influence of various foreign species on the oxidation peak current of 1×10^{-5} M BHA

Foreign species	Concentration	Signal change (%)
BHT	1×10^{-3}	4.8
TBHQ	1×10^{-3}	4.8
Sodium sulfite	1×10^{-3}	2.1
Citric acid	1×10^{-3}	2.8
Sodium chloride	1×10^{-3}	1.9
Acetic acid	1×10^{-3}	2.6
EDTA	1×10^{-3}	3.3
Propyl gallate	1×10^{-5}	9.8
Ascorbic acid	1×10^{-5}	23.1

Table 5.2 Comparison of proposed sensor with other reported voltammetric sensors for the determination of BHA

Electrode	E_p (mV)	Linear range (M)	LOD[a] (M)	References
[1]BDD	896	$3.3 \times 10^{-6} – 5.5 \times 10^{-6}$	7.7×10^{-7}	268
[2]NiHCF / GWCE	312	1.2×10^{-6} - 1.07×10^{-3}	6.0×10^{-7}	279
[3]Pt	700	3.0×10^{-5}- 1.0×10^{-3}	-	280
[4]Pt/MWCNT	340	1.00×10^{-6} - 1.0×10^{-7}	9.5×10^{-8}	281
[5]Poly(L-Cys)/GCE	20	1.00×10^{-6} - 1.0×10^{-5}	4.1×10^{-7}	Proposed sensor

a – limit of detection
[1]BDD –boron doped diamond electrode
[2]NiHCF / GWCE -nickel hexacyanoferrate (NiHCF) surface modified graphite wax composite electrode
[3]Pt – bare platinum electrode
[4]Pt/MWCNT – multiwalled carbon nanotube modified platinum electrode

Table 5.3 Results obtained for the determination of BHA in oil samples by the proposed method

Sample	Added (M)	Found (M)	R.S.D* (%)	Recovery** (%)
Coconut oil	1.00×10^{-5}	0.982×10^{-5}	4.4	98.2
	5.00×10^{-5}	5.09×10^{-5}	1.8	101.8
Sesame oil	1.0×10^{-5}	1.02×10^{-5}	2.7	102.0
	5.0×10^{-5}	5.10×10^{-5}	1.9	102.0

*R.S.D –relative standard deviation
** - average of six replicates

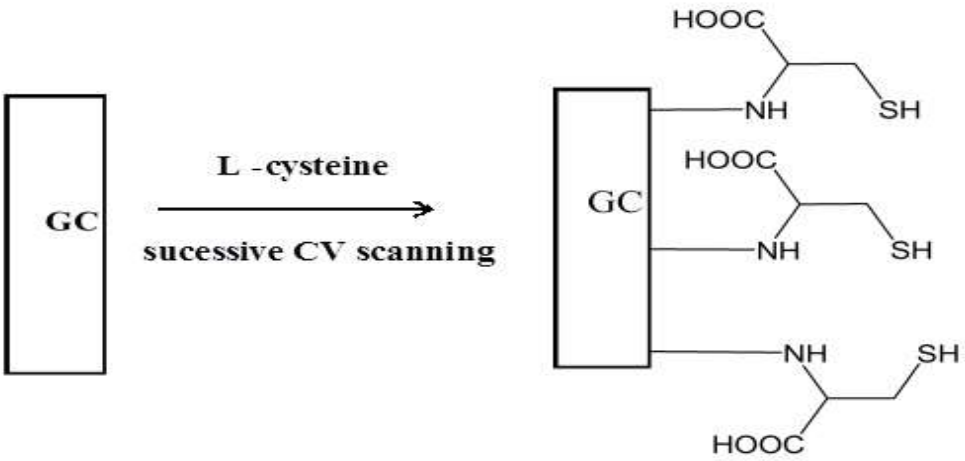

Scheme 5.1 Schematic representation of the fabrication of poly (L-Cys) on GCE

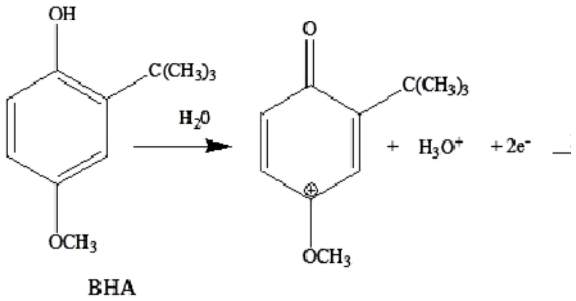

Scheme 5.2 Mechanism for the oxidation of BHA

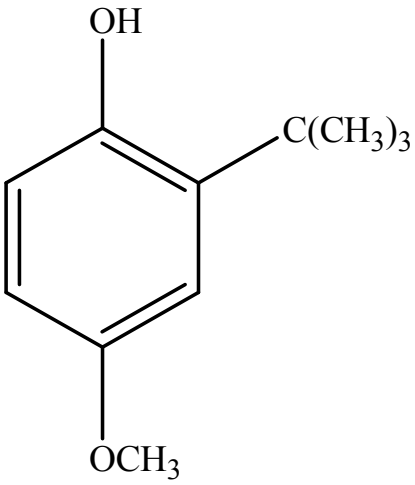

Figure 5.1 Structure of BHA

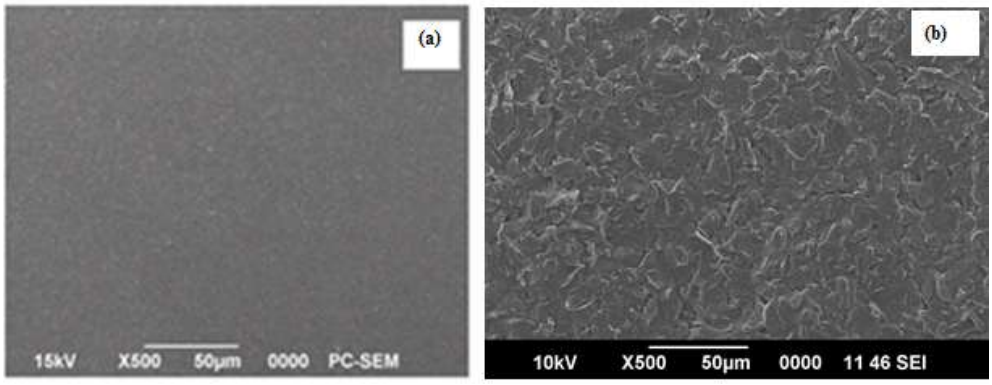

Figure 5.2 SEM images of a) bare GCE and b) poly (L- Cys)/GCE

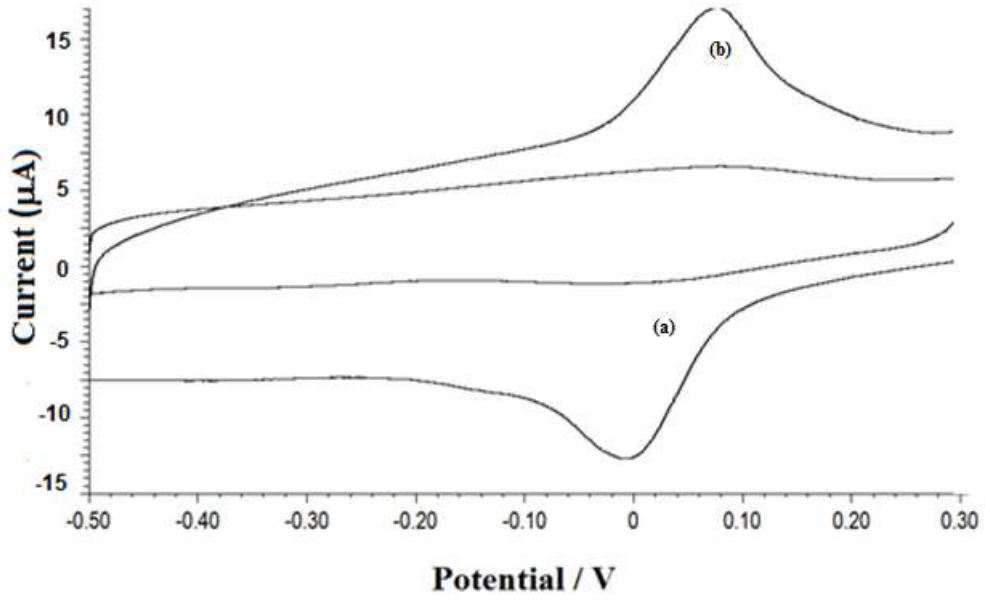

Figure 5.3 Electrochemical response of 1×10^{-5} M BHA at a bare glassy carbon electrode and poly (L- Cys)/GCE in 0.1 M citrate buffer of pH 6.0

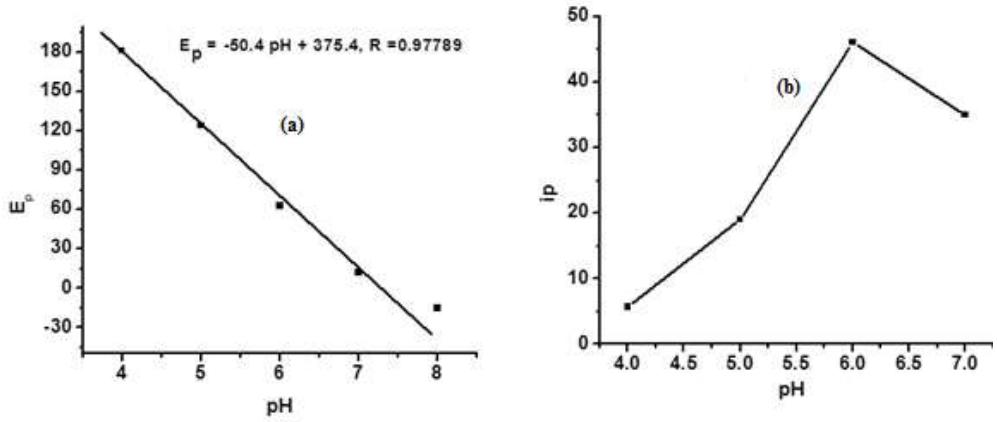

Figure 5.4 Effect of pH on a) peak potential and b) peak current of 1×10^{-5} M

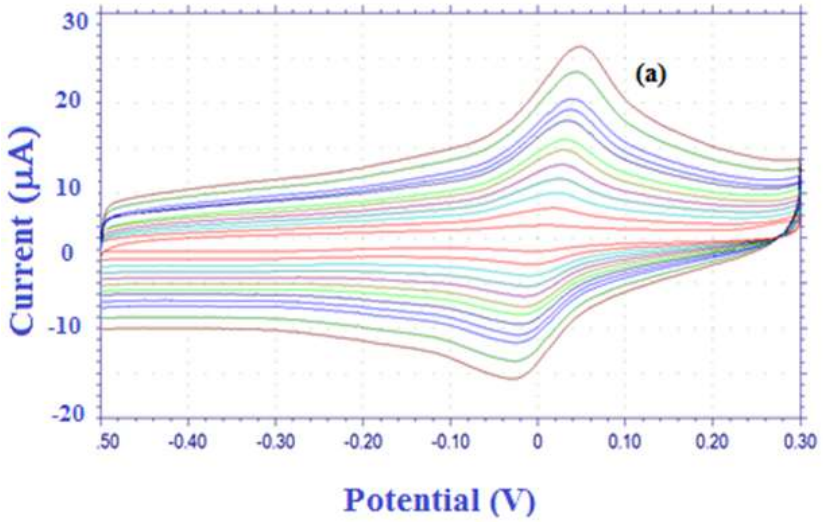

Figure 5.5 Overlay of cyclic voltammogram for oxidation of BHA at different scan rates

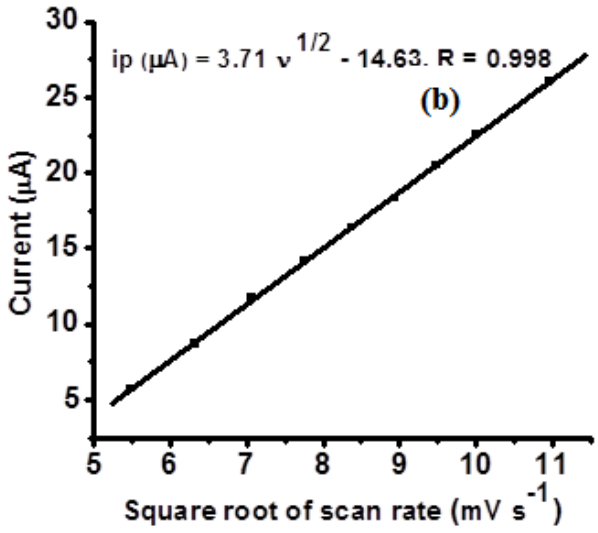

Figure 5.6 Plot of peak current with square root of scan rate

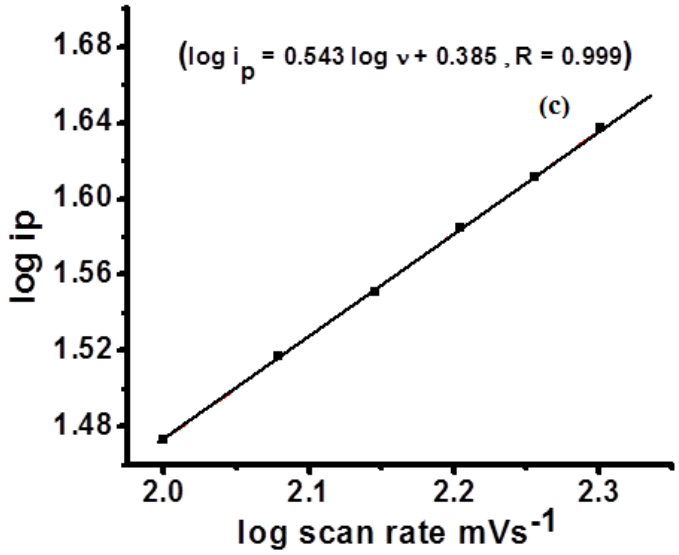

Figure 5.7 Plot of logarithm of peak current vs. logarithm of scan rate

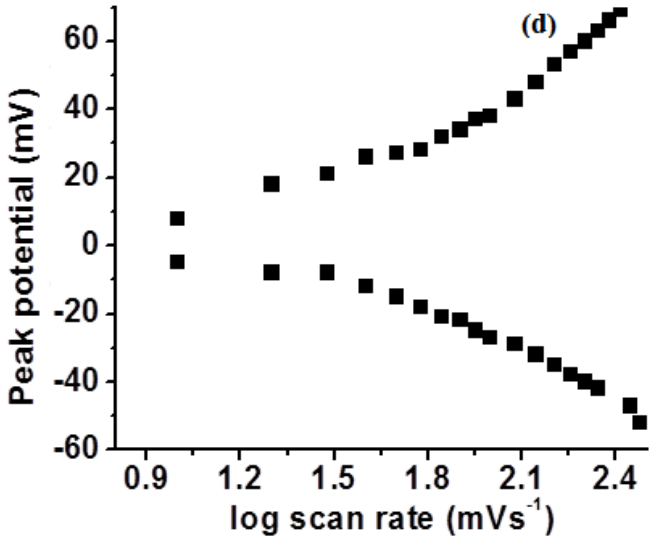

Figure 5.8 Plot of peak potential vs. logarithm of scan rate

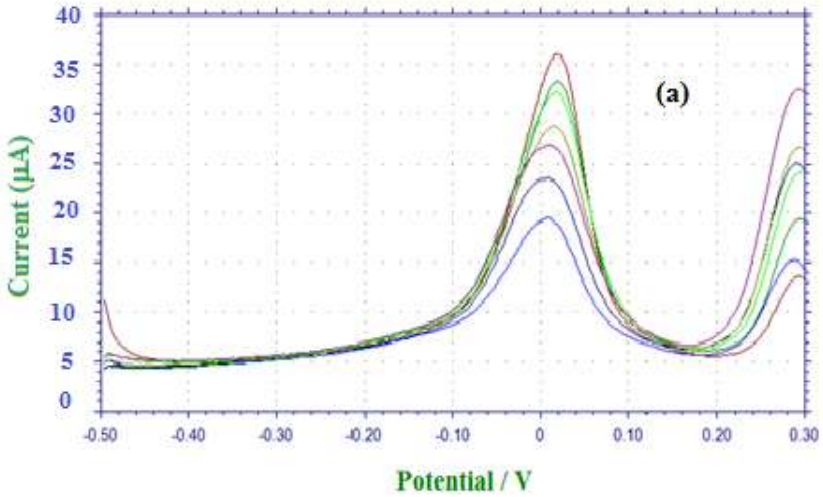

Figure 5.9 Overlay of DP voltammograms for oxidation of BHA at poly (L- Cys)/GCE at different concentrations

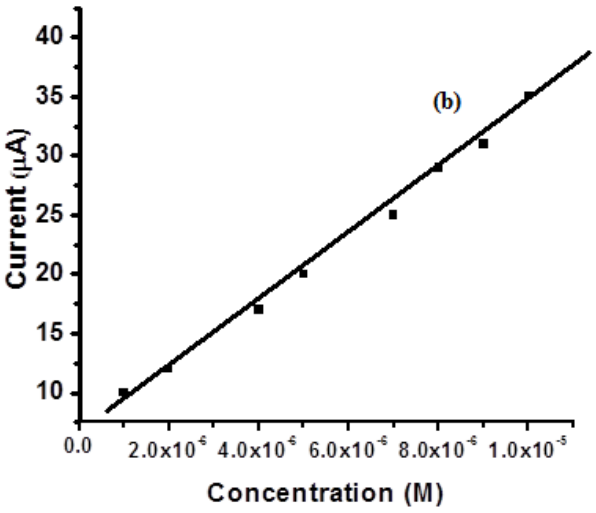

Figure 5.10 Plot of oxidation peak current versus different concentration of BHA

Chapter 6

FLUORESCENT SENSOR FOR NIMESULIDE

Contents

This chapter presents the development of a fluorescent sensor for the determination of nimesulide (NIM) using trioctylphosphine oxide modified CdSe quantum dots (TOPO/CdSe QDS) as fluorescent probe. TOPO/CdSe QDs was synthesized in organic media and its interaction with various non-steroidal anti-inflammatory drugs was studied. From the results it was demonstrated that fluorescence intensity of TOPO/CdSe QDs was selectively quenched by NIM. Under optimal experimental conditions, the intensity of quenching is linearly related to NIM concentration in the range 8.2×10^{-7} - 4.01×10^{-5} M. The mechanism for fluorescence quenching is discussed. Finally, the potential application of the proposed method for the trace determination of NIM in pharmaceutical formulation was carried out and the results were compared with the standard method for NIM analysis.

6.1 Introduction

Non – steroidal anti - inflammatory drugs (NSAIDs) are of great interest in medicine as they are widely used for mild to moderate pain relief as well as in the treatment of osteoarthritis and rheumatoid arthritis. Their action is attributed to the inhibition of cyclooxygenase enzyme, which in turn prevents the biosynthesis of certain prostaglanidins[282].

Nimesulide, (4- Nitro- 2- phenoxy- methanesulfonanilide, NIM, Fig 6.1) is a non-steroidal anti- inflammatory drug (NSAID). It is a sulfoanilide drug and is selective for cyclooxygenase-2 (COX-2) inhibition[283]. It has potent analgesic, anti-inflammatory and antipyretic activities on oral and rectal administration. It is used for the treatment of musculoskeletal disorder, dyemenorrhoea, thrombophlebitis and dental pain. The gastrointestinal safety offered during the consumption of NIM is due to its non - acidic nature. NIM has a pka value of 6.5, which prevents the back diffusion of hydrogen ions responsible for tissue damage[284-285].

NIM is bound to human plasma proteins and is distributed into the synovial fluids. The drug undergoes extensive metabolism in the liver. Both the phenoxy ring moiety and the aromatic nitro group may be responsible for metabolic biotransformation. 4-hydroxynimesulide, the principal metabolite, is responsible for the anti-inflammatory activity of the compound[286]. Even though this drug has been projected as a useful alternative to other NSAIDs, serious hepatic[287-288], renal[289-290] and other adverse effects[291-293] followed by the administration of NIM has been reported.

Several analytical methods such as HPLC[294-296], spectrophotometry[297-298], electrochemical methods[299-300], ion association methods[301], capillary zone electrophoresis[302] etc. have been reported for the quantitative determination of NIM. However, the above methods are expensive and time-consuming.

The unique properties of colloidal luminescent semiconductor nanoparticles or quantum dots (QDs), attributed to quantum confinement effects have elicited intensive research for sensing, labeling and imaging applications. QDs have high quantum yields, broad absorption spectra, narrow size tunable emissions and are resistant to photo bleaching as well as to chemical degradation[303]. The QD surfaces are usually capped by long chain organic moieties such as trioctylphosphine (TOP) and trioctylphosphine oxide (TOPO)[304-305], as part of their stable synthesis. QDs with variable surface capping ligands have been extensively used as fluorescent species for cell labeling, tumor imaging and clinical diagnosis[304, 306]. They have been applied for quantitative determination of biological macromolecules[307-308]and drugs[309-310] based on their fluorescence quenching, which may be due to the changes of the surface states of QDs.

Cyclic voltammetry (CV) is a dynamic electrochemical method that has been successfully employed for quantitative estimation of the HOMO and LUMO levels of electro-active molecular species[311]. The mild experimental conditions made CV superior to other techniques such as photoelectron and tunneling spectroscopy[312]. Semiconductor Q-dots also have discrete energy levels and are expected to undergo electron transfer, mediated through the valence band edge (h1) and the conduction band edge (e1). As long as the vacuum level potentials of the common reference

electrodes are known, the band edge positions of electroactive materials can be estimated[313].

This chapter considers the development of a novel fluorescent sensor for the selective determination of NIM, among other NSAIDs such as mefenamic acid (MEF), rofecoxib (ROF), ibuprofen (IBU) and diclofenac sodium (DIC). The method is based on the quenching of fluorescence intensity of TOPO capped CdSe by nimesulide in organic media. The mechanism of quenching was explained based on Photo Induced Electron Transfer (PET)[314]. In PET the possibility of electron transfer can be predicted from the reduction potential of CdSe QDs and drugs that were obtained using cyclic voltammetric studies. The application of proposed method for the quantification of NIM in pharmaceutical formulation was carried out and the results were compared with the standard potentiometric method[315].

6.2 Experimental

6.2.1 Synthesis of CdSe Quantum dots

The procedure reported in literature was adopted for the synthesis of TOPO/CdSe QDs[316]. The procedure is as follows. 0.0127 g (0.1 mmol) of cadmium oxide (CdO) and 0.1140 g (0.4 mmol) of stearic acid were loaded into a 25 mL three-neck flask and heated to 150 °C under N_2 flow. After complete dissolution of CdO, the mixture was allowed to cool to room temperature. 1.94 g of TOPO and hexadecyl amine (HDA) were added to the flask, and the mixture was heated to 320°C under N_2 flow to form an optically clear solution. At this temperature, the Se solution containing 0.079 g (1 mmol) of Se dissolved in 0.238g (1.18 mmol) of trioctyl

phosphine (TOP) and 1.681 g of dioctylamine was swiftly injected into the reaction flask. After the injection, the temperature was set at 290 °C for the growth of the nanocrystals. 15.0 mL of chloroform was added to the reaction mixture at 30-50°C. The nanocrystal solution was separated from the insoluble reddish solid floating on the top of the chloroform solution by centrifugation and decantation. The nanocrystals were precipitated by adding methanol into the chloroform solution and isolated by centrifugation and decantation. The purified quantum dots were redispersed in chloroform and were left for evaporation in nitrogen atmosphere for 48h.

6.2.2 Preparation of stock solution

A standard stock solution (1×10^{-1} M) was prepared by dissolving 0.3088 g of NIM in 10.0 mL of acetone. Lower concentration of NIM solution was prepared by serial dilution of the stock solution with acetone.

6.2.3 Electrochemical studies

The electrochemical studies were performed with glassy carbon electrode as working electrode, Pt wire as auxiliary and Ag/AgCl as reference electrode. CdSe nanocrystals were dispersed in chloroform within nitrogen atmosphere. Cleaned glassy carbon electrode was dip-coated with this nanocrystal dispersion and dried for 2 h at 120°C. This process led to adsorption of nanocrystals on the electrode surface. Subsequently, the nanocrystal-coated electrodes were transferred to the electrochemical cell. Tetrabutylammonium hexafluorophosphate ($TBAPF_6$) was used as the supporting electrolyte for the voltammetric studies of quantum dots. A 1×10^{-3} M drug solution in phosphate buffer solution was used for voltammetric studies of drugs.

6.2.4 Analytical procedure

For investigating the effect of NIM on the fluorescence intensity of CdSe QD, different concentration of NIM was mixed with 500 µL of QDs and diluted to 2.0 mL with chloroform and fluorescence intensity was measured. All the samples were excited at a wavelength of 365 nm, and the fluorescence emission was scanned from 400 to 900 nm at room temperature.

6.2.5Preparation and analysis of pharmaceutical formulations

Ten tablets (Nise, Dr. Reddy's, India) were powdered well and dissolved in acetone. The solution was filtered through a Whatman No. 41 filter paper. The residue was washed with acetone for several times. The filtrate was collected in a volumetric flask and solution made up to the mark. Solutions of different concentrations were made by serial dilution of stock solution and the amount of NIM was determined as discussed in section 6.2.4.

6.2.6 Standard method for the determination of NIM

The standard method reported in United States pharmacopeia[34] was used for the validation of the proposed method. Stock solutions containing adequate amount of NIM was titrated against 0.1 M NaOH. The end point was determined potentiometrically. A calibration graph was recorded by plotting EMF against concentration of NIM. The solution of pharmaceutical formulation containing NIM was also titrated against 0.1 M NaOH potentiometrically. The amount of NIM in pharmaceutical sample was determined from the calibration graph.

6.3 Results and discussions

6.3.1 Characterization of TOPO/CdSe QDs

The emission spectrum of TOPO/CdSe QDs is as shown in Fig.6.2. The emission intensity was observed at 589 nm. The narrow line width of PL spectra suggests the particles having limited size distribution. Figure 6. 3, displays the absorption spectrum of TOPO/CdSe QDs with a shoulder centered at 564 nm. The optical absorption spectra of TOPO/CdSe QD gave information on the size of the nanocrystals. The particle size of TOPO/CdSe QDs was determined using the empirical formula[317]

$$D= (1.6122 \times 10^{-9})\lambda^4 - (2.6575 \times 10^{-6})\lambda^3 + (1.6242 \times 10^{-3})\lambda^2 - (0.4277)\lambda + (41.57) \quad (6.1)$$

where λ(nm) is the first exciton peak of TOPO/CdSe spectrum. The particle size calculated using Eqn: 6.1 was 3.3 nm. Transmission electron microscopy (TEM) is the most common technique used to determine nanocrystal size. Figure 6.4 shows TEM image of TOPO/CdSe QDs. The average size of TOPO/CdSe QDs observed from TEM analysis was 3.07 nm, which was considerably in the range of that obtained from UV analysis.

6.3.2 Sensor for nimesulide

In order to understand the selectivity of fluorescent sensor, the influence of various NSAIDs of different class, on the fluorescence intensity of TOPO/CdSe QDs was compared. From Fig. 6.5 it was evident that only NIM was able to turn – off the fluorescence intensity of TOPO/CdSe QDs. In order to study the effect of functional groups in NIM on fluorescence quenching of

TOPO/CdSe QDs, the influence of drugs such as sulfamethoxazole (which have a sulfonyl group as in NIM) and tinidazole (contains anitro group) on fluorescence intensity was also studied. From the experimental studies it was found that in presence of the above studied drugs there was no change in the fluorescence intensity of TOPO/CdSe QDs.

6.3.3 Effect of time

The experimental results on effect of reaction time and mixing sequence showed that reactions were complete within 5 min and the relative fluorescence intensity remained stable for at least 1.5 h. Therefore, the fluorescence spectrum was recorded after 5 minutes of mixing.

6.3.4 Mechanism of Quenching

Quenching mechanisms include inner filter effects, non- radiative recombination pathways, electron transfer processes and ion binding interactions[318-319]. In the case of quantum dots, different electron transfer mechanisms have been considered, with and without photoinduction of either QD or receptor. For the NIM receptor to be an effective quencher of QD emission, the suggestion is that it needs to be able to interact directly with one of the QD charge carriers (i.e., valence band holes or conduction band electrons), there by disrupting the radiative recombination process.

The UV- Visible absorption spectra of NIM (Fig 6.6a) shows no absorption band in the range 400- 700 nm, illustrating that the quenching effect is not due to an inner filter resulting from the absorption of the emission wavelength by NIM. There was no obvious change in the absorption spectra of TOPO/CdSe QDs before (Fig 6.6b) and after addition

of NIM (Fig 6.6c). Absence of blue- shift or red-shift in the fluorescence emission spectra with increasing concentration of NIM indicates that the QDs do not aggregates in the presence of NIM. Instead the emission intensity decreases significantly in agreement with the expected photoinduced electron transfer (PET) from the nanoparticles to the quencher[75]. In PET the possibility of electron transfer can be predicted from the redox potentials of the fluorophore and quencher. The energy change for PET is obtained using Rehm-Weller equation[320] (Eqn.6.2) considering the reduction potential of CdSe quantum dots (-0.38V, Fig 6.7) and NIM (-0.64V, Fig 6.8).

$$\Delta G_{PET} = E_{D+/D} - E_{A/A-} - E_{00} \quad \text{.....(6.2)}$$

$E_{D+/D}$ and $E_{A+/A-}$ are the redox potentials of the electron donors and acceptors respectively. The redox potentials were measured using cyclic voltammetry. The electrochemical data gives valuable information and allow the estimation of relative position of HOMO and LUMO levels. The excitation energy of CdSe quantum dots (E_{00}) is estimated using the emission wavelength (λem), where $E_{00} = h\nu = 12398.1/\lambda em$ (A^0). With use of the redox potentials and excitation energy, the ΔG_{PET} values were calculated. ΔG_{PET} values for electron transfer for all the drugs except NIM (ΔG_{PET} = -2.08 eV) was positive (Table 6.1). Therefore, it is assumed that photoinduced electron transfer may take place between CdSe quantum dots and NIM. This demonstrates the selective quenching of fluorescence intensity of CdSe quantum dots by NIM.

Selective quenching of fluorescence intensity of TOPO/CdSe QDs by NIM can be explained on the basis of band gap energy. The conduction

band (LUMO) and valence band (HOMO) edges were calculated using the equations:

$$E_{HOMO} = -(E_{ox} + 4.71)\ eV \quad \text{.....(6.3)}$$

$$E_{LUMO} = -(E_{red} + 4.71)\ eV \quad \text{.....(6.4)}$$

where 4.71 eV is the difference between vacuum level potential of the normal hydrogen electrode and the potential of the Ag/AgCl electrode[321-322], E_{ox} and E_{red} are the onset potentials of the oxidation and reduction process. For quenching to occur the energy of Lowest Unoccupied Molecular Orbital (LUMO) of quencher should lie between the band gap energy of fluorophore. Scheme.1 demonstrates that the LUMO of NIM (-3.76 eV) lies within the band gap of TOPO/CdSe QDs, whereas the LUMO for other drugs under consideration lies above the band gap energy. These results also support the selective fluorescence quenching of TOPO/CdSe QDs by NIM.

6.3.5 Analytical response

Under optimum conditions, the influence of different concentrations of NIM on the fluorescence intensity of TOPO/CdSe QDs is as shown in Fig. 6. 9. Upon addition of NIM to the TOPO/CdSe QDs, a significant decrease in fluorescence intensity was observed. It was found that the fluorescence quenching by NIM is concentration dependent and is best described by a Stern–Volmer equation:

$$I_o/I = 1 + Ksv\,[Q] \quad \text{.....(6.5)}$$

where Io and I are the fluorescence intensity of TOPO/CdSe QDs in the absence and presence of NIM respectively, [Q] is the concentration of NIM and Ksv is the Stern–Volmer fluorescence quenching constant. The calibration plot (Fig.6.10) of I_o/I *vs* concentration of NIM is linear in the range 8.2×10^{-7}- 4.01×10^{-5} M. The limit of detection (S/N=5) for NIM was 4.9×10^{-9} M.

Six replicate experiments were performed with 1×10^{-6} M NIM, and the relative standard deviation (RSD) was 4.5 %. This means the proposed method shows good reproducibility. In addition, after being stored in a refrigerator for one month, the TOPO/CdSe QDs was used for the determination of NIM, and there was no significant change in the fluorescence intensity when compared to the freshly prepared solution. These results suggest that the proposed sensor has a good stability.

6.3.6 Interference Study

The effect of coexisting substances, which pharmaceuticals often contains, on the fluorescence intensity of TOPO/CdSe QDs was also carried out to evaluate the selectivity of the proposed method. From Figure 6.11, it was concluded that the major coexisting species such as ascorbic acid, citric acid, urea, glucose, lactose, Na^+, K^+, SO_4^{2-} and Cl^- did not cause any observable interference when added up to 100 fold excess concentration compared with concentration of NIM [1×10^{-6}M].

6.4 Application studies

The proposed method was successfully applied to the determination of NIM in commercially available pharmaceutical and the results are shown in

Table 6.2. The obtained results were also compared with the standard method. As can be observed, a good agreement was achieved between both the proposed and standard method indicating the utility of present fluorescent sensor for determination of NIM. The agreement is also indicative of noninterference of other ingredients and the excipients which are present in the pharmaceutical formulation.

6.5 Conclusion

In the present chapter the use of TOPO/CdSe QDs for the selective determination of the drug NIM in presence of other non - steroidal anti - inflammatory drugs was demonstrated. Cyclic voltammetry was employed for the estimation of HOMO and LUMO levels and the electrochemical band gap was estimated from the HOMO and LUMO values. The good linear range and lower limit of detection proves the utility of the proposed nanosensor for the trace analysis of NIM.

.

Table 6.1 Calculated ΔG_{PET} values for drugs

Drug	ΔG_{PET}
ROF	+0.15
IBU	+ 0.37
MEF	+0.42
TNZ	+0.44
DIC	+ 0.47
SMZ	+ 0.06

Table 6.2. Determination of NIM in pharmaceutical sample

Sample	Declared amount (mg/tablet)	Method adopted	Found* (mg/tablet ± R.S.D)
Nise (Dr.Reddy's, India)	100.0	Proposed method	100.8 ± 0.19
		Standard method	101.5 ± 0.11

*Average of six determination ± Relative standard deviation

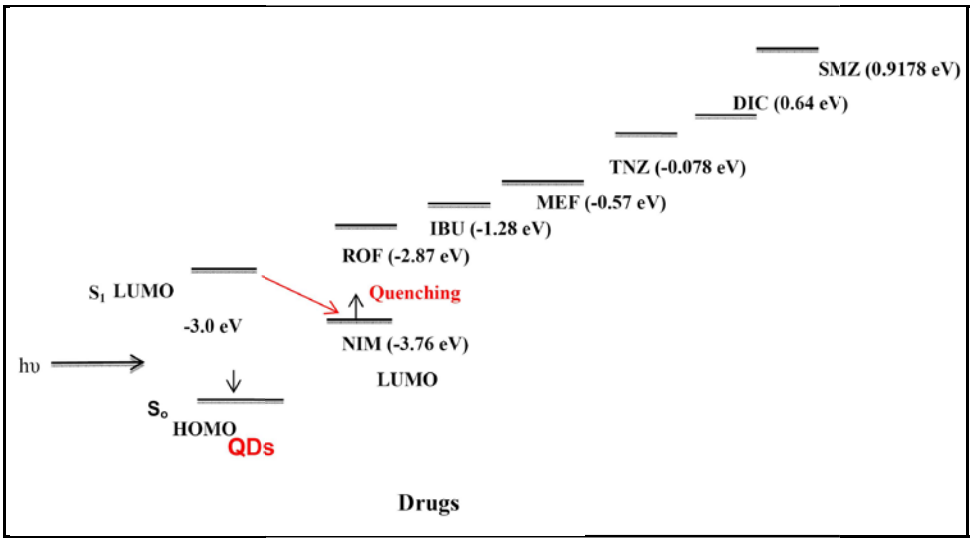

Scheme 6.1 Mechanism for selective fluorescence quenching of TOPO/CdSe QDs by NIM in presence of other drugs

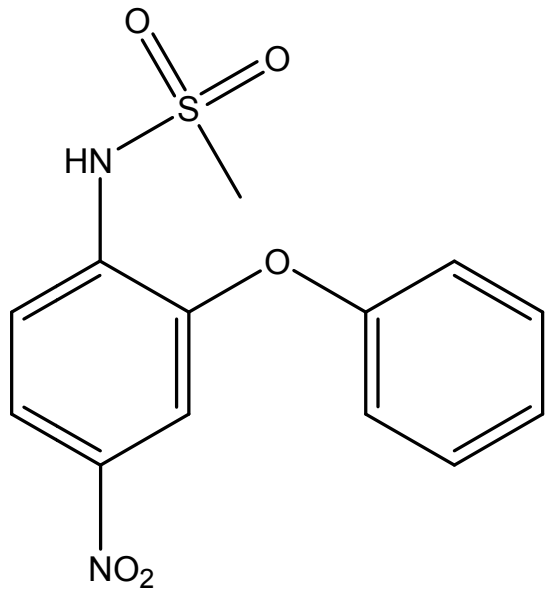

Figure 6.1 Structure of NIM

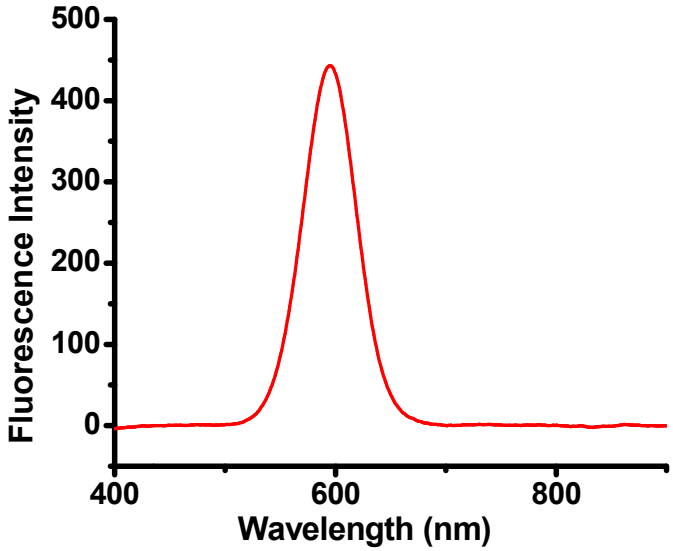

Figure 6.2 Emission spectra of TOPO/CdSe QDs

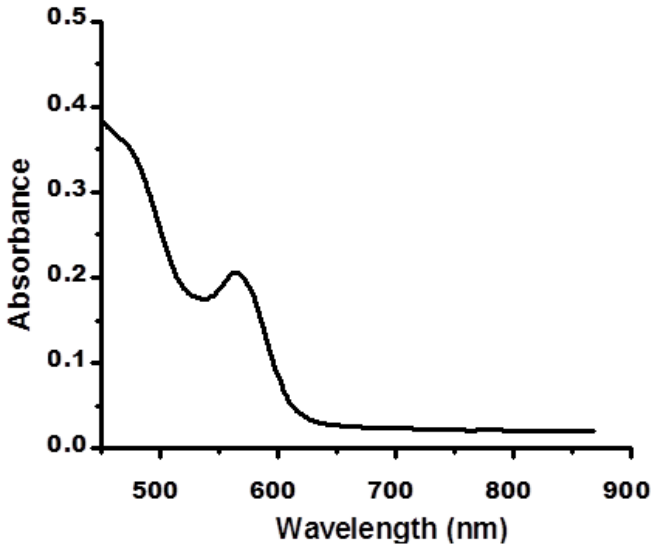

Figure 6.3Absorption spectra of TOPO/CdSe QDs

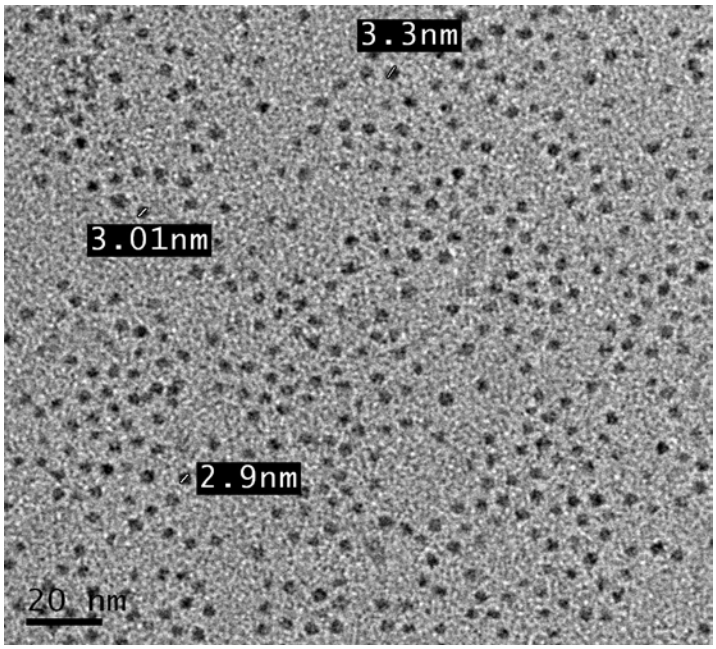

Figure 6.4 TEM image of TOPO/CdSe QDs

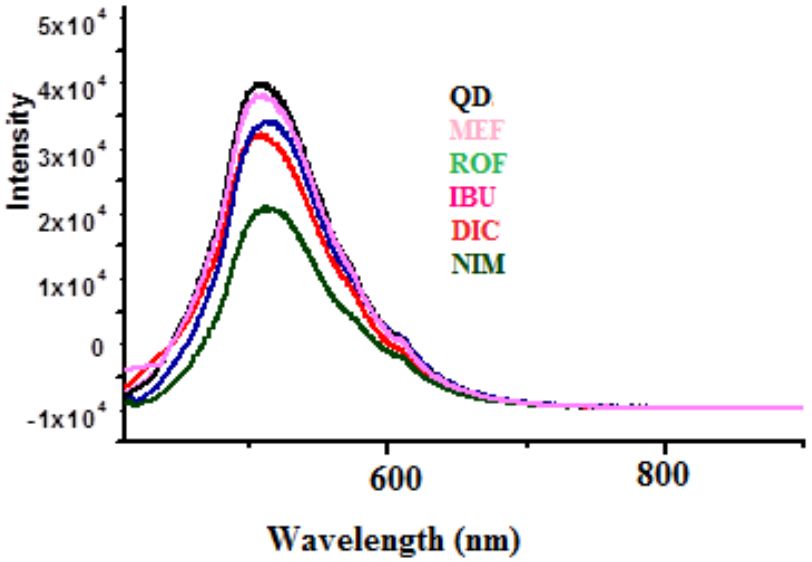

Figure 6.5 Effect of various NSAIDs on fluorescence intensity of TOPO/CdSe QDs

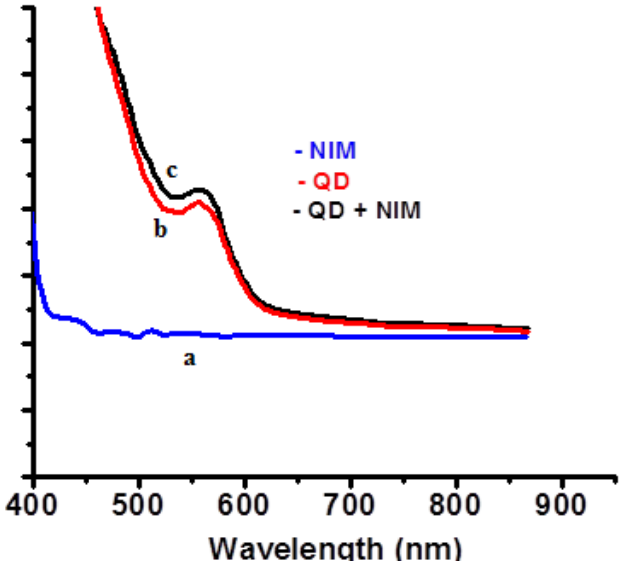

Figure 6.6 Absorbance spectra of (a) NIM alone (b) QD alone and (c) QD + NIM

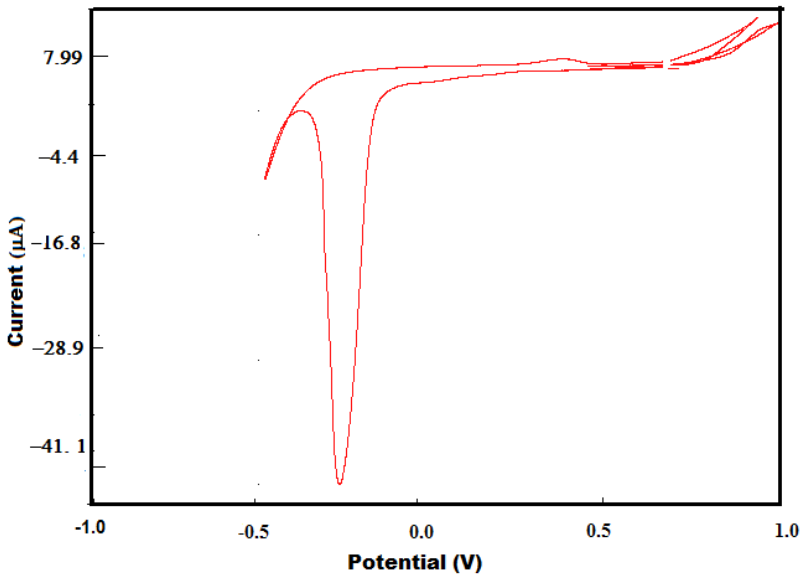

Figure 6.7 Cyclic voltammogram of QDs in 0.1 M tetrabutylammonium hexafluorophosphate

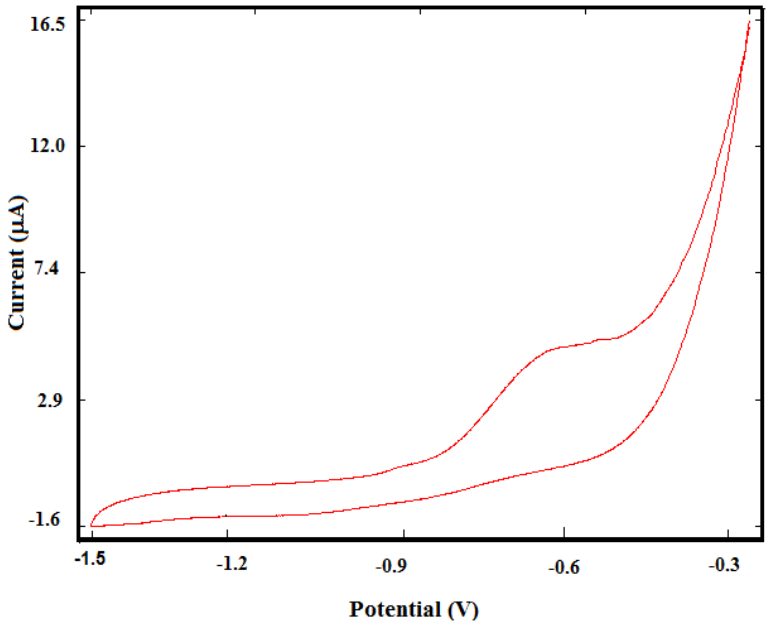

Figure 6.8 Cyclic voltammogram of NIM in 0.1 M PBS

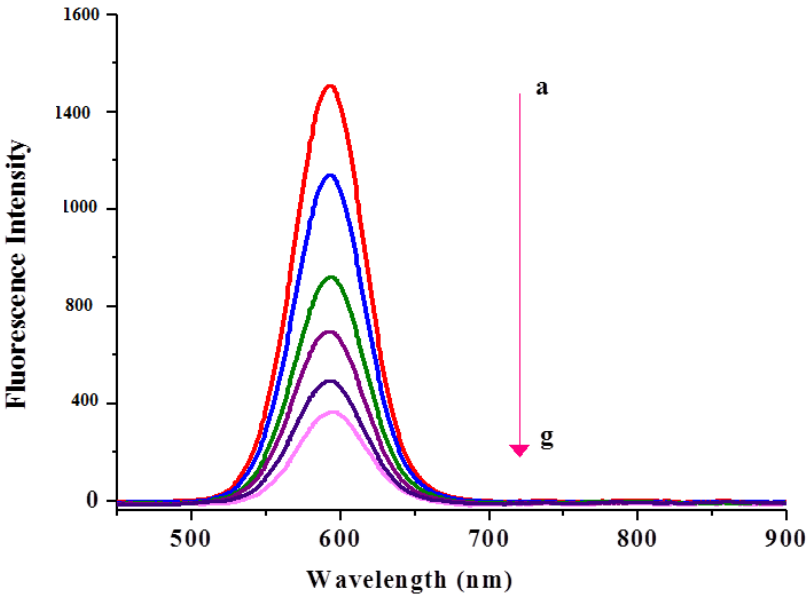

Figure 6.9 Effect of concentration of NIM on the fluorescence intensity of TOPO/CdSe QDs

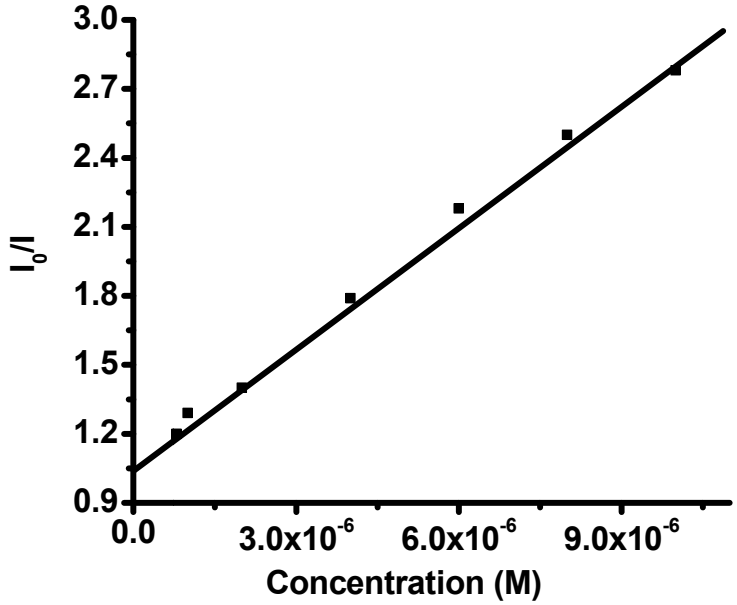

Figure 6.10 Stern – Volmer plot

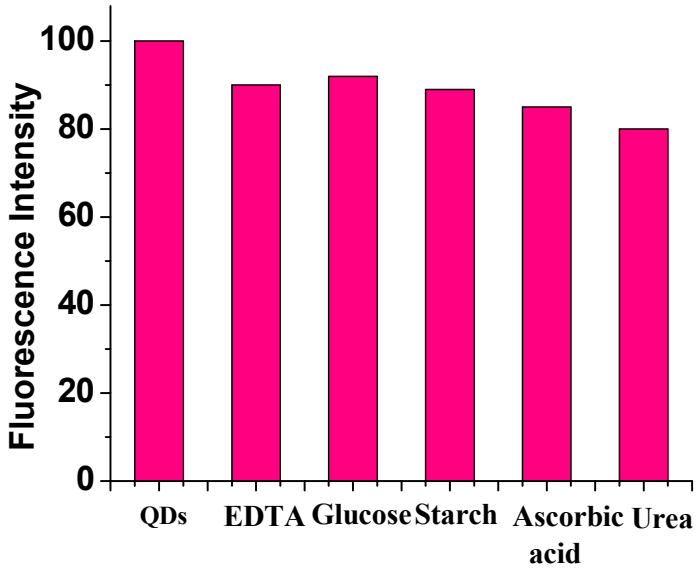

Figure 6.11 Effect of foreign species on the fluorescence intensity of TOPO/CdSe QDs

Chapter 7

FLUORESCENT SENSOR FOR Fe^{3+} ION

Contents

This chapter describes the use of highly fluorescent carbon nitride dots (CNDs) as fluorescent probe for the selective determination of Fe^{3+} ions. Acid driven microwave assisted synthesis strategy was employed for the production of CNDs. The CNDs are found to be sensitive and selective florescent probe for Fe^{3+} ions in aqueous media. Finally, this fluorescence sensor was successfully employed for the determination of Fe^{3+} ions in pharmaceutical formulation and the results agreed with the claimed values. The possible mechanism for quenching was also investigated and discussed in the chapter.

7.1 Introduction

Determination of metal ions from different matrices has continually gained remarkable importance[323-327]. Among the transition metals, iron is not only the most abundant metal but also a micronutrient for human body. Iron can exist in oxidation states ranging from −2 to + 6 and the most common are the ferrous (+2) and ferric (+3) states. Iron has a tendency to switch between the two oxidation states and as result it serve as a co-factor to enzymes involved in redox processess[328]. It also plays an essential role in photosynthesis[329-331].

Iron has many biological functions[332]such as it acts as an electron carrier in plants and animals, as haemoglobin, as oxygen carrier, as myoglobin for oxygen storage, for iron scavenging and storage and in nitrogenase[333]. It is also essential for brain development and function, muscle activity, regulation of body temperature, catecholamine metabolism etc. Both the deficiency and overload of iron can induce serious health problems depending on its concentration in the medium.

The iron concentration in the body is declared to be insufficient when iron losses or requirements exceed absorption. Some of the common causes of iron deficiency are inadequate dietary intake, blood loss, exercise, inability to absorb iron and increased need during the adolescent growth spurt, pregnancy and breast feeding. The consequence of iron deficiency includes anemia, impaired exercise capacity, functional alterations of the small bowel, impaired immunity and inability to maintain body temperature[334]. Gastrointestinal bleeding is a common cause of iron deficiency anemia. Iron is

supplemented as injection or solution or in tablet form when iron deficiency is diagnosed[335].

Although iron is essential for human life and iron deficiency can cause anemia, the unwise use of iron supplements cause harmful effects by inducing pro-oxidant conditions through the interaction of iron with O_2 and H_2O_2 in the body[336-338]. An excess of iron may also lead to neural disorders, such as Parkinson's disease[339-340] and Alzheimer's disease[341-342].

Various methods employed for the determination ofFe^{3+} includes inductively coupled plasma mass spectrometry (ICP-MS)[342-344], fluorescence[345-349], atomic absorption[350-351],colorimetry[352-353], flow injection[354], electrochemical methods[355-356], ion pair chromatography[357] etc. Due to the high sensitivity, non-destructive nature, ability to perform remote sensing etc, fluorescence sensing have recognized as the efficient analytical method for monitoring and quantifying Fe^{3+} ions. Many fluorescent sensors for selective and sensitive determination of Fe^{3+} ion was reported in the literature[358-361]. These sensors were based on organic dyes, fluorescent conjugated polymers, semiconductor quantum dots etc.

Carbon based nanomaterials such as carbon dots, have emerged as new class of florescent materials due to their unique structural and physical properties such as small size (3–10 nm), the ease of surface passivation by organic or other molecules, solubility in water, biocompatibility, photostability, inexpensive nature, strong and tunable photoluminescence[362-363]. Carbon nitride dots (CNDs), obtained by the substitution of carbon atoms in CDs with nitrogen has enhanced photoluminescence. In addition to enhanced photoluminescence, CNDs also exhibits unique properties[364-367]

similar to carbon dots which make them prospecting candidates in catalysis, sensors, and corrosion protection etc.

This chapter details the development of a fluorescent "Turn –Off" sensor for the selective determination of Fe^{3+}ions. Carbon nitride dots were used as the fluorophore for sensor fabrication. The developed sensor was stable for more than one hour and exhibited a good linear range. The mechanism involved in the fluorescence quenching by Fe^{3+} ions was investigated and reported in the chapter. The developed sensor was also satisfactorily applied for the determination of Fe^{3+} ions in pharmaceutical sample.

7.2 Experimental

7.2.1 Synthesis of Carbon Nitride Dots (CNDs)

Fluorescent CNDs were synthesized by microwave irradiation of N, N- dimethylformamide (DMF) in the presence of chlorosulfonic acid (CSA) according to procedure reported in literature[368]. 0.5 mL of chlorosulfonic acid (CSF) was added to 5.0 mL of DMF. The mixture was irradiated at 700 W for 40 seconds in a microwave oven. Finally the solution was transferred to 5.0 mL of distilled water. The excess precursors were removed by dialyzing against water through a dialysis membrane for 1 day.

7.2.2 Preparation of Fe^{3+} ion solution

1×10^{-1} M solution of Fe^{3+} ion was prepared by dissolving 0.482 g of ferric ammonium sulfate in 10.0 mL of double distilled water. In order to prevent hydrolysis, 0.1 M H_2SO_4 was added to the stock solution. Solutions

of different concentrations were prepared by the serial dilution of stock solution.

7.2.3 Analytical procedure

To investigate the sensing potential of the CNDs towards Fe^{3+} ions, a series of standard Fe^{3+} ion solutions of different concentrations were added to CNDs solution. The solution was mixed well and the fluorescence intensity was monitored. The relative fluorescence intensity [Io/I] versus Fe^{3+} ion concentration was used for calibration, where Io and I are the fluorescence intensities of the CNDs before and after adding Fe^{3+}, respectively. All the fluorescence measurements were performed with λex/λem at 365/493 nm.

7.2.4 Analysis of pharmaceutical dosage form

For the pharmaceutical analysis, ten tablets were weighed and powdered in a mortar. The average weight of a tablet was calculated. Powdered tablets were treated with dil. H_2SO_4 and the solution was heated for 30 minutes. The solution was then filtered and transferred to a 100.0 mL volumetric flask and diluted upto the mark. An aliquot of the filtrate was transferred into a calibrated flask and a series of dilutions was made covering the working concentration range (1.0×10^{-4} - 1.0×10^{-5} M). The solution was subjected to fluorescence measurements as mentioned in section7.2.3.

7.3 Results and discussions

7.3.1 Characterization of CNDs

Transmission Electron Microscopy (TEM) image of CNDs are shown in figure 7.1. The TEM image shows that the average size of CNDs is about

7.62 nm. These observations indicate the formation of nanoparticles. Figure 7. 2 represent the UV-Vis absorption spectra of the CNDs dispersion. From the figure it is clear that CNDs shows a strong absorption peak at 270 nm. The photoluminescence (PL) spectrum of the CNDs is depicted in Fig.7. 3. A strong PL emission spectrum centered at 493 nm was observed when it was excited at 365 nm, indicating the production of fluorescent CNDs. The photograph of CNDs dispersion under UV light (365 nm) exhibits a blue colour (Fig.7.4), gives an additional evidence unveiling strong blue fluorescence of CNDs.

7.3.2 Sensor for Fe^{3+} ions

The binding ability of CNDs towards different metal ions in aqueous medium was studied by observing the change in fluorescence intensity before and after the addition of the same amount of different metal ions (such as $Cu^{2+,}$ $Cr^{3+,}$, Zn^{2+}, Cd^{2+}, Hg^{2+}, Pb^{2+}, Co^{2+}, Ni^{2+}, $Cu^{2+,}$ Fe^{2+}). Figure7.5, highlight the sensitivity of fluorescence intensity of CNDs towards Fe^{3+} ions. The results proved that CNDs can be served as a selective fluorescent turn-off sensor for Fe^{3+} ions.

7.3.3 Optimization of experimental parameters

7.3.3.1 Effect of pH

pH plays an important role in the fluorescence intensity of fluorophores. Therefore the effect of pH on the fluorescence intensity of CNDs in the absence and presence of Fe^{3+} ion was investigated from pH 2 to 9. The fluorescence intensity of CNDs in the absence of Fe^{3+} ions was found to increase as the value of pH value varies from 2 to 6. After the addition of

Fe^{3+} ions, fluorescence intensity was found to increase up to a value of 4 and thereafter the fluorescence intensity decreases. The reduced fluorescence intensity of the sensor at higher pH may be due to the complex formation of Fe^{3+} ions with hydroxyl ion, resulting in a decreased concentration of free Fe^{3+} ions in sample solution. Thus a solution of pH 4 was used for further studies.

7.3.3.2 Effect of time

The effect of reaction time between Fe^{3+} ion and CNDs was studied. It was found that fluorescence intensity attained stability within 5 minutes and remained unchanged for more than one hour. The results suggested that the reaction of Fe^{3+}ions with CNDs might be completed very quickly and the sensor had a short response time. Therefore, the fluorescence emission intensity was recorded after the system has reacted for 5 minutes.

7.3.4 Calibration curve

The emission spectra of CNDs and its fluorescence titration with Fe^{3+}ions were recorded in 0.1 M PBS of pH 4. The effect of different concentration of Fe^{3+} ions on the fluorescence emission of CNDs is given in Fig.7. 6. As seen from figure, the fluorescence intensity of CNDs is quenched by the addition of Fe^{3+} ions. Quenching effect of Fe^{3+} ions on the fluorescence intensity of CNDS is found to be concentration dependent and is explained by Stern – Volmer equation[75]

$$I_o/I = 1 + Ksv[Q] \quad \text{.....7.1}$$

where I_o and I are the fluorescence intensity at 493 nm in the absence and presence of Fe^{3+} ions, respectively. K_{SV} is the Stern–Volmer fluorescence

quenching constant, which is related to the quenching efficiency of the quencher, and [Q] is the concentration of the quencher, [Fe^{3+}]. The fluorescence data were then analyzed by plotting Io/I versus [Fe^{3+}]. From Fig.7.7, a linear relationship between the fluorescence response and the concentration of Fe^{3+} ions was obtained in the range of 1.5×10^{-5} - 1×10^{-4} M and found to be Io/I = 1253 [C] + 0.9947 with correlation coefficient 0.999. The limit of detection (LOD) for Fe^{3+} ions was evaluated to be 3.7×10^{-7} M.

7.3.5 Quenching mechanism

The possible explanation for the quenching of the fluorescence intensity of CNDs in the presence of Fe^{3+} ions was investigated. Fe^{3+} ion may form a complex with the surface of CNDs resulting in a strong quenching of fluorescence intensity of CNDs via an electron transfer mechanism. As can be seen from Fig. 7.5, upon adding Fe^{3+}, the strong blue emission of the CNDs solution was quenched. The corresponding emission spectra indicate that the addition of Fe^{3+} ions decreases the fluorescence intensity of the CNDs, but has no effect on the emission wavelength. On the other hand, the emission spectra of CNDs do not overlap effectively with the absorption of Fe^{3+} ions. This observation suggests that resonance energy transfer would not be the dominant pathway for fluorescence quenching.

Quenching of fluorescence can occur as a result of the formation of a non-fluorescent complex between a fluorophore and anon-fluorescent molecule and the mechanism is called ‘static quenching’ or ‘ground sate complex formation’. An electron transfer mechanism is probably accounting for the FL quenching. Fe^{3+} is a paramagnetic ion ($3d^5$ $4s^0$) with empty d shells and can strongly quench the fluorescence of a nearby fluorophore

through electron transfer. This leads to its relatively high charge density with the stronger electron-withdrawing ability and compared with other transition-metal ions, Fe^{3+} has higher thermodynamic affinity and greater chelating processes towards ligands that have nitrogen atoms as the chelating atoms[369]. Since CNDs are nitrogen rich, upon addition of Fe^{3+} ions, there is chance for the formation of a non–fluorescent complex between CNDs and Fe^{3+} leading to the static fluorescence quenching[370]. The characteristic feature of static quenching is a change in the absorption spectra of the two molecules when they form a complex. From figure 7.8 (a and b), it was observed that, the absorption wavelength of CNDs at 270 nm shifted slightly to the right on addition of Fe^{3+} solution. This may be due to the formation of a complex between CNDs and Fe^{3+}[75].

7.3.6 Effect of other ions

To explore the utility of CNDS as a selective fluorescent sensor for Fe^{3+} ions, the interference from other metal ions on the fluorescence intensity of CNDs was investigated. The fluorescence intensity of CNDs upon treatment with 1×10^{-4} M Fe^{3+} ions was measured in the presence of 1×10^{-4} (1:1),1×10^{-3} (1:10) and 1×10^{-2} (1:100) M of other metal ions, including Cr^{3+}, Mn^{2+}, Fe^{2+}, Co^{2+}, Ni^{2+}, Cu^{2+}, Zn^{2+}, Cd^{2+}, Hg^{2+}, Pb^{2+} and Al^{3+} respectively. From the table it was clear that all the tested metal ions did not cause any significant change in the quenching ratio (I_0/I) of CNDs upto 100 fold excess concentration. This showed that the proposed fluorescence method could selectively determine Fe^{3+} ion in the presence of other metal ions.

7.3.7 Application

In order to understand the potential application of the developed sensor, the present method was applied to determine Fe^{3+} ions in tablet. Results are given in Table 7.2. As shown in Table 7.2, the R.S.D. was 1.3 %, and the results obtained by the present method agreed with the labeled values in the tablet.

A comparison of present sensor with other reported fluorescence sensors for Fe^{3+} ions were also carried out and is given in Table 7.3.

7.4 Conclusion

A CNDs based fluorescent sensor for Fe^{3+} ions in aqueous medium was developed. The fluorescence intensity of CNDs was significantly quenched by Fe^{3+} ions. The proposed sensor has proved to be highly selective to Fe^{3+} ions in presence of other metal ions. The mechanism of fluorescence quenching was discussed. The present sensor also explored the use of luminescent CNDs as an optical probe for the determination of Fe^{3+}ions in pharmaceutical formulations.

Table 7.1 Effect of other metal ions on the fluorescence intensity of CNDs

Foreign ions	Tolerance limit
Cu^{2+}	1×10^{-1}
Cr^{3+}	1×10^{-1}
Ni^{2+}	1×10^{-1}
Fe^{2+}	1×10^{-1}
Zn^{2+}	1×10^{-1}
Pb^{2+}	1×10^{-1}
Al^{3+}	1×10^{-1}
Mn^{2+}	1×10^{-1}
Hg^{2+}	1×10^{-1}
Co^{2+}	1×10^{-1}
Cd^{2+}	1×10^{-1}

Table 7.2 Application study

Sample	Declared amount (mg/tablet)	Found* (mg/tablet ± R.S.D**)
Dexoarange (Franco Indian, India)	32.8	31.08 ± 1.3

*average of six replicates
**relative standard deviation

Table 7.3 Comparison of proposed sensor with other fluorescent sensors

Sl. No.	Fluorescent sensors	Linear range (M)	LOD* (M)	References
1	MPA/CdTeQDs	7.5×10^{-8} - 1.8×10^{-6}	2.2×10^{-8}	371
2	NA-GQDs	0.5×10^{-6}-0.5×10^{-3}	0.1×10^{-6}	372
3	TA capped Cu NCs	1.0×10^{-8}-1.0×10^{-6}	1.0×10^{-8}	373
4	BA/GO	5.0×10^{-6}- 5.0×10^{-5}	6.4×10^{-7}	374
5	Proposed method	1.5×10^{-5}-1.0×10^{-4}	3.7×10^{-7}	-

* limit of detection
1. mercaptopropionic acid (MPA)-capped CdTe quantum dots (QDs)
2. nitrogen-doped and amino acid functionalized graphene quantum dots (NA-GQDs)
3. Cu nanoclusters (CuNCs) stabilized by tannic acid (TA)
4. butylamine (BA)-modified graphene oxide (GO)

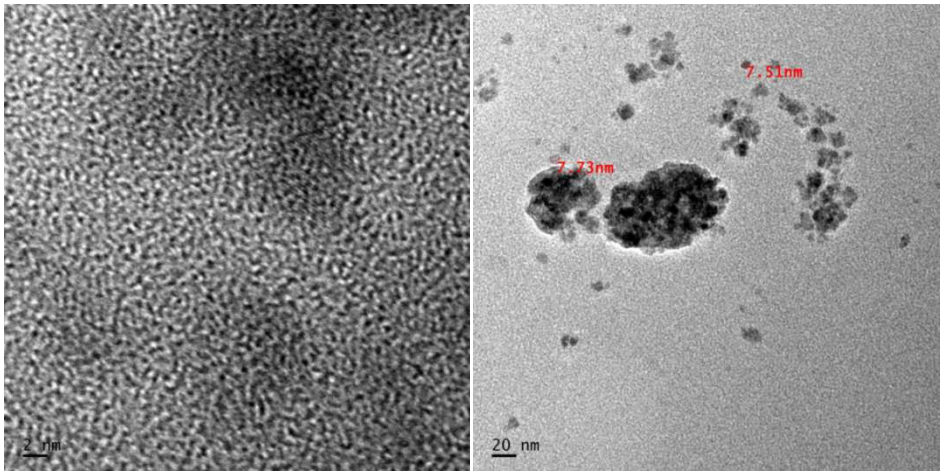

Figure 7.1 TEM image of CNDs

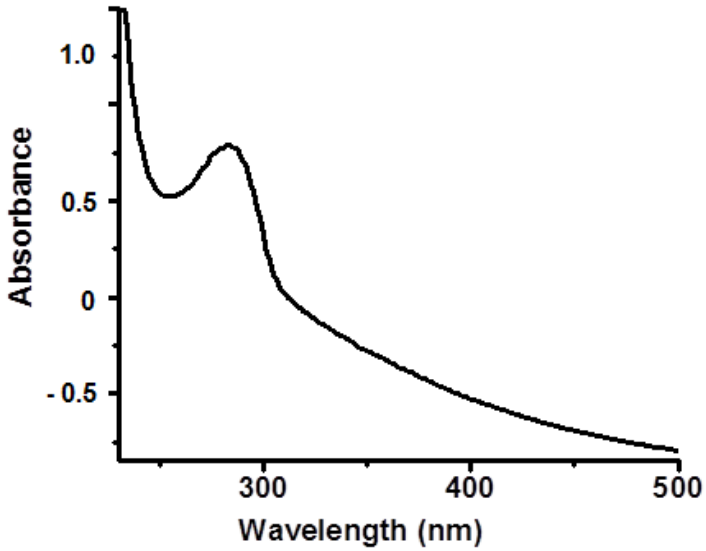

Figure 7.2 Absorption spectra of CNDs

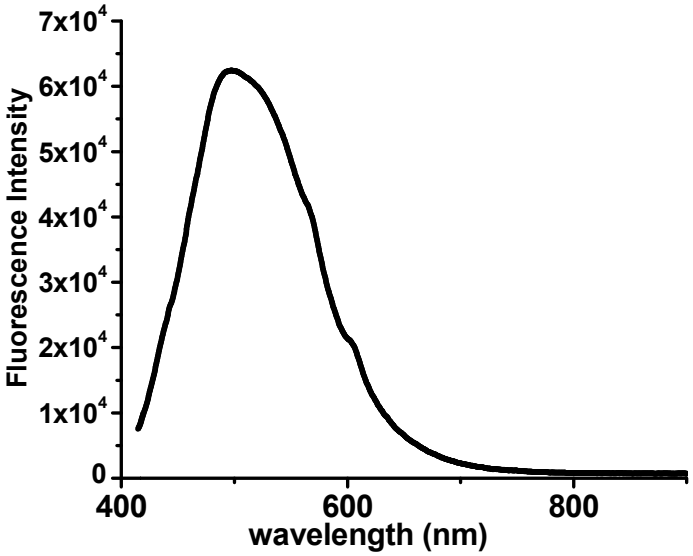

Figure 7.3 Emission spectra of CNDs

Figure 7.4 Photograph of CNDs dispersion under UV light

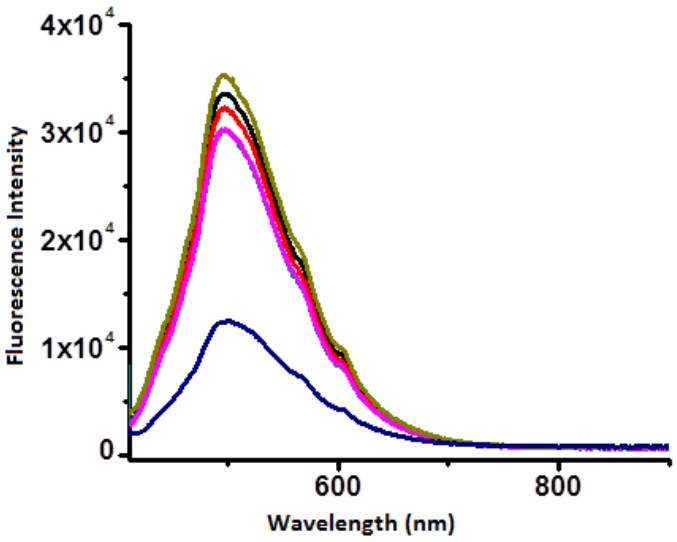

Figure 7.5 Effect of different metal ions on the fluorescence intensity of CNDs

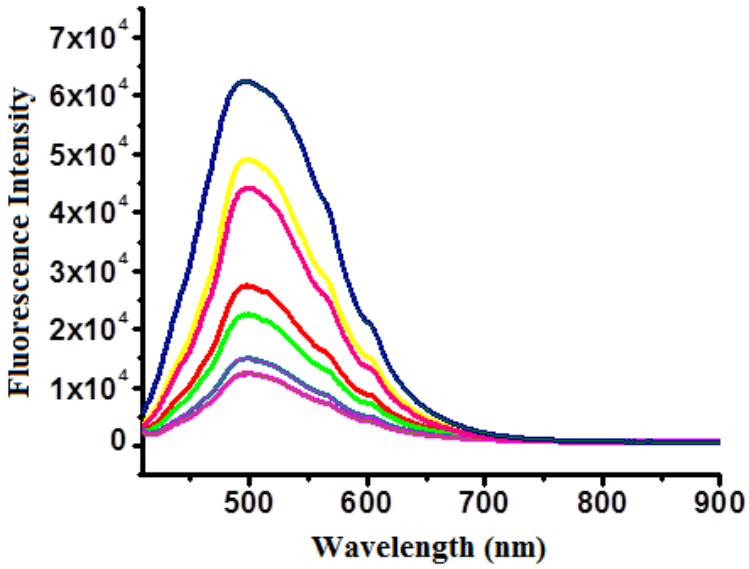

Figure 7.6 Effect of concentration of Fe^{3+} ions on fluorescence intensity of CNDs

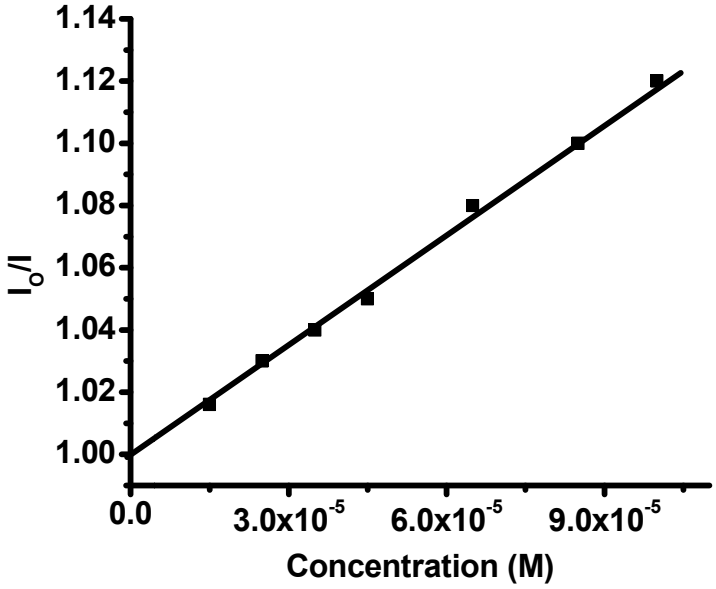

Figure 7.7 Stern – Volmer relationship between CNDs and Fe^{3+} ion

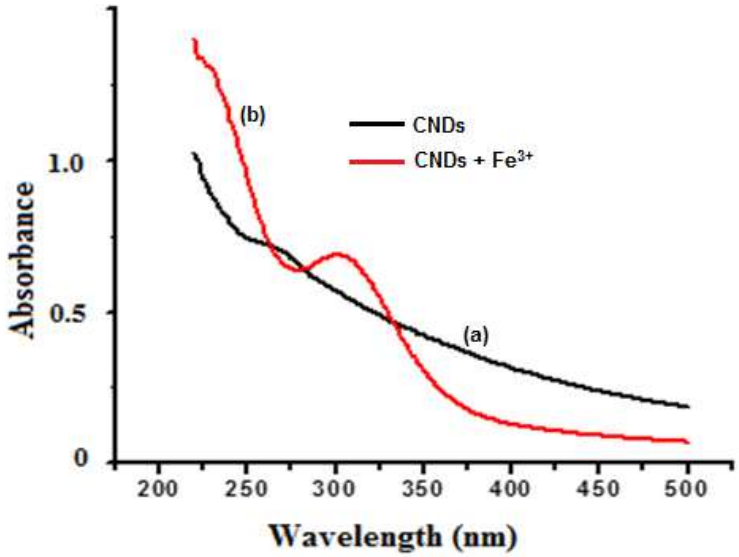

Figure 7.8 Absorption spectra of (a) CNDs alone and (b) CNDs + Fe^{3+} ions

.....ꕥ.....

Chapter 8

FLUORESCENT SENSOR FOR BUTYLATEDHYDROXYANISOLE (BHA)

Contents

A simple fluorescent sensor for the selective determination of butylated hydroxyanisole (BHA) based on the interaction of carbon nitride dots (CNDs) and BHA is reported in this chapter. In the presence of BHA, the fluorescence intensity of CNDs was effectively quenched. The fluorescence quenching effect of CNDs in presence of BHA was concentration dependent and the linear range for the developed sensor was from 1.0×10^{-9} - 1.0×10^{-8} M. The limit of detection was 1.9×10^{-11} M. Mechanism for fluorescence quenching by BHA was also studied. The developed sensor was applied for the determination of BHA in oil samples.

8.1 Introduction

Antioxidant compounds are added as inhibitors of free radical oxidation, to prevent lipids and oils from oxidative deterioration[375]. It is defined as any substance that significantly delays or inhibits oxidation of a substrate. Antioxidants can be divided in two classes; primary (chain breaking) antioxidants and secondary (preventative) antioxidants[376]. The antioxidants scavenge free radicals and form stable low-energy free radicals thereby inhibit the chain propagation of free radicals.

Butylated hydroxyanisole (BHA, E 320), is a white crystalline synthetic antioxidant with a faint characteristic odour. BHA is added in food, cosmetics, pharmaceuticals and plastics[377-380]. The high thermal stability and its ability to remain active in baked and fried foods make them a better choice in the food industry. Even though BHA is widely in food products due to its antioxidant properties, they can also act as oxidizing agents by inducing DNA damage and cell apoptosis and studies have revealed that BHA can be carcinogenic at high doses[381]. An average daily intake (ADI) of 0.5 mg/kg of BHA was established by the Joint FAO/WHO Expert Committee on Food Additives (JECFA) and the European Union Scientific Committee for Food (SCF)[382].

The International Agency for Research on Cancer (IARC) evaluated BHA as a possible class 2B carcinogen. BHA and its major metabolites including glucuronides, sulphates and tert-butyl hydroquinone (TBHQ) has been reported to induce serious health problems such as child hyperactivity, damage to the lungs, liver, and kidneys[383]. Also, it was reported that BHA and TBHQ can induce chromosomal aberrations in vitro

in the presence of metabolic activation. The results obtained from long-term toxicity and carcinogenicity studies with BHA studies have concluded the proliferative changes in the forestomach[384].

A variety of analytical methods reported for the determination of BHA includes spectrophotometry[385-388], liquid chromatography[389-392], gas chromatography[393-395], electrochemical methods[396-400] etc. Most of them suffer many drawbacks, such as expensiveness, complicated and lengthy procedures, and unsuitability for field use. Fluorescence techniques are reported to have simple equipment, rapid response, high sensitivity and easy operation[401-403].

The present chapter considers the efficiency of BHA to selectively quench the fluorescence intensity of carbon nitride dots (CNDs) in presence of other synthetic antioxidants such as butylated hydroxytoluene (BHT), tert-butyl hydroquinone (TBHQ) and propyl gallate (PG). CNDs are fluorescent carbon nanoparticles, with unique optical properties. The fluorescence intensity of CNDs was selectively quenched by BHA. The mechanism of quenching was studied and included in the chapter. The developed fluorescent sensor was applied for the determination of BHA in oil samples.

8.2 Experimental

8.2.1 Synthesis of Carbon Nitride Dots (CNDs)

Fluorescent CNDs were synthesised by microwave irradiation of N, N- dimethylformamide (DMF) in the presence of chlorosulfonic acid (CSA) according to procedure described in section 7.2.1 in chapter 7. Briefly,

0.5mL of chlorosulfonic acid (CSF) was added to 5.0 mL of DMF. The mixture was irradiated at 700 W for 40 seconds in a microwave oven. Finally the solution was transferred to 5.0 mL of distilled water. The excess precursors were removed by dialyzing against water through a dialysis membrane for 1 day.

8.2.2 Preparation of BHA solution

A stock solution of 1×10^{-1} M BHA was prepared by dissolving 0.180 g of BHA in 10.0 mL of methanol. Solutions of different concentrations were prepared by the serial dilution of stock solution.

8.2.3 Sample preparation

8.2.3.1 Treatment of vegetable oil samples

5.0 g of a vegetable oil sample was placed into a 100.0 mL Erlenmeyer flask (with a screw cap) and 5.0 mL of pure methanol was added. After being shaken, with the use of a laboratory shaker for 5 min, the mixture was transferred to a 10.0 mL centrifuging tube and centrifuged at 3000 rpm for 5 min. After a settling time of 2 min, the extracts were transferred into a 25.0 mL flask. The above extraction procedure was repeated twice, all the extracts were collected, and transferred into the 25.0 mL flask; and then the solution was diluted to the mark with methanol[404]. An adequate amount of this sample solution was mixed with CNDs and the fluorescence intensities were measured.

8.2.3 Analytical procedure

The fluorescence measurements were carried in a 3.0 mL cuvette. 500 μL of CNDs solution was mixed with and BHA solution of different

concentration. The fluorescence measurements were performed with λex/λem at 365/493 nm. The relative fluorescence intensity [Io/I] versus concentration of BHA was used for calibration, where Io and I are the fluorescence intensities of the CNDs before and after adding BHA respectively.

8.3 Results and discussions

8.3.1 Characterization

In order to characterize the synthesized CNDs, the fluorescence emission spectra, absorbance spectra and TEM image of CNDs were obtained. The detailed descriptions of these results are given in section 7.3.1 in chapter 7.

8.3.2 Fluorescence turn-off sensing by BHA

The influence of various synthetic phenolic antioxidants such as [1×10^{-3} M] BHA, BHT, TBHQ and PG on the fluorescence intensity of CNDs was carried out and is given in figure 8.1. From the figure it was clear that the fluorescence intensity of CNDs was effectively quenched by BHA alone. The observed result forms the basis of development of a fluorescent sensor for the selective determination of BHA.

8.3.3 Optimization of the experimental conditions

8.3.3.1 Effect of reaction time

According to the experiment, the reaction between CNDs and BHA reached the equilibrium within 5 min at room temperature and the fluorescence of CNDs -BHA system was stable for at least 1 hour (Fig. 8.2). Therefore, the fluorescence signals of the system were recorded after the reaction lasted for 15 min.

8.3.3.2 Effect of pH

As shown in Figure 8.3, the interaction between CNDs and BHA was influenced by the pH of the solution. The fluorescence intensity of CNDs was enhanced with the increase of solution pH from 2 to 4. Further increase of solution pH decreases the fluorescence intensity. Therefore, the fluorescence measurements were carried out in phosphate buffer solution of pH 4.

8.3.4 Effect of concentration

The emission spectra of CNDs and its fluorescence titration with BHA were recorded in aqueous medium and the results of which are shown in Fig. 8.4. When BHA was added to the CNDs, a significant decrease in the fluorescence emission of CNDs was observed. It was found that BHA quenches the fluorescence of CNDs in a concentration dependence manner and the calibration plot (Fig. 8. 5) of I_0/I with concentration of BHA is linear in the range 1.0×10^{-9} - 1.0×10^{-8} M. The limit of detection is 1.9×10^{-11} M. The relative standard deviation for five determinations of 1.5×10^{-9} M BHA was 3.3 %.

8.3.5 Sensing mechanism

Electron transfer process, ion binding interaction, inner filter effect and non radiative recombination pathway are certain mechanisms used to explain the phenomena of quenching[405-407]. The quenching mechanism was studied by fluorescence and UV–Vis absorption spectra. As illustrated in Fig. 8.6, the fluorescence intensity of CNDs was quenched without spectra shift in the presence of BHA. To further understand the quenching

effect, UV– Vis absorption spectra of CNDs in the absence and presence of BHA was investigated. The figure 8.6 clearly indicates that there is shift in the absorbance spectra of CNDs after the addition of BHA. This may be due to the formation of a non- fluorescent complex between CNDs and BHA. Since dynamic and static quenching can be distinguished by absorbance spectra, the shift in the absorbance spectra of CNDs suggests that the decrease in the fluorescence intensity of CNDs in presence of BHA may be due to static quenching[75].

8.3.6 Effect of foreign substance

In order to adopt the CNDs as sensing probe for BHA, it is important to evaluate the interference effect of some common foreign substances. The study of three different ratio of 1:1, 1:10, 1:100 [BHA : foreign substance) coexisting species such as EDTA, ascorbic acid, sulfite and citric acid was carried out and the results are presented in Table 8.1. It can be concluded that upto 100 fold excess concentrations of all these substances did not show any significant interference in the determination of BHA.

8.4 Application

To evaluate the practical utility of CNDs based fluorescent sensor, the developed method was employed to determine BHA in spiked oil samples such as coconut oil and sesame oil. The results are given in table 8.2 and recoveries were ranged from 98.2 to 101.6 %. The results demonstrated the accuracy of the method and prove that the developed method possesses potential applications in the real sample analysis.

8.5 Conclusion

In conclusion, a simple fluorescence probe based on the CNDs has been developed for the selective determination of BHA in aqueous media. Most common coexisting species hardly interfered with the determination of BHA. The concentration-dependent fluorescence quenching could be described by Stern–Volmer equation and the quenching mechanism was attributed to the formation of a non-fluorescent complex between CNDs and BHA. The proposed method was applied to the determination of BHA in oil samples.

Table 8.1 Effect of foreign substances [BHA] = 1×10^{-8} M

Foreign species	Signal change
Sodium sulfite	3.4
Citric acid	2.4
EDTA	1.9
ascorbic acid	4.8

Table 8.2 Application study

Sample	Added (M)	Found (M)	R.S.D (%)	Recovery (%)
Coconut oil	1.00×10^{-8}	0.98×10^{-8}	3.7	98.2
	5.00×10^{-8}	4.95×10^{-8}	2.6	99.0
Sesame oil	1.00×10^{-9}	0.987×10^{-9}	2.2	98.7
	5.00×10^{-9}	5.08×10^{-9}	4.8	101.6

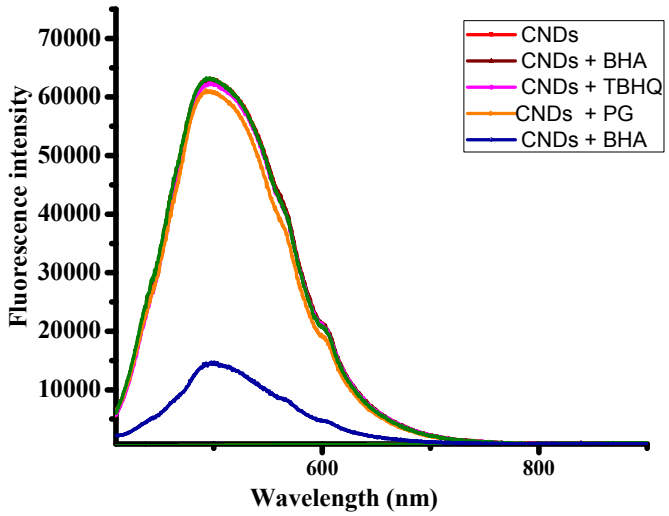

Figure 8.1 Effect of phenolic antioxidants on fluorescence intensity of CNDs

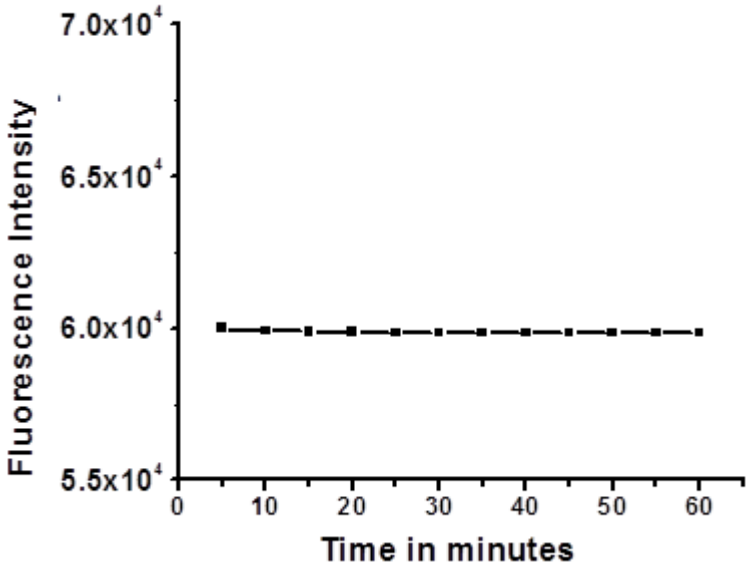

Figure 8.2 Effect of time

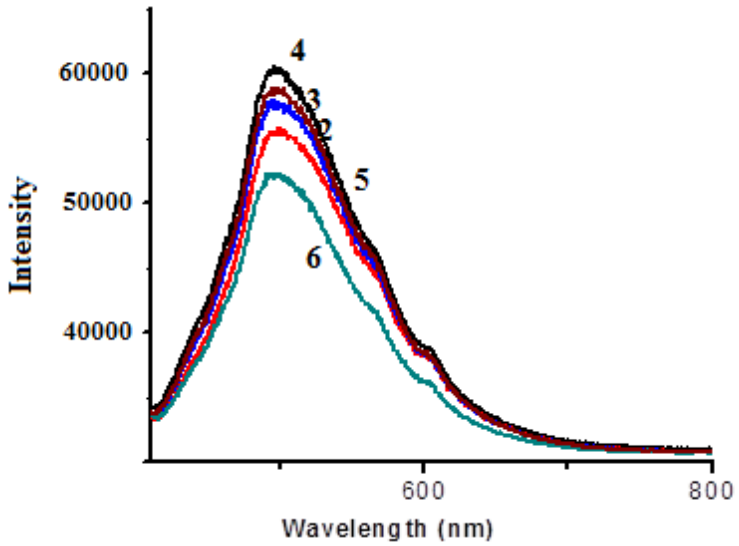

Figure 8.3 Effect of pH

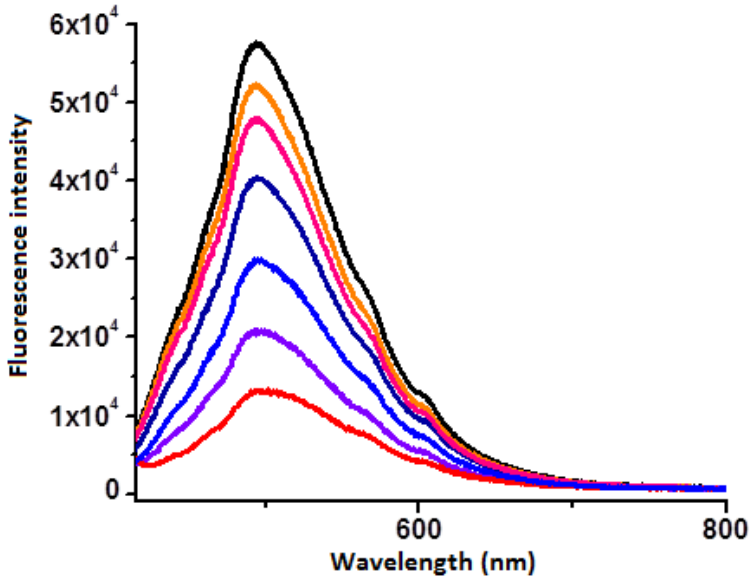

Figure 8.4 Fluorescence spectra of CNDs with the addition of solutions of different concentrations of BHA

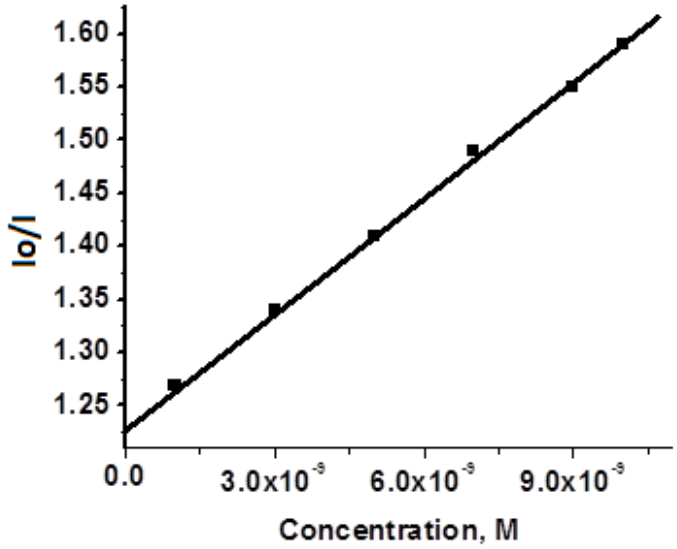

Figure 8.5 Stern–Volmer plot

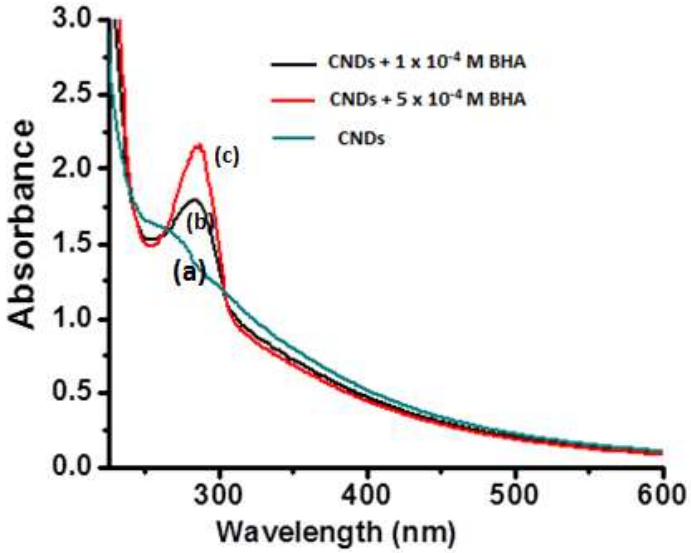

Figure 8.6 Absorbance spectra of (a) CNDs (b) CNDs + 1 × 10^{-4} M BHA and (c) CNDs + 5 × 10^{-4} M BHA

Chapter 9

SUMMARY

Contents

The objectives and brief summary of the present investigations are presented in this chapter.

9.1 Objectives

The major objectives of the work are:

1) Fabrication of chemically modified electrodes (CMEs).

2) Characterization of the CMEs using surface area study and scanning electron microscopy.

3) Development of electrochemical sensors using the above CMEs for determination of food additives.

4) Study of the electrochemical behavior of various analytes on the developed sensors.

5) Synthesis of fluorescent probes such as CdSe quantum dots (QDs) and carbon nitride dots (CNDs).

6) Characterization of the synthesized fluorophores by Transmission Electron Microscopy (TEM) and UV- visible spectroscopy.

7) Development of optical sensors based on the above fluorescent probes for analytes such as Nimesulide (NIM), Fe^{3+} ions and Butylated hydroxyanisole (BHA).

8) Study of the fluorescence quenching mechanism.

9) Determination of analytical figure of merits for various analytes using the developed sensors.

10) Investigation of the developed electrochemical and optical sensors for real samples analysis.

9.2 Summary

As part of the present investigations three electrochemical and three fluorescent sensors were developed for the determination of food additives, pharmaceuticals and metal ions. The details are listed below:

Analyte	Type of analyte	Sensors developed	Limit of detection (M)
Nitrite	Food additive	Electrochemical – TMOPPMn(III)Cl/GE sensor	2.9×10^{-9}
Sudan 1	Food colorant	Electrochemical – AuNP/GCE sensor	1.1×10^{-8}
Butylated hydroxyanisole (BHA)	Antioxidant	Electrochemical – Poly(L-Cys)/GCE sensor	4.1×10^{-7}
		Fluorescent – CNDs based sensor	1.9×10^{-11}
Nimesulide (NIM)	Drug	Fluorescent – CdSe QDs based sensor	4.9×10^{-9}
Fe^{3+} ion	Metal ion	Fluorescent – CNDs based sensor	3.7×10^{-7}

The developed sensors were successfully applied for the determination of analytes in real samples.

Chemical sensors have multidisciplinary applications. The development and application of voltammetric and optical sensors continue to be an exciting and expanding area of research in analytical chemistry. The synthesis of biocompatible fluorophores and their use in clinical analysis, and the development of disposable sensors for clinical analysis is still a challenging task. The ability to make sensitive and selective measurements and the requirement of less expensive equipment make electrochemical and fluorescence based sensors attractive.

References

[1] Hulanicki. A.; Geab. S.; Ingman. F. *Pure Appl. Chem.,* **63,** 1247 (1991).

[2] Bond. A. M.; Oldham. K. B.; Snook. G. A. *Anal. Chem*., **72,** 3492 (2000).

[3] Bockris. J.O.M, Khan. S.U.M. *Surface Electrochemistry*, Plenum Press, New York (1993).

[4] Heyrovsky. J.; Kuta. J. *Principles of polarography,* Academic press, New York (1996).

[5] Bond. A. M.; Scholz. F.*Z Chemie*., **30**, 117 (1990).

[6] Wrona. P.K.; Galus. Z. *Encyclopedia of electrochemistry of the elements*, **IX A**, Marcel Dekker, New York (1977).

[7] Bard. A.J.; Faulkner. L. *Electrochemical Methods*, Wiley, New York (2001).

[8] Osteryoung. J.G.; Schreiner. M.M. CRC *Crit. Rev. Anal. Chem*., **19**, S1 (1988).

[9] Scholz, F. *Electroanalytical Methods,* Springer, New York (2001).

[10] Colon. L.A.; Dadoo. R.; Zare. R.N, *Anal. Chem*., **65**, 476 (1993).

[11] Wasmus S.; Kuver.A. *J. Electroanl. Chem*., **461**, 14 (1999).

[12] Rodgers. P.J.; Shigeru. A. *Anal. Chem*., **77**, 9276 (2007).

[13] Yang. N.; Wang. X. *Coll. Surf. B,* **61**, 277 (2008).

[14] Brainina. K.; Neyman. E. *Electroanalytical Stripping Methods*. John Wiley and Sons, New York (1993).

[15] Wang. J. *Electroanalytical Chemistry*, Wiley-VCH, New Jersey (2006).

[16] Uslu. B.; Ozkan. S.A. *Anal. Lett.,* **40**, 817 (2007).

[17] Harris. P.J.F. *Crit. Rev. Solid State Mater. Sci*., **30**, 235 (2005).

[18] Kinoshita. K. *Carbon: Electrochemical and Physicochemical Properties*, Wiley-VCH, New York (1988).

[19] Kalcher, K.; Svancara, I.; Metelka, R.; Vytras, K.; Walcarius, A. *Heterogeneous carbon electrochemical sensors. Encyclopedia of sensors.* American Scientific Publishers, New York (2006).

[20] Svancara, I.; Vytras, K.; Barek, J.; Zima, *J. Crit. Rev. Anal. Chem.*, **31**, 311 (2001).

[21] Kalcher. K. *Electroanal.*, **2**, 419 (1990).

[22] Kalcher. K.; Kauffmann. J.M.; Wang. J.; Svancara. I.; Vytras. K.; Neuhold. C.; Yang. Z. *Electroanal.*, 7, 5 (1995).

[23] Fick. A. *J. Sci.*, **16,** 30 (1855).

[24] Foresti. M.L.; Guidelli. R.; Nyholm. L. *J. Electroanal. Chem.*, **269**, 27 (1988).

[25] Matsuda. H.; Ayabe. Y. *Z. Electrochem.*, **59**, 494 (1955).

[26] Nicholson. R.S.; *Anal. Chem.*, **37**, 1351(1965).

[27] Klingler. R.J.; Kochi. J.K. *J. Phys. Chem.*, **85**, 1731(1981).

[28] Gileadi. E.; Eisner. U. *J. Electroanal. Chem***. 28**, 81 (1981).

[29] Lane. R.F.; Hubbard. A.T. *J. Phys. Chem.*, **77**, 1401 (1973).

[30] Durst.R. A.; Bâumner. A. J.; Murray.R. W.; Buck. R. P.; Andrieux. C. P. *Pure Appl. Chem.*, **69**, 1317 (1997).

[31] Kutner. W.; Wang. J.; L'Her. M.; Buck. R. P. *Pure Appl. Chem.*,**70,** 1301 (1998).

[32] Lahtinen. R.; Fermin. D.J.; Kontturi. K.; Girault. H.H. *J. Electroanal. Chem.*, **483**, 81 (2000).

[33] Toshifumi. K.; Atsushi. I.; Seiji. S. *Tetrahedron,* **61**, 488 (2005).

[34] Rose. E.; Quelquejeu. M.; Pandian. R.P.; Lecas-Nawrocka. A.; Vilar. A.; Ricart. G. *Polyhedron*, **19,** 581 (2000).

[35] Khairutdinov. R. F.; Serpone. N. *J. Phys. Chem. B*, **103**, 761 (1999).

[36] Baraldi. I.; Carnevali. A.; Ponterini. G.; Vanossi. D. *J. Mol. Struct – Theochem.*, **333**, 121 (1995)

[37] Macdonald. I.J.; Dougherty. T. J. *J. Porphyrins Phthalocyanines*, **5**, 105 (2001).

[38] Dudkowiak. A.; Teslak. E.; Habdas. J. *J. Mol. Struct*.,**792-793**, 93 (2006).

[39] Wrobel. D.; Lukasiewicz. J.; Goc. J.; Waszkowiak. A.; lon. R. *J. Mol. Struct.,* **555**, 407 (2000).

[40] Guldi. D.M. *J. Phys.Chem.,* **109**, 11432 (2005).

[41] Crossley. M.J.; Burn. P.L. *J. Chem. Soc. Chem. Commun.,* **21**, 1569 (1991).

[42] Wagner. R.W.; Lindsey. J.S. *J. Am. Chem. Soc.,* **116**, 9759 (1994).

[43] Kawao. M.; Ozawa. H.; Tanaka. H.; Ogawa.; T. *Thin Solid Films*, **499**, 23 (2006).

[44] Li. Y.; Cao. L.; Tian. H. *J. Org. Chem.*, **71**, 8279 (2006).

[45] Joseph. R.; Kumar. K. G. *Drug Test Anal.*, **2**, 278 (2010)

[46] Joseph. R.; Kumar. K. G. *Anal. Lett.*, **42**, 2309 (2009).

[47] Starowicz. M.; Stypula. B.; Banas. J. *Electrochem. Commun.*, **8**, 227 (2006).

[48] Welch. C.M.; Compton. R.G. *Anal. Bioanal. Chem.*, **384**, 60(2006).

[49] Cavicchioli. A.; La-Scalea. M. A.; Gutz. I. G. R.*Electroanal.*, **16**, 697 (2004).

[50] Hernandez-Santos. D.; Gonzalez-Garcia. M. B.; Garcia. A. C.; *Electroanal.*, **4**, 1225 (2002).

[51] Welch.C.M.; Banks. C.E.; Simm. A.O.; Compton. R.G. *Anal. Bioanal. Chem.,* **382**, 12(2005).

[52] Zhou. N.; Wang. J.; Chen. T.; Yu. Z.G.; Li. G.X. *Anal. Chem.*, **78**, 5227 (2006).

[53] Liu. Y. C.; Yu. C.C.; Yang. K.H.*Electrochem. Commun.,* **8**, 1163 (2006).

[54] Crespilho. F.N, Emilia Ghica. M.; Florescu. M.; Nart. F. C.; Oliveira. O.N., Jr Brett. C.M.A. *Electrochem. Commun*., **8,** 1665 (2006).

[55] Agui. L.; Manso. J.; Yanez-Sedeno. P.; Pingarron. J. M. *Sens. Actuators B*, **113,** 272 (2006).

[56] Kubo. R. *J. Phys. Soc. Jpn.,* **17**, 975(1962).

[57] Tan. Y. W.; Li. Y. F.; Zhu. D. B. *Langmuir*, **18**, 3392 (2002).

[58] Zhang. J.; Oyama. M. *Anal. Chim. Acta*, **540**, 299 (2005).

[59] Fukushima. M.; Yanagi. H.; Hayashi. S.; Suganuma. N.; Taniguchi. Y. *Thin Solid Films*, **39**, 438 (2003).

[60] Zhou. X.; Wei. Q.; Sun. K.; Wang. L. *Appl. Phys. Lett*., **94**, 133101 (2009).

[61] Abidi. W.; Remita .H. *Recent Patents Eng*., **4**, 170 (2010).

[62] Dai. X.; Nekrassova. O.; Hyde. M. E.; Compton. R. G. *Anal. Chem*., **76**, 5924 (2004)

[63] El-Deab. M. S.; Okajima, T.; Ohsaka. T. *J. Electrochem. Soc*., **150**, A851 (2003).

[64] Wang. J. *Analyst*, **130**, 421(2005).

[65] Pumera. S. M.; Sanchez. S.; Ichinose. I.; Tang. J. *Sens. Actuators B,* **123,** 1195 (2007).

[66] Castaneda. M.T.; Alegret. S.; Merkoc. A. *Electroanal*., **19**, 743 (2007).

[67] Katz. E.; Willner. I. *Angew. Chem. Int. Ed*., **43**, 6042 (2004).

[68] Ohnuki. T.; Ohsaka. H.; Matsuda. N.; Oyama. J. *J. Electroanal. Chem.,* **158,** 55 (1983).

[69] Volkov. A.; Tourillon. G.; Lacaze.P. C.; Dubois.J. E. *J. Electroanal. Chem.,* **115,** 279 (1980).

[70] Sun. Y. X.; Ye. B. X.; Wang. Y.; Tang.X. R.; Zhou.X. Y. *Microchem. J.,* **58** 182(1998).

[71] Brett.C. M. A.; Inzelt.G. Kertesz.V. *Anal. Chim. Acta,***385,** 119 (1999).

[72] Vidal. J.C.; Garcia-Ruiz. E. Castillo. J.R. *Microchim. Acta,* **143**, 93 (2003).

[73] Gerard. M.; Chaubey.A.; Malhotra .B.D. *Biosens. Bioelectron*., **17**, 345 (2002).

[74] Guan. J.; Wang. Z.X.; C.Y. Wang, Q.S. Qu, G.J. Yang, X.Y. Hu, *Int. J. Electrochem. Sci.*, **2**, 572 (2007).

[75] Lakowicz. R.J. *Principles of Fluorescence Spectroscopy*, Kluwer Academic and Plenum Publishers, New York (2000).

[76] McNaught. A. D.; Wilkinson. A. *IUPAC. Compendium of Chemical Terminology, 2nd ed. (the "Gold Book*"). Blackwell Scientific Publications, Oxford (1997).

[77] Stokes. G.G. *Phil. Trans. R Soc.,* **142**, 463 (1852).

[78] Kasha. M. *Disc. Faraday. Soc*., **9**, 14 (1950).

[79] Dexter. D.L. *J Chem Phys.,* **21,** 836 (1953).

[80] Inokuti. M.; Hirayama. F. *J. Chem. Phys.,* **43,** 1978 (1965).

[81] Kobayashi. H.; Morita. T. *Chem. Phys. Lett.,* **20,** 376 (1973).

[82] Hasson. S.; Lustig. H.; Rubin. M.B.; Speiser. S. *J. Phys. Chem.,* **88**, 367 (1984).

[83] Sauer. M.; Hofkens. J.; Enderlein. J**.** *Handbook of Fluorescence Spectroscopy and Imaging: From Single Molecules to Ensembles*, Wiley-VCH, (2011).

[84] Ekimov. A.I.; Onushchenko. A.A. *JETP Lett*., **34,** 345 (1981)

[85] Rossetti. R.; Brus. L. *J. Phys. Chem.,* **86,** 4470 (1982).

[86] Reed. M.A.; Randall. J.N.; Aggarwal. R.J.; Matyi. R.J.; Moore. T.M.; Wetsel. A.E. *Phys. Rev. Lett*., **60**, 535 (1988).

[87] Bruchez. M., Jr.; Moronne. M.; Gin, P.; Weiss. S.; Alivisatos, A.P. *Science*, **281**, 2013 (1998).

[88] Chan. W.C.W.; Nie. S. *Science*, **281**, 2016 (1998).

[89] Schmelz. O.; Mews. A.; Basche. T.; Herrmann. A.; Mullen. K. *Langmuir*, **17**, 2861 (2001).

[90] Dennis. A.M.; Rhee. W. J.; Sotto. D.; Dublin. S. N.; Bao. G. *ACS Nano,* **6**, 2917 (2012).

[91] Li. J.; Mei, F.; Li. W. Y.; He. X. W.; Zhang. Y. K. *Spectrochim. Acta A,* **70**, 811 (2008).

[92] Xia. Y.; Song. L.; Zhu. C. *Anal. Chem*., **83**, 1401 (2011).

[93] Boeneman. K.; Deschamps. J. R.; Buckhout-White. S.; Prasuhn. D. E.; Blanco-Canosa. J. B.; Dawson. P. E.; Stewart. M. H.; Susumu. K.; Goldman. E. R.; Ancona. M.; Medintz. I. L. *ACS Nano,* **4**, 7253 (2010).

[94] Thomas. D.; Lonappan. L.; Rajith. L.; Cyriac. S.T.; Kumar. K. G. *J. Fluoresc*, **23**, 473 (2013)

[95] Shi. L.; Paoli. V. D.; Rosenzweig. N.; Rosenzweig. Z. *J. Am. Chem. Soc.,* **128**, 6744 (2006).

[96] Derfus. A.M..; Chan. W.C.W.; Bhatia. S.N. *Nano Lett*., **4,** 11 (2004).

[97] Kirchner. C.; Liedl. T.; Kudera. S.; Pellegrino. T.; Munoz. J.A.; Gaub. H.E.; *Nano Lett.,* **5,** 331 (2005).

[98] Wang. X. C.; Maeda. K.; Thomas. F.; Takanabe. K.; Xin. G.; Carlsson. J. M.; Domen. K; Antonietti. M. *Nat. Mater*., **8**, 76 (2009).

[99] Wohlgemuth. S.A.; White. R.J.; Willinger. M.G.; Titirici. M.M.; Antonietti. M. *Green Chem*., **14**, 1515 (2012).

[100] Li. Q.; Zhang. S.; Dai. L.; Li. L.S. *J. Am. Chem. Soc*., **134,** 18932 (2012).

[101] Guan.W.; Gu. W.; Ye. L.; Guo. C; Su. S.; Xu. P.; Xue. M. *Int. J. Nanomedicine*, **9**, 5071 (2014).

[102] Wang. Y.; Wang. X. C.; Antonietti. M. *Angew. Chem. Int. Ed.,* **51**, 68 (2012).

[103] Thomas. A.; Fischer. A.; Goettmann. F.; Antonietti. M.; Muller. J.O.; Schlogl. R.; Carlsson. J. M. *J. Mater. Chem*., **18**, 4893 (2008).

[104] Lee. E. Z.; Jun. Y.S.; Hong. W. H.; Thomas. A.; Jin. M. M. *Angew. Chem. Int. Ed*., **49,** 9706 (2010).

[105] Lee. E. Z.; Lee. S. U.; Heo. N.S.; Stucky. G. D.; Jun. Y.S.; Hong. W. H. *Chem. Commun*., **48,** 3942 (2012).

[106] Tian. J. Q.; Liu. Q.; Asiri. A. M.; Al-Youbi. A. O.; Sun. X. P. *Anal. Chem*., **85**, 5595 (2013).

[107] Liu. L.; Ma. D.; Zheng. H.; Li. X.; Cheng. M.; Bao. X. *Microporous Mesoporous Mater*., **110**, 216 (2008).

[108] Datta. K. K. P.; Reddy. B. V. S.; Ariga. K.; Vinu. A. *Angew. Chem. Int. Ed.,* **49**, 5961 (2010).

[109] Qiu.Y.; Gao.L. *Chem. Commun*., 2378 (2003).

[110] Li .Y.; Zhao. Y.; Cheng. H. *J. Am. Chem. Soc*., **134**, 15 (2012).

[111] Lu. J.; Yang. J.X.; Wang. J.; Lim. A.; Wang. S.; Loh. K.P. *ACS Nano,* 2009, **3**, 2367 (2014).

[112] Liu. H.; Ye. T.; Mao. C. *Angew. Chem. Int. Ed. Engl*., **46**, 6473 (2007).

[113] Tian. L.; Ghosh. D.; Chen. W.; Pradhan. S.; Chang. X.; Chen. S. *Chem Mater*., **21,** 2803 (2009).

[114] Yang Y, Cui J, Zheng M, *Chem Commun (Camb).***48,** 380 (2012).

[115] Zhu S, Zhang J, Qiao C, Tang S, Li Y, Yuan W, Li B, Tian L, Liu F, Hu R, Gao H, Wei H, Zhang H, Sun H, Yang B.*Chem Commun (Camb).,***47**, 6858 (2011).

[116] Xiao. D.; Yuan. D.; He. H.; Lu. J. *Luminescence*, **28**, 612 (2013).

[117] Jaiswal. A.; Ghosh. S.S.; Chattopadhyay. A. *Chem. Commun. (Camb)*. **48**, 407 (2012).

[118] Zhang. S.; Shi. Z, Wang. *J. Food. Chem*., **173,** 449 (2015).

[119] Yua. L.; Shi. M.; Yue. X.; Qu. L. *Sens.Actuators B,* **209**, 1 (2015).

[120] Silva. E.M.; Takeuchi. R.M.; Santos. A. L. *Food. Chem*., **173**, 763 (2015).

[121] Chandran. S.; Lonappan. L.A.; Thomas. D.; Jos. T.; Kumar. K. G. *Food. Anal. Methods*, **7,**741 (2014).

[122] Wang. M.; Gao.Y.; Sun.Q.; Zhao. J. *Food. Chem*., **172**, 873 (2015).

[123] Zhang. Y.; Hu. L.; Liu. X.; Liu. B.; Wu. K.; *Food Chem.,* **166**, 352 (2015).

[124] Jiang. L.; Ding. Y.; Jiang. F.; Li. L.; Mo. F. *Anal. Chim. Acta*, **833**, 22 (2014).

[125] Jamali. T, Karimi-Maleh. H.; Khalilzadeh. M. A.; *LWT - Food Sci. Technol*., **57**, 679 (2014).

[126] Thomas. A.; Vikraman. A. E.; Thomas. D.; Kumar. K. G. *Food Anal. Methods,* DOI 10.1007/s12161-015-0092-z

[127] Vikraman. A.E.; Thomas. D.; Cyriac. S.T.; Kumar. K. G. *J. Electrochem. Soc.***, 161**, B305 (2014).

[128] Vikraman. A.E.; Rasheed. Z.; Rajith. L.; Lonappan. L. A.; Kumar. K. G. *Food Anal. Methods,* **6,** 775 (2013).

[129] Wang. P.; Hu. X.; Cheng. Q., Zhao. X.; Fu. X.; Wu. K. *J. Agric. Food Chem*., **58**, 12112 (2010)

[130] Yu. L.; Shi. M.; Yue. X.; Qu. L. *Sens. Actuators B,* **209,** 1 (2015).

[131] Gan.T.; Li.K.; Wu. K. *Sens. Actuators B*, **132**, 134 (2008).

[132] Lin. X.; Ni. Y.; Kokot. S. *Anal. Chim. Acta,* **765,** 54 (2013).

[133] Manriquez. J.; Bravo. J.L.; Granados. S.G.; Succar. S.S.; Charreton. C. B.; Ordaz. A.A.; Bedioui. F.; *Anal. Chim. Acta*, **378**, 159 (1999).

[134] Mimica. D.; Zagal. J.H.; Bedioui. F. *Electrochem. Commun.,* **3**, 435 (2001).

[135] Ozoemena. K.I.; Nyokong. T. *Talanta,* **67**, 162 (2005).

[136] Santos. W.J.R.; Sousa. A.L.; Luzb. R.C.S.; Damosb. F.S.; Kubota. L.T.; Tanaka. A.A.; Tanaka. S.M.C.N. *Talanta*, **70**, 588 (2006).

[137] Wu. Y. *Food Chem*., **121**, 580 (2010).

[138] Jin. G. Y.; Zhang. Y. Z.; Cheng. W. X. *Sens. Actuators B*, **107**, 528 (2005).

[139] Li. B.L.; Luo. J.H.; Luo. H.Q.; Li. N.B. *Food Chem*., **173** 594 (2015).

[140] Zhang. K.; Luo. P.; Wu. J.; Wang. W; Ye. B. *Anal. Methods*, **5**, 5044 (2013).

[141] Kalimuthu. P.; John. S.A.; *Electrochem. Commun.,* **11**, 1065 (2009).

[142] Gao.Y.; Wang. M, Yang. X.; Sun. Q.; Zhao. J. *J. Electroanal. Chem*., **735,** 84 (2014).

[143] Pacheco. J. G. Castro. M.; Machado. S.; Barroso. M. F.; Nouws. H. P. A.; Matos. C. D. *Sens. Actuators B*, **215**, 107 (2015).

[144] Liu. Y.T.; Deng. J.; Xiao. X.L.; Ding. L.; Yuan. Y.L.; Li. H.; Ting. X.; Li.; Yan. X.N.; Li. L.; Wang. *Electrochim. Acta,* **56,** 4595 (2011).

[145] Fu. L.; Zheng. Y.; Wang. A.; Cai. W.; Lin. H. *Food Chem*., **181**, 127 (2015).

[146] Beitollah. H.; Goodarzian. M.; Khalilzadeh. M. A.; Karimi-Maleh. H.; Hassanzadeh. M.; Tajbakhsh. M. *J. Mol. Liq.*, **173**, 137 (2012).

[147] Salmanpour. S.; Tavana. T.; Pahlavan. A.; Khalilzadeh. M. A.; Ensafi. A. A.; KarimiMaleh. H. *Mater. Sci. Eng., C,* **32**, 1912 (2012).

[148] Sun, W.; Li. Y.; Duan. Y.; Jiao. K. *Electrochim. Acta*, **54**, 4105 (2009).

[149] Elyasi. M.; Khalilzadeh.M. A.; Karimi-Maleh.H. *Food Chem*., **141,** 4311 (2013).

[150] Liang. J.; Huang. S. Zeng. D. He. Z.; Ji. X.; Ai. X.; Yang. H. *Talanta*, **69**, 126 (2006).

[151] Liu. M.; Xu. L.; Cheng. W. Zeng. Y. Yan. Z. *Spectrochim. Acta A,* **70**, 1198 (2008).

[152] Li. D.; Yan. Z.Y.; Cheng. W. Q. *Spectrochim. Acta A*, **71**, 1204 (2008).

[153] Dong. F.; Hu. K.; Han. H.; Liang. J. *Microchim Acta*, **165,** 195 (2009).

[154] Gong. F.; Wu. D.W; Cao. Z.; He. X. *Biosen. Bioelectronics*, **22**, 423 (2006).

[155] Ling. X.; Deng. D.W.; Zhong. W.Y.; Yu. J.S. *Guang Pu. Xue Yu. Guang Pu. Fen Xi,* **28**, 1317 (2008).

[156] Chen. Y.; Rosenzweig. Z. *Anal. Chem*., **74,** 5132 (2002).

[157] Xie. H.Y.; Liang. J.G.; Zhang. Z.L.; Liu. Y.; He. Z.K.; Pang. D.W. *Spectrochim. Acta A*, **60,** 2527 (2004).

[158] Ding. X.; Qu. L.; Yang. R.; Zhou. Y.; Li. J. *Luminescence*, **30,** 465 (2015).

[159] Yang. T.; He.Q.; Liu. Y.; Zhu. C.; Zhao. D. *J. Anal. Methods Chem*., **2013,** 1 (2013).

[160] Rodrigues. S.S.M.; Lima. A.S.; Teixeira. L.S.G.; Korn. M. G. A.; Santos. J. L.M. *Fuel,* **117**, 520 (2014).

[161] Koneswaran. M.; Narayanaswamy. R. *Sens. Actuators B,* **139**, 91 (2009).

[162] Chen. J.; Zhu. C. *Anal. Chim. Acta,* **546**, 147 (2005).

[163] Zhang. Y.; Zhang. H.; Guo. X.; Wang. H. *Spectrochim. Acta A*. **70**, 1198 (2008).

[164] Cai. C.; Cheng. H.; Wang. Y.; Bao. H. *RSC Adv.***, 4**, 59157 (2014).

[165] Zou. Y.; Yan. F.; Dai. L.; Luo. Y.; Fu. Y.; Yang. N.; Wun. J.; Chen. L.; *Carbon*, **77**, 1148 (2014).

[166] Murphy. C.J. *Anal Chem.***74**, 520A (2002).

[167] Frasco. M. F.; Chaniotakis. N. A. *Semiconductor International Conference CAS***1**, 77 (2009).

[168] Li. H.; Zhang. Y.; Wang. X.; Xiong. D.; Bai. Y. *Mater. Lett*., **61,** 1474 (2007).

[169] Chen. C.Y.; Cheng. C.T.; Lai. C.W.; Wu. P.W.; Wu. K.C.; Chou. P. T.; Chou. Y.; Chiu. H. T. *Chem. Commun*., 263 (2006).

[170] Jin. T.; Fujii. F.; Yamada. E.; Nodasaka.Y.; Kinjo M. *Comb. Chem. High Throughput Screen*, **10**, 473 (2007).

[171] Banerjee. S.; Kara. S.; Santra. S. *Chem. Commun*., 3037 (2008).

[172] Frasco. M. F.; Vamvakaki. V.; Chaniotakis. N.; *J. Nanopart. Res*., **12**, 1449 (2010).

[173] Zhou. M; Chen. X.; Xu. Y.; Qu. J.; Jiao. L.; Zhang. H.; Chen. H.; Chen. X.*Dyes Pigments*, **99**, 120 (2013).

[174] Braida. W.; Ong. S. K. *Water Air Soil Poll.*, **118**, 13 (2000).

[175] Badea. M.; Amine. A.; Palleschi. G.; Moscone. D.; Volpe. G.; Curcilli. A. *J. Electroanal. Chem.,* **509,** 66 (2001).

[176] Casella. I. G.; Gatta. M. *J. Electroanal. Chem.,***568,** 183 (2004).

[177] Santos. W. J. R.; Lima. P.R.; Tanaka. A. A.; Tanaka. S. M. C. N.; Kubota. L. R. *Food Chem.,* **113**, 1206 (2009).

[178] Aydin. A.; Ercan. O.; Tascioglu. S. *Talanta*, **66**, 1181 (2005).

[179] Fann. C. S. B.; Kaneine. J. B. *Vet. Hum. Toxicol*., **35**, 521 (1993).

[180] Mirvish. S. S. *Cancer Lett*., **93**, 17 (1995).

[181] Fox. J. B. *Anal. Chem*., **51**, 1493 (1979).

[182] García-Robledo. E.; Corzo. R.; Papaspyrou. S. *Mar. Chem.*, **162**, 30 (2014).

[183] Filik. H.; Giray. D.; Ceylan. B.; Apak. R. *Talanta*, **85**, 1818 (2011).

[184] Helmke. S. M.; Duncan. M. D. *J. Chromatogr. B.,* **851**, 83 (2007).

[185] Pagliano. E.; Meija. J.; Mester. Z. *Anal. Chim. Acta*, **824**, 36 (2014).

[186] Butt. S.B.; Riaz. M.; Iqbal. M. Z. *Talanta*, **55**, 789 (2001).

[187] Arthur. P. H. M.; Shiva. S.; Gladwin. M. T. *J. Chromatogr B*, **851**, 93 (2007).

[188] Chen. X.; Wang. F.; Chen., Z. *Anal. Chim. Acta,* **623**, 213 (2008).

[189] Wen. Z. H.; Kang. T. F. *Talanta,* **62**, 351 (2004).

[190] Xiao. F.; Liu. L.Q.; Li. J.; Zeng. J.J.; Zeng. B.Z. *Electroanal.,* **20**, 2047 (2008).

[191] Zhao. G.; Liu. K. Z.; Lin. S.; Liang. J.; Guo. X. Y.; Zhang. Z. *J. Microchim. Acta,* **144**, 75 (2004).

[192] Strehlitz. B.; Grunding. B.; Schumacker.W.; Kroneck. P.M.H.; Vorlop. K. D.; Kotte. H. *Anal. Chem.,* **68**, 807 (1996).

[193] Cardoso. W. S.; Gushikem. Y. *J. Electroanal. Chem*, **583**,300 (2005).

[194] Caro. C. A.; Bedioui. F.; Zagal. J. H. *Electrochim. Acta*, **47**, 1489 (2002).

[195] Martins. M. C.; Dodelet. J.P.; Guay. D.; Ladouceur. M.; Tourillon. G.; *J. Phy. Chem.,* **96**, 10898 (1992).

[196] Vijayanathan. V.; Venkatachalam. S.; Krishnamurthy. V.N. *Polymer,***34**, 1095 (1993).

[197] Joseph. R.; Girish Kumar. K. *Drug. Test. Anal*., **2**, 278 (2010).

[198] Leena. R.; Girish Kumar. K. *Drug. Test. Anal*., **2**, 436 (2010).

[199] De Wael. K.; Adriaens. A. *Talanta*, **74**, 1562 (2008).

[200] Randles. J.E.B.; *Trans. Faraday Soc.*, **44**, 322 (1948).

[201] Yi. H.; Wu. K.; Hu. S.; Cui. D. *Talanta*, **55**, 1205 (2001).

[202] Brylev. O.; Sarrazin. M.; Roué. L.; Bélanger. D. *Electrochim. Acta*, **52**, 6237 (2007).

[203] Sun. W.; Zhang. S.; Liu. H.; Jin. L.; Kong. *Anal. Chim. Acta,* **388,** 103 (1999).

[204] Huang, X.; Li. Y.; Chen. Y.; Wang. L. *Sens. Actuators B,* **134**, 780 (2008*)*.

[205] Bard. A. J.; L. R. Faulkner, Electrochemical Methods, Fundamentals and Applications, Wiley, New York 1980, p. 223

[206] Laviron. E.; *J. Electroanal. Chem*., 52, 395 (1974).

[207] Desimoni. E.; Palmisano. F.; Zambonin. P. G. *J. Electroanal. Chem*., **84**, 315 (1977).

[208] Karyakin. A. A.; Karyakina. E. E.; Schmidt. H. L. *Electroanal*., **11**, 149 (1999).

[209] Lubert. K. H.; Guttmann. M.; Beyer. L. *J. Electroanal. Chem.,* **462,** 174 (1999).

[210] Ghorpade. V.M.; Deshpande. S.S.; Salunkhe. D.K. *Food Additive Toxicology*, Marcel Dekker, New York (1995).

[211] Lueck. E. *Antimicrobial food additives*. Springer, Berlin Heidelberg, New York (1980)

[212] EC, Directive of the European Parliament and of the council 94/36/EC of June 30, 1994 on colours for use in foodstuffs, Official J., 10/9/1994, 13, L237.

[213] Baggiani. C.; Anfossi. L.; Baravalle. P.; Giovannoli. C.; Giraudi. G.; Barolo. C.; Viscardi. G. *J. Sep. Sci*., **32**, 3292 (2009).

[214] Niu. L.; Song. Z.; Chen. D. *J. Sci. Food. Agric*., **90,** 338 (2010).

[215] Xu. H.; Heinze. T. M.; Chen. S.; Cerniglia. C. E.; Chen. H. *Appl. Environ. Microb*., **23,** 73 (2007).

[216] Lubet. R.A.; Connolly. G.; Kouri. R.E.; Nebert. D.W.; Bigelow. S.W. *Biochem. Pharmacol*., **32**, 3053 (1983).

[217] Stiborová. M.; Frei. E.; Schmeiser. H.H.; Wiessler. M.; Hradec. J. *Cancer. Lett.,* **68**, 43 (1993).

[218] Levine. W.G. *Drug. Metab. Rev*, **23,** 253 (1991).

[219] Stiborova. M.; Martinek. V.; Rydlova. H.; Hodek. P.; Frei. E. *Cancer Res.*, **62,** 5678 (2002).

[220] Ahlstrom. L.H.; Sparr Eskilsson. C.; Bjorklund. E. *TRAC-Trend Anal. Chem.,* **24,** 49 (2005).

[221] He. L.; Su. Y.; Fang. B.; Shen. X.; Zeng. Z.; Liu. Y. *Anal. Chim. Acta,* **594**, 139 (2007).

[222] Qi. T.; Zeng. Z.; Wen. X.; Liang. X.; Zhang. *Food Chemistry*, **125**, 1462 (2001).

[223] Long. C. Y.; Mai. Z. B.; Yang. X.F., Zhu. B.H.; Xu. X.M.; Huang. X. D.; Zou. X. Y. *Food Chem.,* **126**, 1324 (2011).

[224] Mazzotti. F.; Di Donna. L.; Maiuolo. L.; Napoli. A.; Salerno. R.; Sajjad. A.; Sindona. G. *J. Agr. Food Chem*., **56**, 63 (2007).

[225] Murty. M. R. V. S.; Chary. N. S.; Prabhakar. S.; Raju. N. P.; Vairamani. M. *Food Chem*., **115**, 1556 (2009).

[226] He. L.; Su. Y.; Fang. B.; Shen. X.; Zeng. Z.; Liu. Y.; *Anal. Chim. Acta*, **594**, 139 (2007).

[227] Mejia. E.; Ding. Y.; Mora. M. F.; Garcia. C.D. *Food Chem.,* **102,** 1027 (2007).

[228] Ma. X.; Chao. M.; Wang. Z. *Food Chem.,* **138**, 739 (2013).

[229] Yang. D.; Zhu. L.; Jiang. X.; Guo. L. *Sens. Actuat. B – Chem.*, **141**, 124 (2009).

[230] Yang. D.; Zhu. L.; Jiang. X. *J. Electroanal. Chem*., **640,** 17 (2010).

[231] Mo. Z.; Zhang. Y.; Zhao. F.; Xiao. F.; Guo. G.; Zeng. B. *Food Chem.,* **121,** 233 (2010).

[232] Chao. M.; Ma. X. *Int. J. Electrochem. Sci*., **7**, 6331(2012).

[233] Zhang. J.; Wang. M.; Chao. S.; Wang. W.; He. Y.; Chen. Z. *J. Electroanal. Chem.,* **685**, 47 (2012).

[234] Yin. H.; Zhou. Y.; Meng. X.; Tang. T.; Ai. S.; Zhu. L. *Food Chem*., **127**, 1348 (2011).

[235] Cheng. W.; Dong. S.; Wang. E. *J. Phys. Chem. B,* **108**, 19146 (2004).

[236] Asian. K.; Gryczynski. L.; Malicka. J.; Matveena. E.; Geddes. C.D.; *Curr. Opin. Biotechnol*., **16**, 55 (2005).

[237] Grzelczak. M.; Perez-Juste. J.; Mulvaney. P.; Liz-Marzan. L.M.; *Chem. Soc. Rev.*, **37**, 1783 (2008).

[238] Wang. Z. Ma. L. *Coord. Chem. Rev.*, **253**, 1607 (2009).

[239] Zhou. X.; Wei. Q.; Sun. K.; Wang. L.; *Appl. Phys. Lett.*, **94**, 133101 (2009).

[240] Abidi, W.; Remita. H. *Recent Patents Eng.*, **4**, 170 (2010).

[241] Mohanty. U.S. *J. Appl. Electrochem.,* **41**, 257 (2011).

[242] Laviron. E. *J. Electroanal. Chem. Interfacial Electrochem.*, **101**, 19 (1979).

[243] Dai. X.; Compton. R. G. *Anal. Sci.*, **22**, 567 (2006).

[244] Schmidt. U.; Donten, M.; Osteryoung, J. G. *J. Electrochem. Soc.*, **144**, 2013 (1997).

[245] Finot, M. O.; Braybrook, G. D.; McDermott, M. T. *J. Electroanal. Chem.*, **466**, 234 (1999).

[246] El-Deab, M. S.; Ohsaka, T. *Electrochim. Acta,* **47**, 4255 (2002).

[247] Liu, A.; Zhu, J.; Han, J.; Wu, H.; Jiang, C. *Electrochem. Commun.*, **10**, 827 (2008).

[248] Radmilovic. V.; Gasteiger. H.A.; Ross. P.N. *J. Catal.*, **154**, 98 (1995).

[249] Wang. J. *Analytical Electrochemistry*, Wiley-VCH, New York (2000).

[250] Rahimi. P.; Rafiee-Pour. H.; Ghourchian. H.; Norouzi. P.; Ganjali. M. R.; *Biosen. Bioelectron.*, **25**, 1301 (2010).

[251] Lin. H.; Li. G.; Wu. K. *Food Chem.,* **107**, 531 (2008).

[252] Shahidi. F. *Measurement of lipid oxidation and evaluation of antioxidant activity, in natural antioxidants: Chemistry, Health Effects and Applications.* AOCS Press, Champaign, IL, USA (1997).

[253] Joyner. N. T.; McIntyre. J. E. *Soap,* **15,** 184 (1938).

[254] Madhavi. D. L.; Deshpande. S. S.; Salunkhe. D. K. *Food antioxidants*, Marcel Dekker Inc, New York (1996).

[255] Lam L. K.; Pai R. P.; Wattenberg L. W. *J. Med. Chem*., **22,** 569 (1979).

[256] Shahidi F.; Janitha. P. K.; Wanasundara. P.D. *Crit. Rev. Food Sci. Nutr.,* **32**, 67(1992).

[257] Williams. G.; Iatropoulos. M.; Whysner. J. *Food Chem. Toxicol.,* **37,** 1027 (1999).

[258] Chang. H. C.; Branen. A. L. *J. Food Sci.,* **40**, 349 (1975).

[259] Komaitis. M.E.; Kapel. M. *J. Am. Oil Chem. Soc*., 62 1371 (1985).

[260] Viplava. P. U.; Divakar. T. E.; Hariprasad. K.; Sastry. C.S.P. *Food Chem.,* **25**, 159 (1987).

[261] Wang. J.Y.; Wu. H.L.; Chen. Y.; Sun. Y.M.; Yu. Y.J.; Zhang. X.H.; Yu. R.Q. *J. Chromatogr. A.*, **1264,** 63 (2012).

[262] Kelebek. H.; Selli. S.; Canbas. A.; Cabaroglu, T. *Microchem. J*, **91**, 187 (2009).

[263] Biparva. P.; Ehsani. M.; Hadjmohammadi. M.R. *J. Food. Compos. Anal*., **27**, 87 (2012).

[264] Pezo. D.; Salafranca. J.; Nevin. C. *J. Chromatogr. A*, **1178**, 126 (2008).

[265] Guan. Y.; Chu. Q.; Fu. L.; Ye. J. *J. Chromatogr. A*, **1074,** 201 (2005).

[266] Wang. J.; Zhang. D.; Chu. Q.; Ye. J. *Chin. J. Chem*., **28**, 313 (2010).

[267] Ruiz. M.A.; Calvo. M.P.; Jose. M. P. *Talanta*, **41**, 289 (1994).

[268] Medeiros. R.A.; Rocha-Filho. R.C.; Filho. O. F. *Food Chem.*, **123**, 886 (2010).

[269] Tomaskova. M.; Chylkova. J.; Jehlicka. V.; Navrati. T.; Svancara. I.; Selesovska, R. *Fuel*, **123,** 107 (2014).

[270] Volkov. A.; Tourillon. G.; Lacaze. P.C.; Dubois. J.E.; *J. Electroanal. Chem.***115**, 279 (1980).

[271] Ohnuki. Y.; Ohsaka. T.; Matsuda. H.; Oyama. N.; *J. Electroanal. Chem.,* **158**, 55 (1983).

[272] Cosnier. S. *Anal. Bioanal. Chem.*, **377**, 507 (2003).

[273] Zhang. K.; Luo. P.; Wu. J.; Wang. W.; Ye. B. *Anal. Methods*, **5**, 5044 (2013).

[274] Gu.Y.; Liu. W.; Chen.R.; Zhang.L.; Zhang. Z. *Electroanal.,* **25**, 1209 (2013).

[275] Wang. C.; Li. C.; Wang. F.; Wang. C. *Microchim. Acta*, **365**, 155 (2006).

[276] Ni. Y.; Wang. L.; Kokot. S. *Anal. Chim. Acta*, **412**, 185 (2000).

[277] Borrego. E.; Sicilia. D.; Rubio. S.; Pérez- Bendito. D. *TrAC Trend Anal. Chem*., **20**, 241 (2001).

[278] Ceballos. C.D.; Zon. M.A.; Fernández. H. *J. Chem. Edu.*, **83**, 1349 (2006).

[279] Prabakar. R.S.J.; Narayanan. S.S. *Food Chem.,* **118**, 449 (2010).

[280] Michalkiewicz. S.; Mechanik. M.; Malyszko. *J. Electroanal,* **16**, 588 (2004).

[281] Rasheed. Z.; Vikraman. A. E.; Thomas. D.; Jagan. J.S.; Kumar. K.G. *Food Anal. Methods*, **8**, 213 (2014).

[282] Vane. J.R. *Nat. New. Biol*., **231,** 232 (1971).

[283] Famaey. J.P. *Inflamm. Res.*, **46,** 437 (1997).

[284] Starek. M.; Krzek. J. *Talanta*, **77**, 925 (2009).

[285] Biscarini. L.; Patoia. L.; Favero. A. D. *Drugs Today*, **70**, 23 (1988).

[286] Rainsford. K. D. *Curr. Med. Res. Opin*., **22**, 1161 (2006).

[287] Oliveira. R.J.; Correia. J.; Silvestre. F. *Gastroenterol. Clin. Biol.,* **24**, 592 (2000).

[288] Andrade. R.J.; Lucena. M.I.; Fernandez. M.C.; Gonzalez. M. *J. Hepatol*., **32,** 74 (2000).

[289] Balasubramaniam. J. *Lancet*, **355,** 575 (2000)

[290] Schattner. A.; Sokolovskaya. N.; Cohen. J. *J. Intern. Med.,* **247,** 153 (2000).

[291] Tursen. U.; Kaya. T.I.; Kokturk. A.; Dusmez. D. *Int. J. Dermatol*., **4,** 767 (2001).

[292] Mangalvedhekar. S.S.; Gogtay. N.J.; Phadke. A.V.; Gore. S.; Shah. J.M.; Shah. S.M. *J. Assoc. Physicians India*, **48**, 548 (2000).

[293] Kanwar. A.J.; Kaur. S.; Thami. G.P. *Dermatology,* **201,** 376-376.

[294] Chang. S.F.; Miller. A.M.; Ober. R.E. *J. Pharm. Sci.,* **66,** 1700 (1977).

[295] Carini. M.; Aldini. G.; Stefani. R.; Marinello. C.; Facino. R.M. *J. Pharm. Biomed. Anal.,* **18**, 201 (1998).

[296] Sadhana. G.S.; Ghogare. A.B. *J. Chromatogr*., **542**, 515 (1991).

[297] Lakshimi. C.S.R.; Reddy. M. N. *Microchim. Acta*, **132,** 1 (1999).

[298] Nagaraja. P.; Yathirajan. H.S.; Arunkumar. H.R.; Vasantha. R.A. *J. Pharm. Biomed. Anal.,* **29**, 277 (2002**).**

[299] Zhang. J.; Tan. X.; Zhao. D.; Tan. S.; Huang. Z.; Mi. Y.; Huang. Z. *Electrochim. Acta,* **55**, 2522 (2010).

[300] Wang. C.; Liu. X.Q.; Qu. Q.; Yang. G.; Hu. X. *J. Pharm. Biomed. Anal.*, **42,** 237(2006).

[301] Constantinescu. I.C.; Florea. M.; Arama. C.C.; Nedelcu. A.; Monciu. C.M. *Farmacia,* **57**, 267 (2009).

[302] Dogrukol-Ak. D.; Tuncel. M.; Aboul-Enein. H.Y. *J. Sep. Sci*., **24**, 743 (2001).

[303] Brucher. M Jr.; Morrone. M.; Gin. P.; Weiss. S.; Alvisatos. A.P. *Science,* **281**, 2013 (1998).

[304] Medintz. I.L.; Uyeda. H.T.; Goldman. E.R.; Mattoussi. H. *Nat. Mater*., **4,** 435 (2005).

[305] Murray. C.B.; Norris. D.J; Bawendi. M.G. *J. Am. Chem. Soc.,* **115**, 8706 (1993).

[306] Gao. X.; Cui. Y.; Levenson. R.L.; Cheng. W.K.; Nie. S. *Nat. Biotechnol*., **22,** 969 (2004).

[307] Wang. L.; Chen. H.; Wang. L.; Li. L.; Xu. F.; Liu. J.; Zhu. C. *Anal. Lett*., **37,** 213 (2004).

[308] Chen. X.; Wang. X.; Liu. L.; Yang. D.; Fan. L. *Anal. Chim. Acta*, **542**, 144 (2005).

[309] Liang. J.; Huang. S.; Zeng. D.; He. Z.; Ji. X.; Ai. X.; Yang. H. *Talanta*, **69,** 126 (2006).

[310] Ma. Y.; Yang. C.; Li. N.; Yang. X. *Talanta*, **67,** 979 (2005).

[311] Lai. R. Y.; Fleming. J. J.; Merner. B. L.; Vermeij. R. J.; Bodwell. G. J.; Bard. A. J. *J. Phys. Chem. A,* **108**, 376 (2004).

[312] Kucur. E.; Riegler. J.; Urban. G. A.; Nann. T. *J. Chem. Phys.,* **119**, 2333 (2003).

[313] Trasatti.V. *Electrified Interfaces in Physics, Chemistry and Biology*, Kluwer Academic, Dordrecht (1992).

[314] Callan. J.F.; de Silva. A.P.; Mulrooney. R.C.; McCaughan. B. *J. Incl. Phenom. Macrocycl. Chem.,* **58**, 257 (2007).

[315] United States Pharmacopoeia, United States Pharmacopoeial Convention Inc, Rockevile, 209 (2005).

[316] Qu. L.; Peng. X. *J. Am. Chem. Soc.*, **124**, 2049 (2002).

[317] Yu. W.W.; Qu. L. H.; Guo. W. Z.; Peng. X. G. *Chem. Mater.*, **15**, 2854 (2003).

[318] Chen. Y.F. ; Rosenweig. Z. *Anal. Chem.*; **74,** 5132 (2002).

[319] Youngjin. K.; Robert. J.C.; Joseph. H.T. *Nano Lett*., **1,** 165 (2001).

[320] Weller. A. *Pure Appl. Chem*., **16,** 115 (1968).

[321] Kucur. E.; Riegler. J.; Urban. G.A.; Nann. T. *J. Chem. Phys*., **119**, 2333 (2003).

[322] Hyun. B.R.; Zhong. Y.W.; Bartnik. A.C.; Sun. L.; Abrun. H.D.; Wise. F.W.; Goodreau. J.D.; Matthews. J.R.; Leslie. T.M.; Borrelli. N.F. *ACS Nano,* **2**, 2206 (2008).

[323] Fernández-Calviño. D.; Rodríguez-Suárez. J. A.; López-Periago. E.; Arias-Estévez. M.; Simal-Gándara. J. *Geoderma*, **145**, 91 (2008).

[324] Xiao. Y.; Rowe. A.A.; Plaxco. K.W. *J. Am. Chem. Soc.,* **129,** 262 (2007).

[325] Wu. J.S.; Hwang. I.C.; Kim. K.S.; Kim. J.S. *Org. Lett*., **9**, 907 (2007).

[326] Wu. P.; Li. Y.; Yan. X.P. *Anal. Chem*., **81,** 6252 (2009).

[327] Kabehie. S.; Xue. M.; Stieg. A.Z.; Liong. M.; Wang. K.L.; Zink. J.I. *J. Am. Chem. Soc.*, **132**, 15987 (2010).

[328] Madhavan N. K.; Vasuprada. I. *Indian J. Med. Res*., **130**, 634 (2009).

[329] Riley. L.P.; Chester. R. *Introduction to Marine Chemistry*, Academic Press, New York (1971).

[330] Martin. J.H.; Fitzwater. S.E. *Nature,* **331,** 341 (1988).

[331] Martin. J.H.; Gordon. R.M.; Fitzwater. S.E. *Nature*, **345**, 156 (1990).

[332] Huheey.J.E.; Keiter.E.A.; Keiter.R.I.; Medhi.O.K.; *Inorganic Chemistry; Principles of Structure and Reactivity*, 4th Edn, Person Education,

[333] Lee. J.D. *Concise Inorganic Chemistry*, 5th edn, pp 754.

[334] Oski. F.A. *N. Enql. J. Med*., **329**, 190 (1993).

[335] Andrews. N.C. *Curr. Opin. Chem. Biol*., **6**,181 (2002).

[336] Meneghini. R. *Free Radic. Biol. Med*., **23**, 783 (1997).

[337] Toyokuni. S. *Free Radic. Biol. Med*., **20**, 553 (1996).

[338] Berg. D.; Gerlach. M.; Youdim. M.B.H.; Double. K.L.; Zecca. L.; Riederer. P.; Becker. G. *J. Neurochem.,* **79**, 225 (2001).

[339] Kaur. D.; Yantiri. F.; Cherny. R.A.; Bush. A.I.; Andersen. J.K. *Neuron*, **37,** 899 (2003).

[340] Duce. J.A.; Tsatsanis. A.; Cater. M.A.; James. S.A.; Robb. E.; Wikhe. K.; Leong. S.L.; Rogers. J.T.; Bush. A.I. *Cell,* **142**, 857 (2010).

[341] Mandel. S.; Amit. T.; Bar-Am. O.; Youdim. M.B.H.; *Prog. Neurobiol.*, **82**, 348 (2007).

[342] Wu. J.; Boyle. E.A. *Anal. Chim. Acta*., **367**, 183 (1998).

[343] Jong. J. de.; Schoemann. V.; Lannuzel. D.; Tison. J.L.; Mattielli. N. *Anal. Chim. Acta*., **623**, 126 (2008).

[344] Sharma. A.K.; Singh. I.; *Food Anal. Methods.* **2,** 221 (2009).

[345] Lee. M.H.; Giap. T.V.; Kim. S.H.; Lee. Y.H.; Kang. C.; Kim. J.S. *Chem. Commun*., **46**, 1407 (2010).

[346] Yanyan. D.; Chen. M.; Zhang. Y.; Luo.F.; He.C.; Li. M.; Chen. X.; *Talanta*, **106**, 261 (2013).

[347] Shamsipur. M.; Sadeghi. M.; Garau. A.; Lippolis. V.; *Anal. Chim. Acta,* **761**, 169 (2013).

[348] Du. Y.; Chen. M.; Zhang. Y.; Luo. F.; He. C.; Li. M.; Chen. X. *Talanta*, **106**, 261 (2013).

[349] Xiang. Y.; Tong. A. *J.Org. Lett.*, **8,** 1549 (2006).

[350] Giamarchi. P.; Cabon. J.Y.; Le Bihan. A. *Anal. Chim. Acta*, **664**, 114 (2010).

[351] Saracoglu. S.; Soylak. M.; Peker. D.S.; Elci. L.; Santos. W.N.; Lemos. V.A.; Ferreira. S.L. *Anal. Chim. Acta*, **575**, 133 (2006).

[352] Liang. Z.Q.; Wang. C.X.; Yang. J.X.; Gao. H.W.; Tian. Y.P.; Tao. X.T.; Jiang. M.H.; *J. Chem.,* **31**, 906 (2007).

[353] Wu. S.P.; Chen. Y.P.; Sung. Y.M. *Analyst*, **136**, 1887 (2011).

[354] Ussher. S.J.; Milne. A.; Landing. W.M.; Attiq-ur-Rehman. K.; Seguret. M.J.; Holland. T.; Achterberg. E.P.; Nabi. A.; Worsfold. P.J. *Anal. Chim. Acta*, **652**, 259 (2009).

[355] Lu. M.; Compton. R.G.; *Electroanal*., **25,** 1123 (2013).

[356] Favaron. R.; Aleixo. L.M. *Fresenius J. Anal. Chem*., **368**, 611 (2000).

[357] Garcia-Marco. S.; Torreblanca. A.; Lucena. J.; *J. Agric. Food Chem*., **54**, 1380 (2006)

[358] Gupta.T.; van der Boom. M. E. *J. Am. Chem. Soc.*, **129,** 12296 (2007).

[359] Fan. L.; Jones. W. E.; *J. Am. Chem. Soc.*, **128,** 6784 (2006).

[360] Bricks. J. L.; Kovalchuk. A.; Trieflinger. C.; Nofz. M.; Büschel. M.; Tolmachev. A. I.; Daub. J.; Rurack. K. *J. Am. Chem. Soc.*, **127,** 13522 (2005).

[361] Han. J.; Zhou. Z.; Bu. X.; Zhu. S.; Zhang. H.; Sun. H.; Yang. B.; *Analyst,* **138**, 3402 (2013).

[362] da Silva J.C.G.; Gonçalves H.M.R. *Trends Anal. Chem*., **30,** 1327 (2011).

[363] Baker. S.N.; Baker. G.A. *Angew. Chem. Int. Ed. Engl*.; **49**, 6726 (2010).

[364] Datta. K. K. P.; Reddy. B. V. S.; Ariga. K.; Vinu. A.; *Angew. Chem., Int. Ed.,* **49**, 5961 (2010).

[365] Y. Qiu and L. Gao, *Chem. Commun*., 2003, 2378

[366] Yang. G. W.; Wang. J. B.; *Appl. Phys. A: Mater. Sci. Process*., **71**, 343 (2000).

[367] Ghosh. K.; Kumar. M.; Wang. H.; Maruyama.T.; Ando. Y.; *J. Phys. Chem. C*, **114**, 510714 (2010).

[368] Liu. S.; Wang. L.; Tian. J.; Zhai. J.; Luo. Y.; Lua. W.; Sun. X.; *RSC Adv*, **1**, 951 (2011).

[369] Li. X.; Liao. Y.; Huang. M.; Strong. V.; Kaner. R.B.; *Chem. Sci.*, **4**, 1970 (2013).

[370] Ernst. Z.L.; Menashi. J. *Trans. Faraday Soc*., **59**, 2838 (1963).

[371] Rodrigues. S.S.M.; Lima. A.S.; Teixeira. S.G.L.; Korn. M.G.A.; Santos. L.M. *Fuel*, **117**, 520 (2014).

[372] Li. L.; Li. L.; Wang. C.; Liu. K.; Zhu. R.; Qiang. H.; Lin. Y.; *Microchim. Acta*, **182**, 763 (2015).

[373] Cao. H.; Chen. Z.; Zheng. H.; Huang. Y. *Biosens. Bioelectron*., **62,** 189 (2014).

[374] Mei. Q.; Jiang. C.; Guan. G.; Zhang. K.; Liu. B.; Liu. R.; Zhang. Z. *Chem. Commun*., **48**, 7468 (2012).

[375] Frankel, E. N. *Lipid Oxidation*. The Oily Press, Bridgwater, England (2005).

[376] Antolovich. M.; Prenzler. P. D.; Patsalides. E.; Mcdonald. S.; Robards. K. *Analyst*, **127**, 183 (2002).

[377] Irache. J.M.; Vega. F.A.; Ezpeleta. I. *Pharma. Acta Helv*., **67,** 152 (1992).

[378] Egsgaard. H.; Larsen. E.; Pederson. W.B.; Carlsen. L. *Trends Anal. Chem*., **11**, 164 (1992).

[379] Cabanillus. A.G.; Diaz. T.G.; Salinas. F.; *Analysis*, **19**,262 (1991).

[380] Boussendaji. R.; Porthault. M.; Berthod. A. *J. Pharm. Biomed. Anal*., **11**, 71 (1993).

[381] Williams. G.; Latropoulos. M.; Whysner. J. *Food Chem. Toxicol*., **37**, 1027 (1999).

[382] FAO/WHO, J. (1995). *Codex general standard for food additives*. http://www.who.int/ipcs/food/jecfa/en/index.html.

[383] Whysner. J.; Wang. C. X.; Zang. E.; Iatropoulos. M. J.; Williams. G.M.; *Food Chem. Toxicol.*, **32,** 215 (1994).

[384] Ito. N.; Hirose. M.; Fukushima. S.; Tsuda. H.; Shirai. T.; Tatematsu. M. *Food Chem.Toxicol*., **24,** 1071 (1986).

[385] Capitan-Vallvey. L.F.; Valencia. M.C.; Nicolas. E.A. *Anal. Chim. Acta,* **503,** 179 (2004).

[386] Kulys. J.; Bratkovskaja. I. *Talanta*, **72**, 526 (2007).

[387] Tabart. J.; Kevers. C.; Pincemail. J.; Defraigne. J.O.; Dommes J. *Food Chem.*, **120**, 607 (2010).

[388] Versari. A.; Parpinello. G.P.; Scazzina. F.; Del Rio. D. *Food Control,* **21,** 786 (2010).

[389] Pezo, D.; Salafranca. J.; Nevin. C. *J. Chromatogr. A*, **1178,** 126 (2008).

[390] Kelebek. H.; Selli. S.; Canbas.A.; Cabaroglu. T.; *Microchem. J.,* **91**, 187 (2009).

[391] Biparva. P.; Ehsani. M.; Hadjmohammadi. M.R. *J Food Compos. Anal.,* **27**, 87 (2012).

[392] Wang. J.Y.; Wu. H. L.; Chen. Y.; Sun. Y.M.; Yu. Y.J.; Zhang. X.H. *J. Chromatogr. A,* **1264**, 63 (2012).

[393] Yang. M.H.; Lin. H.J.; Choong. Y.M. *Food Res. Int*., **35,** 627 (2002).

[394] Lin. H.J.; Wang. M.L.; Choong. Y.M.; Chen. C.W.; Hwang. B.S.; Tsai. S.L. *J. Food Drug Anal*., **11,** 141 (2003).

[395] Ding. M.; Zou. J.K. *Food Chem*., **131**, 1051 (2012).

[396] Caramit. R.P.; Andrade. A.G.D.; de Souza. J.B.G.; de Araujo. T. A.; Viana. L.H.; Trindade. M.A.G. *Fuel*, **105**, 306 (2013).

[397] Robledo. S.N.; Zon. M.A.; Ceballos. C.D.; Fernandez. H. *Food Chem.,* **127,** 1361 (2011).

[398] Medeiros. R.A.; Lourencao. B.C.; Rocha-Filho. R.C.; Fatibello-Filho. O. *Anal Chem.,* **82**, 8658 (2010).

[399] Medeiros. R.A.; Rocha-Filho. R.C.; Fatibello-Filho. O. *Food Chem*., **123**, 886 (2010).

[400] Freitas. K.H.G.; Fatibello-Filho. O.; *Talanta*, **81,** 1102 (2010).

[401] Tae. J.; Yang. Y.K.; Yook. K.J. *J. Am. Chem. Soc*., **127**, 16760 (2005).

[402] Zhang. X.; Shiraishi. Y.; Hirai. T. *Tetrahedron Lett*., **48**, 5455 (2007).

[403] Wei. Y.; Qin. G.; Wang, W.; Bian. W.; Shuang. S.; Dong. C. *J. Lumin.*, **131**, 1672 (2011).

[404] Ni. Y.; Wang. L.; Kokot. S. *Anal. Chim. Acta*, **412**, 185 (2000).

[405] Chen. Y.F.; Rosenzweig. Z. *Anal. Chem*., **74**, 5132 (2002).

[406] Cai. Z.X.; Yang. H.; Zhang. Y.; Yan. X.P.; *Anal. Chim. Acta*, **559**, 234 (2006).

[407] Chen. B.; Yu. Y.; Zhou. Z.T.; Zhong. P. *Chem. Lett*., **33**, 1608 (2004).

…..ஜ۞ஜ…..

Publications

[1] **Divya Thomas,** Anuja E. Vikraman, Theresa Jos, K. Girish Kumar, Kinetic approach in the development of a gold nanoparticle based voltammetric sensor for Sudan I, *LWT - Food Science and Technology* (2015, DOI: 10.1016/j.lwt.2015.04.020).

[2] **Divya Thomas,** Zafna Rasheed, Jesny Siri Jagan, K. Girish Kumar, Study of kinetic parameters and development of a voltammetric sensor for the determination of butylated hydroxyanisole (BHA) in oil samples. *Journal of Food Science and Technology*, (2015, DOI 10.1007/s13197-015-1796-1).

[3] Ambily Thomas, Anuja E. Vikraman, **Divya Thomas,** K. Girish Kumar, Voltammetric Sensor for the Determination of TBHQ in Coconut Oil, *Food Analytical Methods,* (2015, DOI 10.1007/s12161-015-0092).

[4] Zafna Rasheed, Anuja E. Vikraman, **Divya Thomas**, Jesny Siri Jagan, K. Girish Kumar, Carbon-Nanotube-based sensor for the determination of butylated hydroxyanisole in food samples. *Food Analytical Methods,* **8,**213 –221 (2015).

[5] Anuja E. Vikraman, **Divya Thomas**, Soumya Cyriac, K. Girish Kumar, Kinetic and thermodynamic approach in the development of a voltammetric sensor for sunset yellow. *Journal of Elelctrochemical Society*, **161,** 305-311 (2014).

[6] Sobhana Mathew, **Divya Thomas**, Anuja E. Vikraman, K. Girish Kumar, Manganese (II) –Selective Potentiometric Sensor Based on Calix [4] resorcinarene in PVC Matrix. *Frontiers in Sensor,* **1,** 74-80 (2014).

[7] Sreejith Chandran, Laina Lonappan, **Divya Thomas**, Theresa Jos, K. Girish Kumar, Development of an electrochemical sensor for the determination of Amaranth: A synthetic dye in soft drinks. *Food Analytical Methods,* **7**, 741-743 (2014).

[8] Theresa Jos, **Divya Thomas**, Sowmya T Cyriac, Meera Jacob, K. Girish Kumar,Effect of anionic surfactant on the reduction of tinidazole at a gold nano particle modified glassy carbon electrode. *Indo American Journal of Pharmaceutical Research,* **3,** 8434-8439 (2013).

[9] **Divya Thomas**, Laina Lonappan, Leena Rajith, Soumya T. Cyriac, K. Girish Kumar, Quantum dots based fluorescent probe for the selective determination of nimesulide. *Journal of fluorescence*, **23**, 473-478 (2013).

[10] **Divya Thomas**, Leena Rajith, Laina Lonappan, Sindhu Issac, K. Girish Kumar, Sensitive determination of nitrite in food samples using voltammetric technique, *Food Analytical Methods,* **5,** 752-758 (2012).

[11] Laina Lonappan, Sindhu Issac, Renjini Joseph, **Divya Thomas**, K. Girish Kumar, Electrochemical studies of tamsulosin hydrochloride using multiwalled carbon nanotube-modified carbon sensor. *Micro and Nano Letters,* **6,** 867-870 (2011).

Conference papers

[1] Gold Nanoparticle modified glassy carbon electrode sensor for the voltammetric determination of Sudan 1 in food samples. (23rd Swadeshi Science Congress, Kottayam, 2013).

[2] Carbon nitride dots based fluorescent sensor for the determination of BHA in food samples. (Current Trends in Chemistry (CTric), Cochin University of Science and Technology, Kochi, 2013).

[3] Voltammetric determination of nitrite in food samples. (22nd Swadeshi Science Congress, Kasargod, 2012).

[4] Quantum dots based fluorescent probe for the selective determination of Nimesulide. (24th Kerala Science Congress, Kottayam, 2011).

[5] A TMOPPMn(III)Cl modified gold sensor for the determination of nitrite in food samples. (1st Kerala Women Science Congress, Kochi, 2010).